Analysis of 5G Cellular Radio Network Deployment over Several Scenarios

Alexandre Botelho Vieira

Thesis to obtain the Master of Science Degree in

Electrical and Computer Engineering

Supervisor: Prof. Luís Manuel de Jesus Sousa Correia

Examination Committee

Chairperson: Prof. José Eduardo Charters Ribeiro da Cunha Sanguino

Supervisor: Prof. Luís Manuel de Jesus Sousa Correia

Members of Committee: Prof. António José Castelo Branco Rodrigues

: Eng. João Miguel Sotomayor Calvário

November 2018

I declare that this document is an original work of my own authorship and that it fulfils all the requirements of the Code of Conduct and Good Practices of the *Universidade de Lisboa*.

To my family, friends and colleagues.

Acknowledgements

The first acknowledgement is naturally to sincerely thank Prof. Luís M. Correia for the opportunity of developing this thesis throughout the past few months. It has truly been a pleasure to work under his supervision with the continuous series of effective, righteous and straight to the point advices, recommendations and stories regarding not only the thesis work, but also other aspects in life.

It has been a great experience to develop the thesis in collaboration with KPMG, for whom I present my thanks the opportunity of collaboration, especially to Eng. José Teixeira and Eng. João Calvário, who have always provided a valuable assistance and feedback throughout the development of this thesis, strongly contributing to improving the quality of this work.

In these months a special thanks must be made to my estimated GROW colleagues, in the names of André Ribeiro, Anna O.A, Ismael Belchior and Pedro Delgado for all of our discussions, advices and recommendations.

To all of those who have joined me in this journey I thank my good friends from IST, Afonso, Tiago, Pereira, Luís, Tomás, Girão, Rei, Ratinho, Guedes e Charana, as well as all my friends from Lisbon Toastmasters Club, Lério, Rui, Campello, Costa, Flor, Neto, Ribeiro and Braga, who have helped, encouraged and motivated me throughout the academic journey in all these years.

At last, but most important, I present my special gratitude/appreciation to all my family, especially to my parents for all the dedication and hard work which made my academic journey possible, to my brothers, sisters, nephews and nieces for all their support, understanding and motivation throughout these five years.

Abstract

The main purpose of this thesis was to study and develop a model for cellular planning for 5G-NR networks. The goal was to compute the number of required cells to cover a given target area, with well-defined reference model parameters and different traffic profiles. The model was developed considering coverage and capacity planning characteristics related to 5G-NR, for the 700 and 3 500 MHz bands, in three different environments (urban, suburban, rural) with the inclusion of different numerology configurations. With the developed simulator, one can easily assess the impact of varying input parameters, such as user density, target area, frequency band, bandwidth, numerology, throughput at cell edge, traffic profile, among others, on the number of cells. Regarding capacity dimensioning, the process of resource allocation has been redeveloped from scratch due to the inclusion of numerology configurations. An increase on the total number of cells is observed when the density of users increases or when the available bandwidth decreases, and with more users more resources are needed to fulfil coverage and capacity requirements. Most of the cells in urban scenarios are limited by capacity regardless of the frequency band, whilst for suburban and rural ones there is a shift from coverage to capacity limited cells when an increase of frequency occurs. Also, regarding the traffic profile, the results show that changing the service mix or the services' throughput values can severely impact on the number of required cells, with a relative increase in the number of cells up to 40%.

Keywords

5G-NR, cellular dimensioning, coverage, capacity, number of cells, Lisbon

Resumo

O objetivo principal desta tese foi o estudo e o desenvolvimento de um modelo de dimensionamento de rede celular para redes 5G-NR. O propósito foi o de calcular o número de células necessárias para cobrir uma certa área, com parâmetros de referência e diferentes perfis de tráfego. O modelo foi desenvolvido tendo em conta as características de cobertura e capacidade impostas pelo 5G-NR, para as frequências de 700 e 3 500 MHz, para três ambientes de propagação (urbano, suburbano, rural), com a inclusão de diferentes configurações de numerologias. Com o simulador desenvolvido, é possível verificar o impacto da variação de parâmetros de entrada, tais como a densidade de utilizadores, frequência, largura de banda, numerologia, velocidade no limite da célula, perfil de tráfego, entre outros, no número de células. No dimensionamento de capacidade, o processo de alocação de recursos foi desenvolvido de raiz devido à inclusão das configurações de numerologia. Verifica-se um aumento no número de células quando a densidade de utilizadores aumenta e quando a largura de banda disponível diminui, e com mais utilizadores mais recursos são necessários para cumprir os requisitos a nível de cobertura e capacidade. A maior parte das células em ambiente urbano são limitadas por capacidade independentemente da frequência, enquanto que nos ambientes suburbano e rural há uma transição de células limitadas por cobertura para capacidade, quando esta aumenta. Sobre perfis de tráfego, os resultados mostram que a variação da quota de serviço ou da velocidade pode impactar severamente no número de células, com um aumento até 40%.

Palavras-chave

5G-NR, dimensionamento, cobertura, capacidade, número de células, Lisboa

Table of Contents

List of Figures

List of Tables

List of Acronyms

16 QAM	Quadrature Amplitude Modulation (4 bits per symbol)
256 QAM	Quadrature Amplitude Modulation (8 bits per symbol)
3G	Third Generation of mobile communications
3GPP	Third Generation Partnership Project
4G	Fourth Generation of mobile communications
5G	5th Generation of Mobile Communications
64 QAM	Quadrature Amplitude Modulation (6 bits per symbol)
ANACOM	National Communications Authority (Portugal)
BH	Backhaul
BS	Base station
CA	Carrier Aggregation
CN	Core Network
CP	Control Plane
CP	Cycle Prefix
DL	Downlink
DN	Data Network
E2E	End-to-end
EIRP	Effective Isotropic Radiated Power
eMBB	Enhanced Mobile Broadband
EPC	Evolved Packet Core
EPS	Evolved Packet System
E-UTRAN	Evolved Universal Terrestrial Radio Access
FDD	Frequency Division Duplex
FH	Fronthaul
FTP	File Transfer Protocol
GSM	Global System for Mobile Communications
ICT	Information and Communication Technology
INI	Inter-Numerology Interference
IoT	Internet of Things
LTE	Long Term Evolution
MAPL	Maximum Allowed Path Loss
MBB	Mobile Broadband
MIMO	Multiple-input Multiple-output

MME	Mobility Management Entity
MMTC	Massive machine type communication
MT	Mobile Terminal
MVNO	Mobile Virtual Network Operator
NFV	Network Functional Virtualisation
NG-RAN	New Generation Radio-Access Network
NR	New Radio
OFDM	Orthogonal Frequency Division Multiplexer
P2P	Peer-to-peer
PRB	Physical Resource Block
QoS	Quality of Service
QPSK	Quadrature Phase Shift Keying (2 bits per symbol)
RAN	Radio Access Network
RAT	Radio Access Technology
RB	Resource Block
RLB	Radio Link Budget
ROM	Residential, Office and Mix scenario
SCS	Sub-carrier spacing
SDN	Software-Defined Network
SINR	Signal to Interference Noise Ratio
SNR	Signal to Noise Ratio
TDD	Time Division Multiplex
TMA	Tower Mounted Amplifier
TP	Throughput
TTI	Transmission Time Interval
UL	Uplink
UMTS	Universal Mobile Telecommunications System
UP	User Plane
UPF	User Plane Function
URLLC	Ultra-reliable, Low-Latency communication
VNF	Virtual Network Function
VoIP	Voice over IP
VoLTE	Voice over LTE

List of Symbols

Δf	Carrier Frequency
η	User Density
μ	Type of Configuration
α_{pd}	Average Power Decay
G_r	Gain of the Receiving Antenna
G_t	Gain of the Transmitting Antenna
L_p	Path Loss
m	Order of Modulation
$N_{slot}^{frame,\mu}$	Number of slots per Frame for a given configuration
$N_{slot}^{subframe,\mu}$	Number of slots per subframe for a given configuration
$N_{streams}$	Number of streams
N_{sym}^{slot}	Number of symbols per slot
$N_{RB,DL}^{max,\ \mu}$	Maximum number of RBs in Downlink for a given configuration
$N_{RB,DL}^{min,\ \mu}$	Minimum number of RBs in Downlink for a given configuration
$N_{RB,UL}^{max,\ \mu}$	Maximum number of RBs in Uplink for a given configuration
$N_{RB,UL}^{min,\ \mu}$	Minimum number of RBs in Uplink for a given configuration
N_{RB}	Number of resource blocks
N_{RB}^{u}	Number of resource blocks per UE
N_{SC}^{RB}	Number of subcarriers per RB
N_{sym}^{SF}	Number of symbols per subframe
N_u	Number of users in the system
$N_{u,cell}$	Number of users in a cell
$P_{r,min}$	Power sensitivity at the receiver antenna
$R_{b,teo}$	Theoretical data rate / throughput
R	Cell radius
S	Coverage area
$T_{S\,[s]}$	Sampling Time
T_{SF}	Period of subframe

List of Software

Microsoft Visual Studio 2017	C# App Development Environment
Microsoft Office Excel 2016	Spreadsheet application
Microsoft Office Word 2016	Word processor
Draw.io	Online flow chart and diagram software

Chapter 1

Introduction

This chapter provides a brief overview of the mobile communications systems evolution, focusing on the most important aspects of 5G network, in terms of motivation and scope of work to be developed.

1.1 Overview

According to [BEEC14], advances in wireless networks are driving commerce as well as enhancing society in new, unexpected and fortuitous ways. A key driving gear for the wireless of the future will be the widespread deployment of 5G wireless networks. Radio access in 5G will be built from existing wireless radio access technologies (RAT) e.g., LTE and Wi-Fi, combined with entirely new ones.

Future wireless systems are expected to use more bandwidth more efficiently by exploiting spatial diversity techniques with massive MIMO and beamforming. Higher user throughput will be achieved mainly through carrier aggregation and the use of new frequency bands. The overall cell density is therefore projected to increase, while more devices with lower transmission power, transmission or reception gains are expected to be supported by 5G networks.

Therefore, the concept of linking more and more devices to the Internet is a strong door opener for more efficient and economical industry frameworks, due to the development of new use-cases, such as machine communication systems in MMTC, Smart Cities, Virtual Reality or Augmented Reality, in Figure 1.1. This, together with the increasing number of mobile devices and growing data rates demandsfrom customers, e.g., enhanced mobile broadband, has driven the need for the development of a new mobile communications network, the 5th Generation. The key advantage points are better or more efficient techniques to provide better network capacity, latency, mobility and transmission speeds.

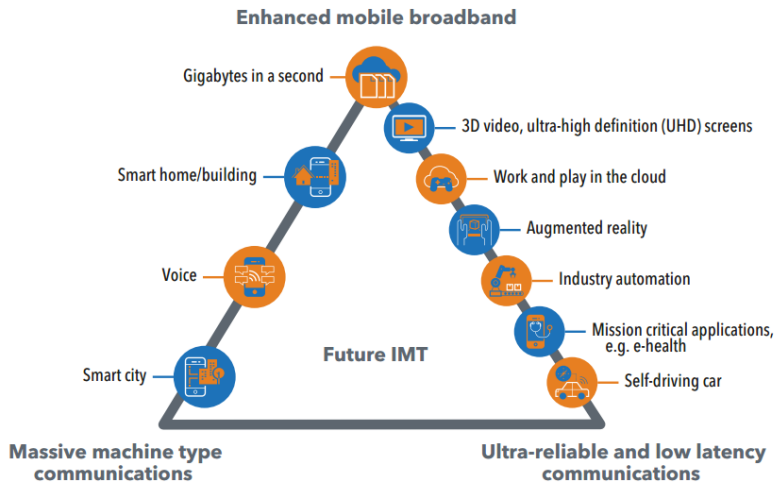

Figure 1.1. Proposed use-case scenarios for 5G | ITU (extracted from [ITUn17]).

Although the 5th Generation is still currently in late development stages (2018-2020), some operators and mobile phones manufacturers have already started proposing network deployments in 2019. At the present moment the first outline prospects of what the 5G network architecture will consist of have already been established, with the comprehensive release version by 3GPP to come still in 2018. Consequently, many operators, chip and phone manufacturers are starting to be in the possession of enough material to conduct substantial studies and testing on 5G technologies. Figure 1.2 exhibits the 5G study target roadmap established by Next Generation Mobile Networks (NGMN) in 2015.

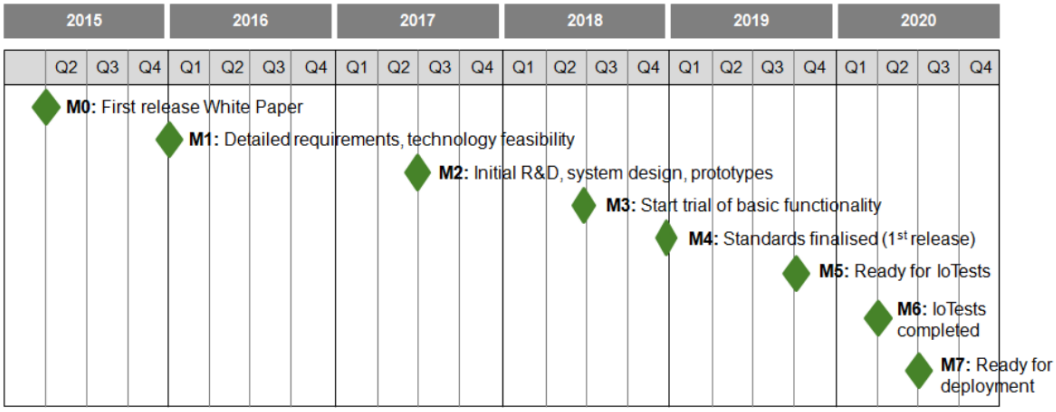

Figure 1.2. NGMN 5G Roadmap (extracted from NGMN15).

However, works related to a comprehensive simulator approaching the coverage and capacity elements of 5G-NR network have not still been widely studied or widely published. Therefore, the novelty this thesis brings is the study of coverage and capacity characteristics for initial 5G-NR deployments in three propagation environments, urban, suburban and rural, for a much higher diversity of spectrum options compared to LTE, with more bandwidth values and the inclusion of numerology configurations, for the 0.7 and 3.5 GHz bands. Therefore, the ultimate goal of the simulator is to compute the number of cells from three key elements, the model reference parameters (link budget, propagation models, capacity requirements), the reference traffic profile (service priority, mix share, throughput requirement) and the municipality/district database within the geographical target deployment area (location area, propagation environment, user density). Since the model should withstand any modification in the input parameters, it should also be time accessible to test the impact of different configurations of input parameters on the number of cells.

In terms of coverage, the model should be focused on the new frequency bands expected to be deployed in early 5G implementations. While the 0.7 GHz is lower than the LTE's 0.8 GHz, which could provide better coverage to network users, the main goal frequency-wise is to analyse the impact on the higher 3.5 GHz band of 5G compared to LTE's 2.6 GHz, in terms of higher propagation losses both indoors and outdoors. In terms of capacity, the model should be able to support every valid spectrum configuration defined by 3GPP. This includes new bandwidth configurations as well as the numerologies in use for these frequency bands. The ultimate goal is to determine the maximum number of users in the cell and in the network for a reference traffic profile, which measures the performance for a variety of services demanded by users.

1.2 Motivation and Contents

According to [ERIC17], increasing demands from consumers and tough pricing competition are causing market revenue stagnation for the industry, despite the high growth in both mobile subscriptions and

mobile data traffic, overall mobile service revenue growth has flattened out compared to the 10-15% growth in the previous decade. Thus, the main financial motivation concerning 5G technology is about aiding telecommunications operators convert the growth of usage of mobile data services into a greater, more solid source of revenue.

[ERIC16] defines the interoperability with previous generations of mobile communications as one of the key principles concerning the Information and Communications Technologies (ICT) industry, while also establishing that 5G network access capabilities must extend far beyond those of past generations of mobile communications, both in terms of incorporating a wider range and variety of devices, and in delivering data with a much lower cost per bit.

Regarding frequency spectrum, 5G is planned to extend its usage far as 30 to 80 GHz for increased system capacity, and two of the main frequencies of operation are anticipated to be 0.7, 3.5 and 28 GHz. Although the length of spectrum usage increases, 5G networks are expected to use only higher frequencies as a complement to lower frequency bands for providing either additional capacity, or very wide transmission bandwidths for specific extreme data rates, such as in dense deployments.

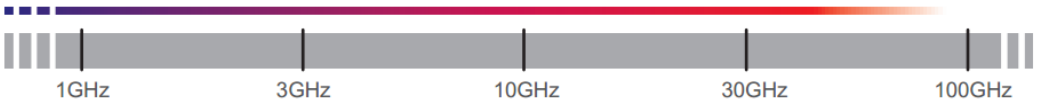

Figure 1.3. Projected spectrum for 5G | Ericsson (extracted from [ERIC16]).

The concept of beamforming is discussed in [ERIC15] and [ERIC16]. According to [ERIC15], it is about taking the already existing concept of multi-antenna technologies (MIMO) to a higher level. The more antenna elements the narrower the beam, and this with the transmitter-receiver tracking in real-time allows for maximising the power of the received signal in a specific direction. However, some transmissions regarding synchronisation and system information from base stations still need to reach several users at once, which is not possible with beamforming. The main advantages of this concept are allowing a more efficient spectrum and energy utilisation. The transmitter and receiver use beam-forming to track one another, and by focusing the transmission power in a specific direction it improves energy transfer, plus it improves the radio environment around the base station by limiting interference to specific fractions of the space around the transmitter

At the level of network architecture, the key point for minimising network signalling is the concept of ultra-lean radio access design. It consists of minimising any transmissions not directly related to the delivery of user data, such as synchronisation, network acquisition or channel estimation. Besides, it is also planned that 5G networks should decouple user data and system control functionality, allowing for a separate process of scaling user-plane capacity and basic system control functionality.

This thesis was done in collaboration with KPMG Portugal, which is one of the largest IT consulting companies in Portugal. The main conclusions taken as a result of this work are intended to give some guidelines to the company for consulting in the context of mobile communications operators, by

providing the essential framework for cost estimating in a future occasion derived from coverage and capacity analysis performed in this thesis.

In terms of contents, this thesis is divided into five chapters, followed by a set of annexes that add complementary information and results to the main work. The present chapter presents a brief overview of the mobile communications' history evolution, showing the motivation behind the thesis.

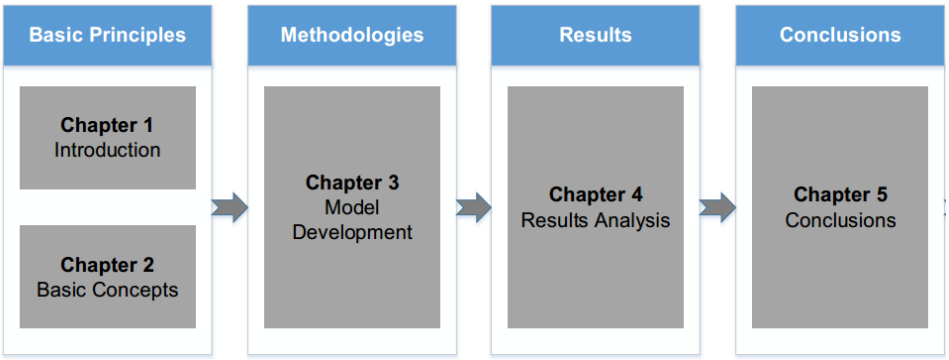

Figure 1.4. Thesis Structure.

In Chapter 2, the fundamental characteristics of the key elements of 5G-NR networks are presented. It provides a characterisation of the network architecture, the radio interface where the novelty aspects concerning 5G-NR are highlighted and some aspects regarding coverage and capacity dimensioning. It also presents a description of the main use cases in terms of services and applications expected to be supported in 5G deployments through performance metrics, such as throughput or latency requirements. Furthermore, a comprehensive view on the state of the art is presented on topics that relate to the work developed in the thesis from academic theses, industry reports and official telecommunications standards.

In Chapter 3, the most important and relevant models applied in the simulator are described. It consists of models and assumptions taken for simulator elements, such as coverage, capacity and throughput calculations, as well as the inclusion of numerology configurations. The simulator implementation is also explained in this chapter through means of routine inputs and outputs, as well as through means of workflows. In the end, an assessment on key simulator elements is performed in order to guarantee that results are valid and correct for further study.

In Chapter 4, the scenarios to be considered in the simulator are described, as well as the model reference parameters in terms of link budget, propagation models' configurations and capacity related metrics, such as the throughput at cell edge, which numerologies are active, among others, and the reference traffic profile. From these reference parameters a number of analysis are performed from diverse results in order to study the impact of different input parameters mainly on the cell radii, number of active users and number of cells. The traffic profile is modified to study the impact on different service mix share configurations, as well as the impact on changing the average throughput per service. At last, in Chapter 5 the main conclusions from the simulation results are taken, presenting the most relevant

and important results and a brief analysis on them. Besides, some recommendations for future work are presented, based on 5G-NR standards still to be released and on some key assumptions taken for the model development.

In the end, a number of complementary models or data used in the context of this thesis is presented. In Annex A, the expressions relating SNR with the throughput per RB is defined. In Annex B, the propagation models for both indoors and outdoors used in the model are described in their full extension. In Annex C, the district and municipality database in terms of the reference scenario is presented, showing the area, propagation environment and user density per location. Finally, Annex D presents some additional assessment results which validate the results produced by the propagation distance models and a description of the secondary model routines is presented in Annex E.

Chapter 2

Fundamental Concepts and State of the Art

This chapter provides an overview on 5G, primarily focusing on the network, coverage and capacity aspects and required performance parameters. A concise description of the state of the art is also presented.

2.1 Network Architecture

The most important key aspects on 5G's architecture and radio interface are provided in this section, primarily based on the works of [NGMN15], [5GPP17] and [AM5G16].

According to [NGMN15], 5G networks are expected to leverage the structural separation of hardware and software, as well taking advantage of function customisation offered by SDN and NFV. In essence, the 5G architecture is a native SDN/NFV scheme, which covers needs from devices, infrastructure, network functions, value enabling capabilities and the entire set of management functions to orchestrate the system. Besides, APIs are provided to support multiple use cases, value creation and business models. The Figure 2.1 displays an abstract view on the different components and layers proposed for the 5G network architecture, by showing the association between end-users (5G devices) and the Radio Access Technology (RAT) element, as well as its connection to the bottom network layer (infrastructure resources layer). From this, the second layer deals with network function configurations, linked upwards to the third layer with the final business-projected use-cases.

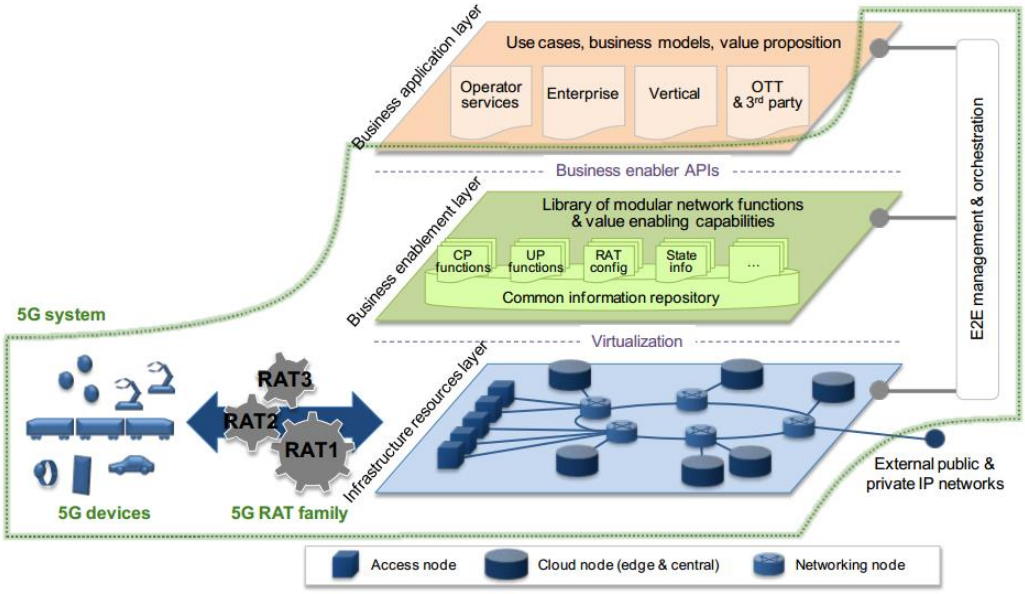

Figure 2.1. Abstract 5G Network Architecture (extracted from [NGMN15]).

From Figure 2.1, the architecture comprises three layers plus an end-to-end management and orchestration entity:

- **Infrastructure resource layer (IRL):** consists of physical resources, comprised of access nodes, cloud nodes (processing or storage), 5G devices, networking nodes and associated links. Resources are exposed to higher layers and to the E2E management and orchestration entity through relevant APIs, from which performance and status monitoring are an intrinsic part.
- **Business enablement layer (BEL):** library of the entire set of functions required within a network to form a modular architecture building blocks. This includes functions realised by software-designed modules and a set of configuration parameters for certain components of the network, such as radio access. These functions and capabilities are used when requested by

the orchestration entity.

- **Business application layer (BAL):** consists of specific applications and services in the optics of operators or companies. The interface to the E2E management and orchestration entity allows, e.g., to build dedicated network slices for a specific application.
- **E2E management and orchestration unity:** consists on the contact point translating the use cases and business model requirements into actual network functions and slices. It is responsible for defining network slices for a given network demand, linking the relevant modular network functions, assigning relevant performance configurations and mapping it into the infrastructure resources. It will not be a monolithic piece of functionality but a collection of modular functions integrating advances in different domains, such as NFV, SDN or SON. At last, this unity is expected to have the ability of sharing capabilities with third party organisms, such as MVNOs, to create and manage their own network slices, as well as using data-aided intelligence to optimise the full set of service composition and delivery characteristics.

To meet and carry out the specifications of the 5G network architecture, the underlying point consists of applying a clear separation of Control Plane (CP) and User Plane (UP), with open interfaces defined between them, via SDN principles. Between the remote radio units (RRUs) and baseband units (BUs), the fronthaul interface(s) should also be as open and flexible as possible, with a good forward and backward compatibility.

According to [5GPP17] and [AM5G16], future networks are expected to be an integration of cross-domain networks, where multiple virtual networks can be created on top a common shared physical infrastructure, creating a flexible network. The virtual networks are then customised in a series of aspects, such as latency, transmission speed, bandwidth requirements to meet the specific needs of applications, services, devices, costumers of operators. Figure 2.2 exhibits an example of some applications using slice resources and its link with corresponding core network (CN) slices.

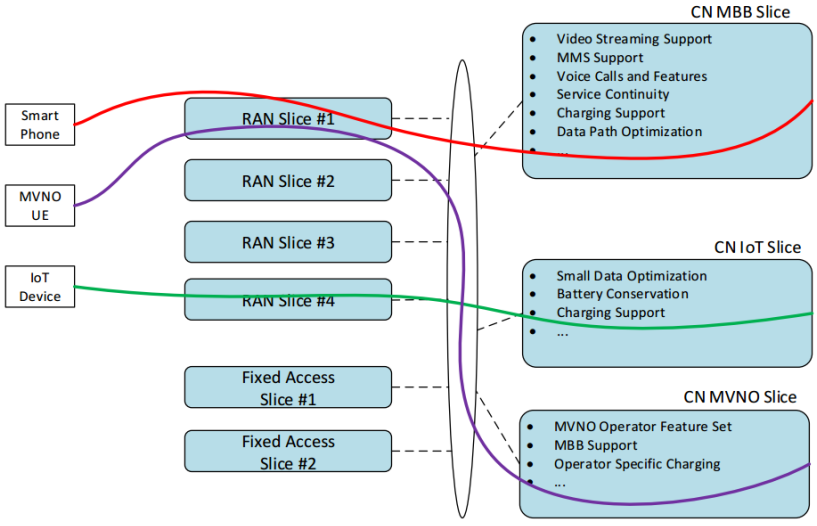

Figure 2.2. Network slicing abstraction | 5G Americas (extracted from [NGMN15]).

Network slicing technology will be particularly important for operators since it will be possible to deploy

new services with a much shorter time-to-market. This is expected to drive development of new use cases in the optics of generating new sources of revenue.

The abstraction shown in Figure 2.2 states that each slice is a feature type-ready configuration batch, which can then be assigned and transported to the corresponding core network slice. For example, a mobile virtual network operator end-user (MVNO UE) can require a service that demands an explicit, limited, set of features. For this, it re-uses the RAN slice #1 in order to achieve the CN MVNO slice. According to [AM5G16], a network slice is the key supporter of communication services of a particular connection type with a specific way of handling the CP and the UP for the given service. It is composed of a collection of 5G network functions (NF) and specific RATs settings combined together for the specific use case or specific business model, as it can be seen in Figure 2.3.

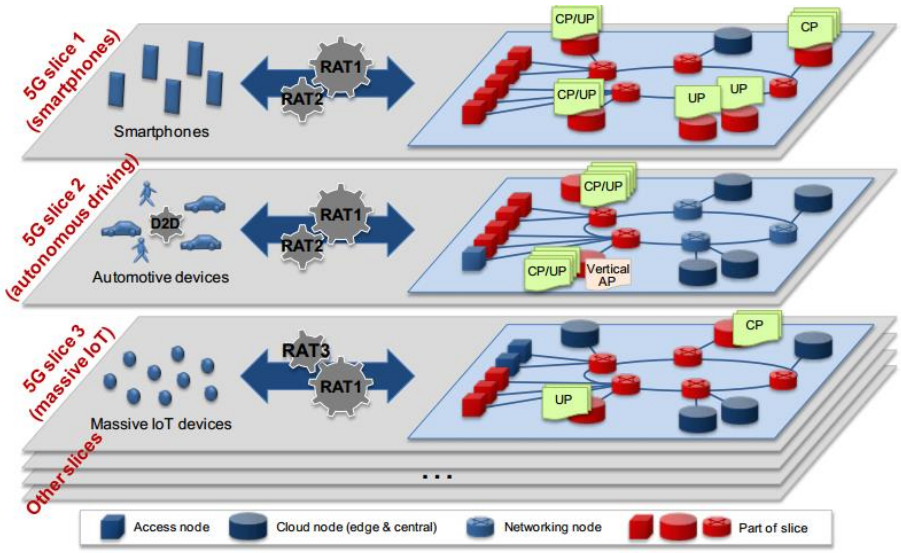

Figure 2.3. Network slicing abstraction (extracted from [NGMN15]).

Figure 2.3 illustrates multiple 5G network slices being operated at the same on the same infrastructure, slicing for smartphone performed by using established network functions distributed across the network, for Autonomous Driving performed by giving maximum value to security, reliability and latency and for massive IoT: some basic Control-plane functions (CPF) can be configured, and/or omitted (e.g., mobility functions).

It is important to emphasise that not all slices will need to contain the same network functions. The purpose of network slicing is to provide the minimum required traffic commitment as possible for any given use case. This adds a layer of flexibility to the 5G network architecture, since it avoids unnecessary functionalities to be dealt with, but also by being a key enabler into expanding existing and creating new use-cases, and consequently, business models. An illustration of this is the possibility of allowing third-party entities to acquire a varying degree of utilisation and control of certain aspects of network slicing from a given operator, in order to provide relevant tailored services.

For each slice, all the required dedicated functions can be instantiated at the cloud edge node (CEN) including vertical compression due to latency constraints. In due time there may be unknown use cases and traffic, thus the 5G network must contain enough functionality blocks to ensure controlled and

secure operation of the network E2E at any circumstance. Although the goal of network slicing is to minimise the simultaneous use of dedicated and shared infrastructure resources, the use of both is still required for some critical functions, e.g., radio scheduler.

2.2 Radio Interface Novelties

The radio interface in 5G can be primarily described in this chapter with NR, the RAT schemes and the technical migration roadway, where different migration options are described depending on operator's requirements and equipment. In agreement with [HUAW16], the new radio air interface is a key differentiator technology from previous generations of mobile communications, comprising key enabling technologies, such as fundamental waveforms, multiple access schemes, channel coding, access protocols and frame structures, among others, as it can be seen in Figure 2.4.

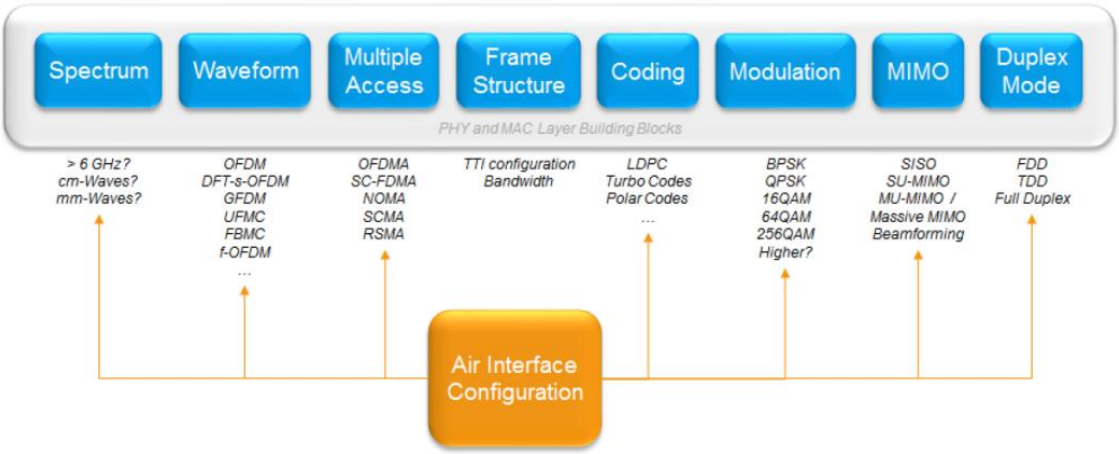

Figure 2.4. Network slicing abstraction | NGMN (extracted from [ROSC16a]).

From Figure 2.4, a brief overview, based on [HUAW16]), on the main topics is carried out:

- **Filtered-OFDM (waveform):** it enables a unified air interface supporting flexibility and spectral efficiency. Since in 5G different applications will have different requirements on AI technology, using a pure OFDM will no longer be sufficient to support requirements due to the lack of flexibility. Therefore, the candidate waveforms proposed thus far are CP-OFDM, W-OFDM and f-OFDM;
- **Sparse Code Multiple Access (multi-access):** allocation of AI resources. It is a key technique for managing and increasing the number of connections and spectral efficiency.
- **Polar Codes (coding):** have a clear and simple encoding and decoding structure, with the error correction performance being superior to the previously used Turbo codes.

Regarding the new concept of radio in 5G, New Radio will support the wide variety of services, devices and deployments 5G will encompass, as well as it ensures backward and forward compatibilities. 5G-NR can provide multiple OFDM numerologies in the same bandwidth through multiple subcarrier spaces

(SCS), allowing it to be used for different carrier frequencies for different services. The sampling time is defined by (2.1) and the numerology configuration by (2.2).

$$T_{s[\mathrm{ms}]} = \frac{1}{\Delta f_{max[\mathrm{kHz}]} \cdot N_f} \tag{2.1}$$

where:

- Δf_{max} is the maximum subcarrier frequency (480 kHz);
- N_f is the maximum number of carrier frequencies (4096);

The numerology configuration bandwidth (SCS) is given by:

$$\Delta f_{[\mathrm{kHz}]} = \Delta f_{ref[\mathrm{kHz}]} \cdot 2^{\mu} \tag{2.2}$$

where:

- Δf_{ref} = 15 kHz
- μ is the numerology configuration number (integer);

Depending on frequency, cell size and latency characteristics of a given application or service, there can be a plenitude of numerology configurations, as seen in Figure 2.5. For example, to achieve very low latency at high frequencies the transmission from the BS to the MT should be established through micro-cells, using a SCS of 60 kHz. For MTs moving at high speed higher SCSs must be considered due to Doppler effect, and for very low latency since the TTI must be low, higher SCSs must be used.

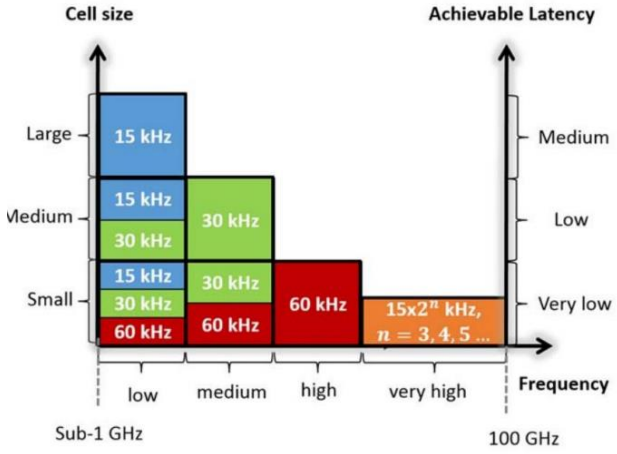

Figure 2.5. Configuration of multiple numerologies (extracted from [MMMA17]).

There are two schemes in 5G-NR that support multiple numerologies within the same carrier bandwidth, FDD and TDD. Due to adjacent frequency resources being used at the same time in FDD there is inter-numerology interference, while in TDD it does not exist since each Transmission Time Interval (TTI) segment has its own, single, numerology. On the other hand, FDD has a higher flexibility scheduling MTs due to a wide range of subcarriers, while TDD is limited to a specific set of subcarriers decreasing, thus its scheduling flexibility. The major impact TDD has, due to its flexibility limitation, is at the level of system latency. The number of OFDM symbols depends on two aspects – the subcarrier spacing and the cycle prefix (CP) in use. For a set of numerology configurations, its characteristics are defined in Table 2.1, such as the number of OFDM symbols per slot, the number of slots per frame and per sub-frame.

Table 2.1. Characteristics for a set of numerologies (based on [3GPP17a]).

μ	$N^{slot}_{OFDM\ symb}$	$N^{frame,\mu}_{slot}$	$N^{subframe,\mu}_{slot}$	Cycle Prefix
0	14	10	1	Normal
1		20	2	
2		40	4	
3		80	8	
4		160	16	
2	12	40	4	Extended

The elementary modulation schemes 5G-NR is expected to support are QPSK, 16QAM, 64QAM and 256QAM, supporting code rates between 1/3 and 8/9. The resource grid allocation in 5G-NR depends on the numerology in use, as described in Table 2.2, although the number of subcarriers per PRB is 12, regardless of the numerology.

Table 2.2. Number of RBs for a set of numerologies (based on [3GPP17a]).

μ	Downlink		Uplink	
	Min	**Max**	**Min**	**Max**
0	20	275	20	275
1				
2				
3				
4		138		138

In the context of RAT infrastructures, as stated by [NGMN15], two configuration schemes are forecasted for 5G radio-access technology, single-unified RAT (SU-RAT) and multiple RATs (M-RAT).

SU-RAT is the ideal for long term network development, as operators avoid the management of multiple access network configurations, and it can be optimised for different frequencies, as well as use cases, through parameter configuration of common air interface (AI). It builds on a minimum group of defined 5G features for a diversity of use cases. The challenge in SU-RAT is designing an AI with such degree of flexibility, while maintaining performance and efficiency over not only a wide range of frequencies, but also a wide range of use cases. Besides, SU-RAT may require re-farming of already existing spectrum by the introduction of a monolithic RAT.

The cost of migration to a SU-RAT in 5G must be carefully studied, since even if the new unit improves overall spectral efficiency, more techniques are needed beyond the simple re-farming of 4G spectrum. Therefore, aggregation with LTE/LTE-A will be a fundamental key aspect to achieve good performance in the initial migration phase to the SU-RAT. For operators without relevant investments in 4G network infrastructure, preference should not be given to a SU-RAT scheme.

M-RAT enables the integration of different AIs complementing each other and working as single unit. This scheme allows the operator to design and deploy at its own pace integrated services for a variety of use cases, demanding and requiring specific RAT characteristics. It is deemed to be technically easier

to achieve due to the independence of RAT modules, as well being more economically sounding especially for operators starting investment in 5G networks. For example, consider the possible M-RAT schemes:

- An optimised RAT for higher frequency bands (above 6 GHz) used in dense urban areas to provide capacity and high data rates, plus an optimised RAT for lower frequency bands (below 6 GHz) for coverage, due to limited coverage of former RAT.
- An optimised RAT designed to support ultra-low latency, or ultra-high reliability.

As reported by [NGMN15], due to the wide range of capabilities required to be developed for 5G, its network interface is expected to be comprised of more than one RAT. The established common ground is to have each RAT optimised for certain use cases, or for certain spectrum lot. However, one must pay attention not to consider unnecessary development of RATs to attend niche optimisations, as doing so would hinder RATs economy of scale development. The underlying approach is to have different RATs being defined as modes of operation of a single, unified RAT. At last, there have been proposed three possible technical migration paths from previous generations of mobile communications to 5G-NR, according to [NGMN15]. Assuming the best choice the M-RATs, the technical migration paths towards 5G are provided in Figure 2.6.

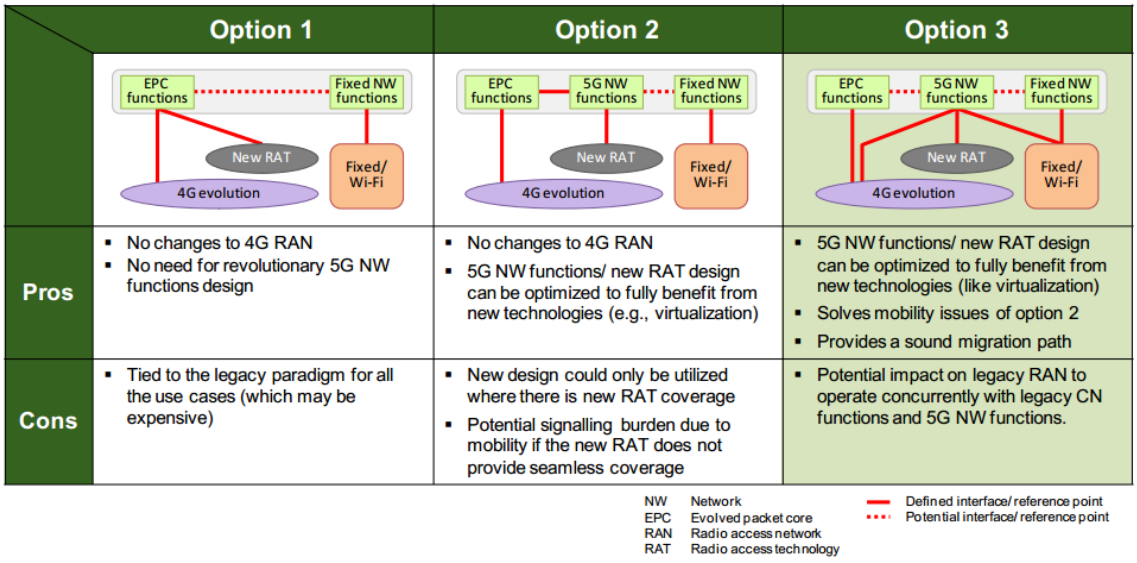

Figure 2.6. AT Interfacing options for 5G | NGMN (extracted from NGMN15).

Since this thesis proposes to deal with a green-field implementation approach, hence in agreement with [AM5G16], the interface option 3 (third) is the optimal one, since all RATs, e.g., 4G evolution can promptly benefit from 5G network functions, even in areas without (new) RAT coverage.

2.3 Coverage and Capacity

The main coverage and capacity characteristics for 5G-NR networks are provided in this section. The

main objective is to analyse the fundamental concepts in terms of modelling both coverage and capacity in the core of this thesis, in order to reach the number of required cells to cover a given geographical target area supporting a specific capacity and coverage requirement profile.

2.3.1 Coverage Overview

The main objective of coverage estimation is the computation of the site cell radius and consequently the number of cells. Therefore, the key element here are coverage distances, which are computed from the appropriate propagation models and the maximum path loss (MAPL) given by the radio link budget formulation.

According to [METIS17a], the frequency spectrum under consideration for 5G-NR networks spans from the 0.6 to 86 GHz frequency bands, with expected different deployment dates. This wide spectrum range has to do with different entities being interested in a wide range of devices to be served by 5G-NR. However in this thesis, one considers the initial spectrum bands that are considered for the first 5G field deployments, the cm-spectrum, specifically the 0.7 and 3.5 GHz frequency bands. Therefore, this thesis is focused on the propagation and coverage effects related to these frequency bands.

The cell radius is given by the distance parameter in the MAPL formulation, which is dependent on the propagation scenario (urban, suburban, rural), frequency band and other characteristics, such as the BS and MT heights. The generic formulation is defined in [Corr16]:

$$d_{max\,[\mathrm{km}]} = 10^{\frac{L_{p,max_{[\mathrm{dB}]}} - L'p_{[\mathrm{dB}]}}{10\,\alpha_{PD}}} \tag{2.3}$$

where:

- $L_{p,max}$: maximum path loss (MAPL) given by the link budget computation;
- L'_p: path loss given by the sum of the outdoors and indoors path loss;
- α_{PD}: average power decay (model and configuration dependent);

Compared to the previous generation of mobile communications, LTE/4G, and according to [ADRA17], 5G networks are expected to provide not only higher data rates to users, but also more access at anytime and anywhere. Thus, in 5G path loss estimation plays a crucial role, even more if one considers that around 80% of mobile traffic is generated inside buildings [Pire15]. The propagation models in use in this thesis are present in Table 2.3, for outdoors coverage estimation.

Table 2.3. Propagation Models for Outdoors Coverage Estimation.

Propagation Scenario	Frequency Band [GHz]	
	0.7	**3.5**
Urban	Okumura-Hata	WINNER II
Suburban		
Rural		

In outdoors propagation a heavy dependence on the signal frequency is expected. From literature research, a description for the models in use is done:

- **Okumura-Hata model** [MoLi11] – the standard model is an urban flat environment from which

correction factors are considered. It takes urban, suburban and open area scenarios into account from 1 to 20 km, with a BS height between 30 and 100 m and UE terminal height between 1 and 10 m. Its frequency range goes from 150 to 1 500 MHz, being a suitable model for the 700 MHz band;

- **WINNER II model** [WINN07] – it presents a variety of distinct propagation. For macro-cells it outputs valid results for urban, suburban and rural areas. It considers distances from 0.05 to 5 km and is based on having a BS height around 25 m and UE terminal height around 1.5 m;

Taking outdoors-indoors attenuation environments, studies have been performed to estimate typical penetration values in a wide range of frequencies, path loss that can then be added to the outdoors one into variable L'_p from (2.3), such as:

- **Experimental Indoors Path Loss Model** [HTZA16] – the work is based on field tests from Samsung and Nokia, consisting of an approximate for estimating this penetration loss on the premise of low and high-loss buildings, essentially given by the presence of strongly reflective surfaces, such as glass walls, including both 0.7 and 3.5 GHz bands;

It is possible to provide the best coverage with more power although at the cost of increased interference with adjacent areas using the same frequency, while on the contrary there is a strong possibility of blind spots and thus lack of coverage at cell edges. There is then the need to establish a compromise between path loss models and interference when designing a network for a frequency of 3.5 GHz.

2.3.2 Capacity Overview

The main objective of capacity estimation is to compute the number of required resources, defined in 5G-NR as *resource blocks* (RBs), which support the traffic profile in consideration within a certain quality of service (QoS), such as, for example, defining the maximum acceptable service throughput reduction of 10% in the case of capacity overload in the cell.

The initial, and maximum, number of users is given by the coverage estimation, from which the capacity estimation indicates if such users can be served with the required traffic profile. If there is cell capacity overload, the number of users is reduced through cell radius reduction, until or if there is possibility of the cell withstanding the required number of RBs. After this estimation, the final number of users in the cell and in the network can be computed. The throughput per user can be given by:

$$R_{b,user_{[\text{kbps}]}} = N_{RB/U} \cdot N_{SC/RB} \cdot N_{streams} \cdot N_{sym/SF} \cdot N_{bits/sym} \cdot \frac{1}{\tau_{SF_{[\text{ms}]}}} \quad (2.4)$$

where:

- $N_{RB/U}$: number of RBs per user;
- $N_{SC/RB}$: number of subcarriers per RB (12 in 5G-NR);
- $N_{streams}$: order of MIMO configuration;
- $N_{sym/SF}$: number of symbols per subframe;
- $N_{bits/sym} = \log_2 M$: number of bits per symbol;
- τ_{SF} : time of subframe;

As it can be seen in (2.4), if the MIMO configuration is assumed to be equal for all users, the remaining variables are fixed in the context of 5G-NR, and thus the conclusion is that the throughput per user is only dependent on the number of RBs each user has allocated to itself and the modulation curve in use, responsible for the number of bits per symbol.

Hence, if the global cell capacity is to be defined, it will depend on the total number of allocated RBs, the throughput per each RB, and the modulation in use at the RB, given by:

$$N_{users} = \left\lfloor \left(N_{RB} \cdot N_{SC/RB} \right) \cdot \frac{N_{sym/SF} \cdot N_{bits/sym}}{\tau_{SF_{[\mathrm{ms}]}} \cdot R_{b/user_{[\mathrm{kbps}]}}} \right\rfloor \quad (2.5)$$

There are essential elements that must be clear concerning the evaluation of cell capacity. The first is the signal-and-noise to interference ratio (SINR), essentially dependent on the MT distance to the BS, and the channel spectrum efficiency (SE), dependent on the level of quantisation. Both these elements will defined the appropriate modulation coding scheme (MCS) to be assigned to each user, which in 5G-NR is defined as from QPSK, 16-QAM, 64-QAM and 256-QAM. The implications of the MCS order can be defined as:

- **Lower MCS orders (m < 32):** more robust and tolerant to higher values of interference at the cost of lower transmission throughput, thus it performs better on low SNR;
- **Higher MCS orders (m > 64):** much higher transmission throughput at the cost of lower tolerance to noise and interference, and increased transmission and channel estimation errors.

Generically speaking, since radio spectrum resource management and optimisation is a fundamental concept in wireless communications, it is important to consider improvements in the field of spectrum efficiency. [WJSW17] states that advances in RF architecture, domain processing and network architecture are important steps towards a higher spectral efficiency, as well as improvements in physical layer technologies, such as multiple access scheme, channel coding scheme and waveform. This presents a key advantage of 5G towards 4G, since with an equivalent amount of spectrum. It can transmit a greater number of bits, leading to faster UE experienced bit rates.

In regard to carrier aggregation techniques, according to [LETM14] they are to provide the operator with the opportunity of combining and operating separate, often non-contiguous, blocks of spectrum as one block with the goal of maximising available and future spectrum, in order to provide a higher level of performance consistency. There are three configurations for carrier aggregation:

- **Contiguous frequency band:** carriers are contiguous and located within the same frequency band. In this case the MT can handle signals using a single trans receiver.
- **Non-contiguous frequency band | intra-band:** carriers are located within the same frequency bands, but they are not adjacent to each other. In this case the MT may require a separate transceiver for each carrier.
- **Non-contiguous frequency band | inter-band:** carriers are in different, distinct parts of the radio spectrum. It requires a transceiver for each carrier and the MT must operate in multiple bands at the same time. It is very useful for operators with limited or fragmented spectrum, though at the cost of increased system design complexity, cost and power consumption.

Due to a commercial competition for spectrum at lower bands, operators have often to use carrier aggregation techniques to make use of their non-contiguous frequency band. Although there have been successful tests in LTE-A with advanced carrier aggregation producing data rates up to 600 Mbit/s per user in controlled environments, they were based on higher MIMO order (8x8) and on limited/research spectrum, thus it does not and can not still apply to most of real-life deployments.

Regarding bandwidth in 5G-NR, the main difference with LTE (4G) is that 5G-NR will consider a single bandwidth of up to 100 MHz, whereas in LTE the maximum is 20 MHz, for single channels. Hence, this is a clear indicator of the potential of 5G-NR to achieve even higher data rates since with carrier aggregation, in the future, the maximum achievable bandwidth will be even considerably higher than those in LTE with the same techniques.

2.4 Services and Application Requirements

The main goal of this section is to analyse and define the main service and applications' requirements and characteristics in the context of expected 5G use-cases. In detail, the goal is to analyse the requirements in terms of throughput, latency and other relevant KPIs of services and applications, such as video streaming, augmented reality, Internet of Things (IoT) and self-driving cars.

The network development behind 5G networks has the objective of making possible the creation of a wide range of new and unique use cases to be deployed by operators, which were not yet available or efficient to implement in previous generations of mobile communications, such as with UMTS or LTE. Therefore, the current panorama for use cases can be split into three main groups [DTUG16]:

- **Enhanced Mobile Broadband (eMBB):** diverse services (download file, streaming), usually larger packets. It includes services such as virtual reality and infotainment for vehicles.
- **Massive Machine Type Communications (MMTC):** periodic communication, small packet size. It includes IoT services such as Smart Cities and Domotics.
- **Ultra-reliable and Low-Latency Communications (URLLC):** usually small packets, latency critical. It includes services such as communication between vehicles (V2V) and industry automation.

Nevertheless, service categories defined for previous generations of mobile communications are anticipated to still be supported by 5G networks, with the four classes of services defined by [3GPP15]:

- **Conversational Services** – voice and real-time multimedia messaging, it is the most delay sensitive service class due to bidirectional data flow.
- **Streaming services** – delay requirements are not as strict as in Conversational, since these have unidirectional data flow.
- **Interactive services** – web browsing, characterised by a single access, continuous or not, to a remote equipment containing data (e.g., website server).
- **Background services** – e-mail, SMS, databases download, reception of measurement

records, it is defined as the process of sending and receiving data in the background, with no specific time frame to be processed. It is the least delay sensitive service.

A more comprehensive description of these service categories can be seen in Table 2.4.

Table 2.4. Service class summary according to 3GPP (extracted from [3GPP15]).

Service Class	Conversational	Streaming	Interactive	Background
Real-time	✓	✓	×	×
Symmetry	✓	×	×	×
Throughput	Guaranteed		Non-Guaranteed	
Delay	Min. fixed	Min. variable	Mod. variable	Highly variable
Buffer	×	✓	✓	✓
Burst	×	×	✓	✓
Example	Voice/video call	Video streaming	Web browsing	SMS, E-Mail

From the three groups [DTUG16] and the service classes defined by [3GPP15], the KPIs for the main network services are defined from [Corr16] [Alco17] and [GOBR18], in Table 2.5.

Table 2.5. Throughput requirements (adapted from [Corr16], [AnJa15], [Alco17] and [GOBR18]).

Class	Service	Throughput [Mbit/s]			
		DL		UL	
		Min	Max	Min	Max
Conversational	VoIP	0.032	0.064	0.032	0.064
	Chat	0.064	0.384	0.064	0.384
Interactive	Video-streaming	1	90	1	90
	Web browsing & Social Media	1	10	1	5
	FTP	1	150	1	10
	P2P				
Background	E-mail	1	5	1	5

The definition of minimum and maximum throughput values per class service is established from QoS requirements in [AnJa15] for VoIP and Chat, while the remaining services are adapted from [Alco17] and [GOBR18], serving as an indicative recommendation. While video-streaming is a part of the *Interactive* class, a more detailed description of the service characteristics is presented in Table 2.6. [ANDR17] states there are many aspects (e.g., compression rate, variable based-on-network-conditions delivery quality, mobile cache) that can influence the actual experienced bit-rate, hence one considers an average and a recommended throughput for different levels of video quality as seen in Table 2.6.

Table 2.6. Video-streaming throughput requirements (based on [ANDR17], [NETF16] and [NBNC18]).

Quality	Resolution	Throughput [Mbit/s]		Data in 1 hour [GB]
		Recommended	Average	
Low	240p / 360p	< 1	0.7	0.32
Standard	480p	3	1.6	0.72
High-Definition	720p	5	2.0	0.90
	1080p	5	3.3	1.49
	2K	10	6.7	3.02
Ultra-High-Definition	4K	[15; 25]	15.6	7.02
	8K	[80; 100]	90	40.50

From Table 2.6 two analysis can be done. The first is in the actual context of video-streaming services available in the market, where it would be unlikely for a network to support service throughput values above the 10 Mbit/s, the threshold for 2K video, according to a study by [DEVA17] that states that the most common mobile screen resolution in the market in 2017 was 720p. Hence, the main advantage of the capacity increase in 5G systems would be merely the possibility of creating more capacity to support more users in the same geographical target deployment area. On the other hand, the second analysis considers the perspectives in future developments where the increase of mobile services through different user equipements are expected with screen resolutions up to 4 or 8K, though the trend points to the 1080p resolution as being the widespread resolution in the upcoming years, in streaming services such as Netflix and Amazon Prime. Nevertheless, as the network evolves and the user equipements associated to the industry development, screen resolutions above 1080p can become the standard with data-intensive applications such as smart-TV video-streaming hotspot or in the field of virtual reality (VR).

Regarding the use cases for IoT in 5G, [SMKS17] acknowledges the classification of the main applications into two classes, massive machine-type communications (**MMTC**) characterised by large numbers of low-cost devices with high requirements on scalability and increased battery lifetime, and ultra-reliable low-latency communications (**URLLC**), related to mission-critical applications, where uninterrupted and robust exchange of data is of utmost importance. According to [AVID16], based on a GSMA report, Figure 2.7 shows the main considered application profiles for IoT in 5G.

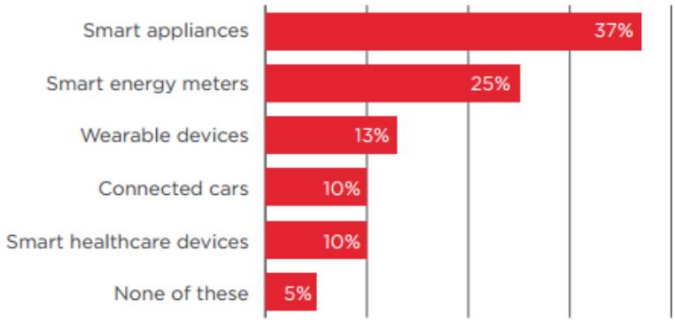

Figure 2.7. Main applications for 5G-based IoT (extracted from [AVID16]).

While the main IoT areas considered by [AVID16] are present in Figure 2.7, the sensor manufacturer Libelium (in [LIBE12]) presents a description of the main services and applications likely to be created or improved through IoT in 5G:

- **Domotics & Home Automation:** energy and water use, remote control appliances, intrusion detection systems, arts and goods preservation;
- **Healthcare:** patient fall detection, medical fridges, sportsmen care, patient surveillance, ultraviolet radiation;
- **Industrial control:** machine-to-machine (M2M) applications, indoor air quality, temperature monitoring, ozone presence, indoor location;
- **Logistics:** location tracking (indoors, outdoors), fleet management (e.g., airports, warehouses, delivery services)**;**
- **Smart Agriculture:** wine quality enhancing, green houses, golf courses, meteorological station network, humidity and temperature measurements;
- **Smart Cities:** smart parking, structural health, noise urban maps, smartphone detection, electromagnetic field levels, traffic congestion, smart lightning, waste management, smart roads;
- **Smart Environment:** forest fire detection, air pollution, snow level monitoring, landslide and avalanche prevention, earthquake early detection;
- **Smart Water:** potable water monitoring, chemical leakage detection, swimming pool remote measurement, pollution levels in the sea, river floods;

Regarding the extreme low-latency possibilities of 5G, [NETM18] considers that it might not actually be necessary for most IoT devices or applications, since for many IoT applications there is no need for strict time control, only for periodic communication over time. Some latency-critical applicational IoT applications requirements are set in Table 2.7.

Table 2.7. Characteristics for latency critical IoT applications (extracted from [SMKS17]).

Use Case	Latency [ms]	Update time [ms]	Device density [m^{-2}]	Range [m]	Mobility [km/h]	Location
Factory automation	[0.25; 10]	[0.5; 50]	[0.33; 3]	[50; 100]	< 30	Indoors
Precision Machinery	0.25	0.5				
Packaging machines	2.5	5				
Process automation	[50; 100]	[100; 5 000]	10 k /plant	[100; 500]	< 5	
Smart Grids	[3; 20]	[10; 100]	[10; 2 000]	< 1 000	0	Outdoors
Traffic safety urban[1]	[10; 100]	100	3 000	500	< 100	
Traffic safety highway[1]			500	2 000	< 500	

[1]Use case belongs to the Intelligent Transportation Systems (ITS) category;

The use cases presented in Table 2.7 are taken as the four most important use cases for latency critical

IoT applications, and are defined by [SMKS17] as:

- **Factory automation:** need for real-time control of machines and systems in fast production and manufacturing lines, e.g., high-speed assembly, packaging and palletising. These are highly challenging in terms of latency and reliability;
- **Process automation:** applications for monitoring and diagnosing industrial elements and processes, such as heating, cooling and pumping procedures. The nature of measured values for these applications change relatively slowly, therefore latency is not of highest importance.
- **Smart Grids:** have fewer restricting requirements both on latency and reliability compared to factory and process automation, however communication range can extend up to a few km;
- **Intelligent Transport systems (ITS):** characterised by autonomous driving and optimisation of road traffic. The key aspects in these applications are latency, reliability and moderate communication distance ranges.

In [UhSH17], self-driving cars services and applications are divided into three main segments, logistics, vehicle telematics and automotive insurance industries, as well as the transportation sector (e.g., self-driving vehicles in ports, airports, railways and shipping industries). There are two main categories of potential automotive solutions, according to the 5G-PPP classification in [CARS15]:

- **Wide-area infrastructure-based communications**: vehicle to network (V2N) communication, are likely to require a reliable, contiguous coverage. Preferable spectrum is set to be cm-waves;
- **Short-range user-based communications:** vehicle-to-vehicle (V2V), vehicle-to-infrastructure (V2I), vehicle-to-person (V2P). Focus on short-range and traffic-density scenarios, thus preferable spectrum should be mm-waves;

The main requirements are defined by 5G-PPP in terms of KPIs as latency, reliability, throughput, communication range, node mobility and device density. Since there is a wide range of applications and services in the context of self-driving cars, [CARS15] proposes some key metrics for some use cases, present in Table 2.8.

Table 2.8. Characteristics of V2X services (extracted from [CARS15]).

Service / Application	Latency [ms]	Reliability	Data rate [Mbit/s]
Automated overtake	< 10	$< 10^{-5}$	Low
Collision Avoidance	< 100		
High-density Platooning	< 10		

The KPIs provided in Table 2.8 must be achieved under certain conditions, such as distance and relative speed of transmitting and receiving vehicles. Therefore, not all conditions present in Table 2.9 are likely to be exist simultaneously, since the increase in some of the conditions may affect negatively or positively others, e.g., if vehicle density is increased it is likely the average vehicle speed will decrease, or if one considers a speed increase one should expect a longer communication distance.

Table 2.9. Conditions under which latency and reliability are achieved (extracted from [CARS15]).

Scenario	Vehicle density [/km^2]	Relative speed [km/h]	Communication range [m]
Urban	[1 000; 3 000]	[0; 100]	[50; 100]
Suburban	[500; 1 000]	[0; 200]	[100; 200]
Highway	[100; 500]	[0; 500]	[200; 1 000]

The main KPIs for some of expected use-cases in the context of 5G are presented in Table 2.10 following the works of [NGMN15] and [Pere17].

Table 2.10. Service requirements per use-case (extracted from [NGMN15] and [Pere17]).

Class	Use Case	Throughput [Mbit/s]		Latency [ms]	Device Density [km^{-2}]
		DL	UL		
eMBB	Ultra-high broadband access (V.R)	1 000	500	10	75 000
	Broadband access in dense areas	300	50	10	[200; 2 500]
	Broadband access in a crow	25		10	150 000
	50 Mbit/s in suburban scenario	50	25	50	400
	50 Mbit/s in rural scenario			50	100
	Mobile vehicular broadband			10	2 000
MMTC	Massive low-cost, long-range, low-power MTC	< 0.1	< 0.1	-	200 000
URLLC	Ultra-low latency	50	25	< 1	-
	Ultra-high reliability, ultra-low latency	[0.005; 10]	< 10	1	-

The metrics that are not defined in Table 2.10 are considered to be irrelevant for the associated use-case. The mobility metric represents the maximum speed at which the MT can be guaranteed by the network to be assigned the necessary throughput (both DL and UL) and latency requirements. The traffic and device density are related to a certain extent, the first consists of the cell capacity (throughput) per unit of area requirement per type of use-case, e.g., if an operator decides to deploy a broadband access in a dense area, it should offer 750 Gbit/s (DL) per every square kilometre of network field implementation. The second is a measure on the estimated number of users the cell can serve from the previous metrics (throughput, mobility, traffic density) depending on the network traffic profile, e.g., if many users are doing HD video-streaming at the same cell, but for short amount of time, the device density value can be higher than if it is for long periods of time.

The most relevant metrics for eMBB are the throughput and mobility tolerance, which take cell capacity and handover into analysis, while for MMTC the most relevant metrics are latency and mobility which can be dealt mainly with in the network architecture plane and in the handover planning. In the case of URLLC, there is a very strong emphasis on latency being as low as possible although in some use-cases the throughput is also very important.

2.5 State-of-the-Art

The main works of research and investigation from other authors regarding subjects related to coverage and capacity in 5G networks are provided in this section. Research is considered mainly from three sources, academic works, IEEE based literature and institutional research from entities such as METIS, 5G Americas, 3GPP or 5G-PPP. In terms of frequency band studies for cellular network design, literature research has been noted to consist essentially of three elements, the first on previous cellular network design studies for LTE networks from the 0.8 to the 2.6 GHz bands, the second on proposals for developing networks based on the mm-wave spectrum band (28 GHz) where additional propagation effects may provide usefulness when analysing the impact of 5G's 3.5 GHz band, and the third on early proposals for dealing with frequency band elements in 5G-NR such as numerology and propagation effects.

Starting with the works based on the first element, [Alco17] provides a comprehensive work on cellular network design for three LTE frequency bands (0.8, 1.8 and 2.6 GHz) in different propagation scenarios, with different traffic load profiles and service profile/share profiles, as well as having some elements that are transversal to early versions of 5G-NR deployment, such as the number of sub-carriers per RB (12). It is based on a number of works from other authors and serves as a key element in this thesis for the lower frequency band study of 700 MHz.

Regarding works based not only but mostly on the mm-wave spectrum, [Jian15] is focused on coverage, capacity and protocol design layers for mm-waves, basing the studies on features such as data-rate, latency, energy and cost requirements, as well the implications in terms of propagation characteristics, channel modelling, link outage scenarios and deployment configurations and scenarios. [Vihe16] has investigated characteristics of indoor coverage at high frequency ranges, but also focused on outdoor to indoor coverage modelling by adapting already existing models into a single one. [Anni17] has established methods for computing capacity and coverage solutions for mobile broadband in rural and remote areas at the mm-wave spectrum. [Jan16] has presented the case for propagation mechanisms at mm-waves and characterisation of wireless channels in site-specific and stochastic channel approaches, both for narrow and wideband configurations, proposing a method to estimate capacity provisioning.

[Hish16] has researched cell capacity implications in the context of mm-wave cellular networks, proposing a method based on a set of use cases' requirements and based on cell and device centric architectures, taking noise and interference conditions, cell association schemes, spectral efficiency and carrier aggregation into account. Still on capacity, [Chan16] has developed works for 5G cellular systems by proposing a methodology based on application workload requirements, such as outage probability and throughput, to create a network system model. Since massive MIMO will be, along with mm-waves, the main facilitator for much higher capacity in 5G, [Tian16] has been found to provide a comprehensive study on massive MIMO and mm-wave coverage and capacity implications in the context of 5G cellular networks.

[3GPP17b] has compiled the most comprehensive studies made on coverage for a wide spectrum

range, including both cm and mm-waves. The methodology is based on aspects such as characterisation of scenarios, antenna modelling, different types of pathloss, fast fading and other additional modelling components, and the main works on channel models are described:

- METIS - has proposed 5G requirements in terms of frequency range, bandwidth, massive MIMO and polarisation modelling, and performed channel measurements at various bands between 2 and 60 GHz with different channel model methodologies, map, stochastic and hybrid models, covering a wide variety of scenarios.
- ITU-R M and NYU Wireless have performed studies in propagation and atmospheric loss on mm-waves, focusing on dense urban environment, proposing characterisation in the context of blockage modelling, wideband power delay profiles and physics-based path loss model.
- mmMAGIC has undertaken channel measurements in the 6 to 100 GHz range, while IMT-2020 is doing similar work based on China.

In broader terms, regarding general 5G network schemes, MiWEBA is focused on the study of millimetric waves in the access radio, fronthaul and backhaul contexts, in a variety of scenarios. The group has performed analysis on the use of mm-waves in micro-cells for dense radio-access areas in indoors and outdoors, to infer the technical feasibility of network increase capacity. The Fantastic 5G project has researched the primary key indicators needed to be achieved to improve capacity, coverage, reliability and latency for networks operating below 6 GHz, based on LTE E-UTRAN for model simulations. The Sungkyunkwan University of South Korea has developed a model that computes capacity and coverage for millimetric waves in the 27 GHz band, in an urban scenario. The Polytechnic University of New York has presented a project on the implementation of mm-waves for future 5G networks, having as underlying modelling interface an open source software NS-3, capable of simulating 5G-network parameters with a 1 GHz bandwidth.

At last, the works that relate more to the frequency spectrum in the scope of this thesis and network characteristics, such as numerology or MIMO, [ERIC18a] presents a simplified but comprehensive overview on 5G deployment considerations, from use-cases to frequency bands' implementation roadway, as well as interoperability architectures with LTE core network. [HTZA16] proceeds to study the requirements for new channel models, from frequency bands, bandwidth, types of antenna arrays, mobility and handover issues, as well as presenting an experimentation and validation method for typical outdoors propagation scenarios in micro and macro-cells and outdoor-to-indoor penetration loss. For this method, it considers elements such as signal blockage, path loss models and shadow fading.

[YaAr17], [YaAr18a] and [YaAr18b] agglomerate studies on different perspectives regarding the multi-numerology schemes in 5G-NR, based on a number of technical configurations such as the power difference for edge users of different numerologies, being an early technique in the numerology-management context, through the use of allocation fairness. Similar work on the numerology field is presented by [DGDR18] and [YLPY18]. Concerning experimentation on the 3.5 GHz band propagation effects and MIMO antennas, there have been field trials by [ERIC18b], [LiSL18] and [BSCW16], the last one proposes an antenna configuration allowing for MIMO configuration in small devices for 3.5 GHz

Chapter 3

Models and Simulator Description

A description of the models used in this thesis is provided in this chapter, in which their mathematical formulation and implementation are detailed. At the end of this chapter, a brief assessment of the developed simulator is done.

3.1 Scenarios Development

This section provides the characteristics of the scenarios to be considered in this thesis, focusing primarily on the spectrum bands and propagation scenarios.

A considerable number of spectrum regions for 5G are currently being considered, at both the cm-wave (e.g., 700, 3 500 MHz) and the mm-wave spectra (e.g., 28 GHz) [AM5G17], in terms of technical and economic feasibility. Due to the very different and complex nature of mm-wave propagation and economic implications in terms of operator network configuration, such as with the need for much denser base station scheme, mm-waves are unlikely to be the first choice in early 5G deployment phases.

The main objective is to study the coverage and capacity implications in different scenarios for the cm-wave spectrum, the most likely spectrum to be considered in first network deployments, more specifically in the 0.7 and 3.5 GHz bands. The former will provide MTs general access to the network, while the latter will be able to provide MTs with higher data rates from larger bandwidth allocation or higher MIMO orders. Regarding the possibility of using MIMO at these frequencies, Table 3.1 shows the highest achievable MIMO order for different MT devices from (3.1) where the number of antennae is the rounding to the closest multiple of 2.

$$N_{antennae} = \left\lceil d_{[\mathrm{m}]} / \frac{c_{[\mathrm{m/s}]}}{f_{[\mathrm{Hz}]}} \right\rceil \quad (3.1)$$

where:

- d: device distance (length or width);
- c: speed of light;

Table 3.1. Maximum number of antennas per equipment dimension.

Equipment	Dimensions [cm]		Frequency [MHz]			
			700		3 500	
	Length	Width	Length	Width	Length	Width
Waspmote sensor[1]	12	12	-	-	2	2
Smartphone	7	14	-	-	-	2
Tablet	24	19	-	-	2	2
V.R glasses	21	9	-	-	2	2
15” Laptop	32	21	-	-	4	2
Car roof (A.V)	125	100	2	2	14	12
Bus roof (A.V)	220	140	6	4	26	16

[1]A general-purpose sensor device from IoT manufacturer Libelium [LIBE18]

From Table 3.1 it is possible to formulate the observations based on the most common devices to be supported in 5G networks. For devices such as smartphones, tablets or laptops, in most cases even at the 3.5 GHz band it will not be possible to assure a MIMO configuration higher than 2x2, posing a serious limitation for the very high throughput values normally referred for 5G deployments. In the case of very high throughput-demanding devices, such as in the context of virtual reality (e.g., Samsung Gear V.R

glasses) or autonomous vehicles' devices (e.g., vehicle rooftop serving as antenna for infotainment), in the first the requirement for high throughput may not be sufficiently met with the maximum MIMO order of 2x2 at 3.5 GHz, while for the second there is the possibility of achieving interesting MIMO orders, especially at the 3.5 GHz band, for cases such as V2V communications or infotainment. Even in difficult propagation scenarios, at the 0.7 MHz band achieving up to 4x4 MIMO in a bus/train scenario is feasible.

In what concerns the present commercial, military or other spectrum usage at the two bands mentioned, the 700 MHz band has been issue of a frequency refarming initiative from the European Union in 2018 [ANAC18] to guarantee an available band to 5G mobile communications by 2020 while the 3 500 MHz band is currently on the process of being opened from previous satellite and non-licensed services, according to [MEDI18]. In some countries, such as the United Kingdom, spectrum auctions are currently being held for the 700 and 3 500 MHz bands [5GCO18]. Regarding the frequency bands and bandwidths for early 5G-NR, they have been defined for the 700 MHz band, although for the 3 500 MHz the specific and differential values (DL, UL) are still to be defined officially, present in Table 3.2.

Table 3.2. 5G-NR Frequency Bands (extracted from [3GPP17c]).

Band [MHz]	NR Band	UL band [MHz]		DL band [MHz]		Duplex Mode	Bandwidth [MHz]	
		Min	Max	Min	Max		UL	DL
700	n28	703	748	758	803	**FDD**	45	45
3 500	n78	3 300	3 800	3 300	3 800	**TDD**	500	500

In most countries the main band for the 700 MHz spectrum usage will be the n28 NR-band [5GCO18], whose maximum available bandwidths have already been defined by 3GPP (45 MHz per channel). For the 3 500 MHz band, the maximum available bandwidth value per channel has not yet been fully defined by 3GPP although a total available bandwidth of around 500 MHz is expected to be the norm. Although in the context of this thesis the distinction is of no relevant effect, it may be important to note the 700 MHz band will be FDD based while the 3 500 MHz band will be TDD based.

The main propagation scenarios to be examined are urban, suburban and rural for the cm-wave spectrum (700 and 3 500 MHz), whose main differences consist of the presence and distribution of obstacles, the density of buildings and the density of users. Besides the geospatial distribution, the model will consider an empirical measure of traffic density fluctuation throughput the day with the ROM configuration metric (Residential, Office, Mixed).

3.2 Model Development

This section provides the description of the models developed during this thesis, focusing primarily on their mathematical formulation. The main objectives are to describe the model generically, define the model inputs and outputs and which propagation models are to be used.

The model dimensioning should be as objective and detailed as possible, while also permitting changes in input parameters for different network deployment configurations. This process can be seen as a high-level approach to network dimensioning, where by the use of propagation models and specific algorithms it is possible to produce an output solution with an acceptable degree of accuracy.

The input and output parameters are generically described in the next section, as well as the propagation models used for coverage planning. The most relevant models for coverage and capacity are defined in the next section. Besides these essential elements for cellular network planning there is the traffic density/volume and share/mix profile throughout a typical load day.

From the input parameters the first step is to compute the maximum cell distance through link budget and propagation models, given the reference throughput, then to define the maximum network load, from the traffic profile, which produces an estimation cell radius for the different propagation scenarios from which the cell density configurations are retrieved, as seen in Figure 3.1.

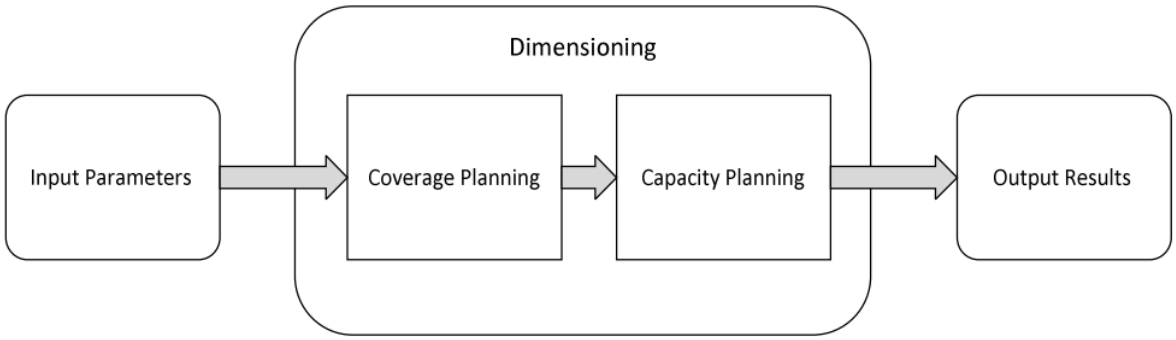

Figure 3.1. Generic network dimensioning (extracted from [Alco17]).

The main parameters considered in this thesis are segmented both in the capacity/coverage metrics and in the network/MTs perspective [Table 3.3].

Table 3.3. Capacity and coverage metrics for network and UE perspective.

Metrics	Parameters	
	Network	**MTs**
Capacity	Device/connection density, throughput, cell size, latency	Throughput, latency, traffic volume profile
Coverage	Propagation scenario, penetration losses, cell size, obstructions	Signal strength, mobility

While there may exist the same parameter in the capacity and coverage field, its meaning is not necessarily the same. For example, a macro-cell could be a suitable solution for coverage purpose while femto-cells could be the most adequate solution to support or increase network capacity in the same coverage area. On the other hand, it is the received power at the MTs that will define their access to the network, but it is through network capacity that MTs can achieve certain parameters.

The fundamental model inputs and outputs are defined in Figure 3.2. Besides these, there are others

specifically relevant to 5G-NR network deployments, such as the numerology configuration and the maximum supported MIMO order. Although not considered in the early model development in this thesis, latency requirements could be added at a later stage. In this case, after having computed the cell radii and density for different propagation scenarios, it could very well be useful to consider the work from [Silv16] for estimating backhaul infrastructure to support certain latency requirements.

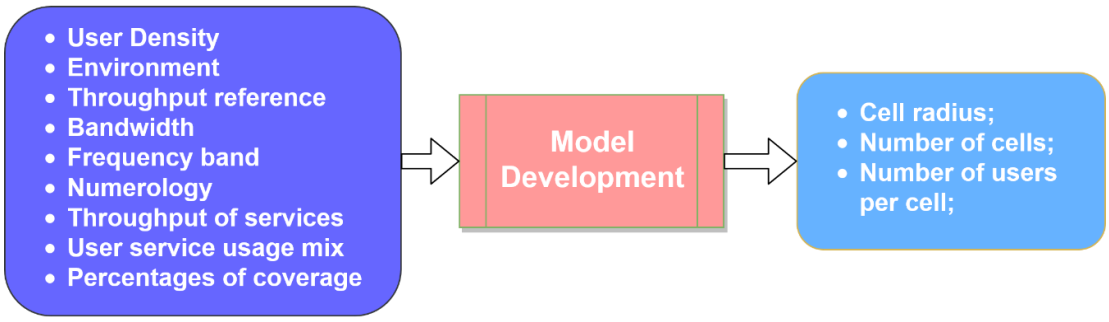

Figure 3.2. Model development input/output dimensioning (adapted from [Alco17]).

The main output will be the number of base stations in the target area, given by the cell radius computed at the level of coverage and/or capacity evaluation. The former has predominance in terms of network planning over the latter, except for when network capacity is exceeded – then the predominant value is the capacity computed cell radius. Nevertheless, it is from capacity evaluation that the metrics of throughput and maximum number of users are determined.

The fundamental aspects on the propagation model characteristics is presented Table 3.4. The goal is to, essentially, have an outdoors propagation model for both frequency bands (Okumura-Hata for the 0.7 GHz and WINNER II for the 3.5 GHz frequency band) and an indoors model that accepts both frequency bands. The outdoors models are valid for the three propagation scenarios (urban, suburban, rural) while the indoors one is an empirical and site-generic model, meaning it is an abstraction based only on the fact if the main wall to be crossed represents a high or low-loss material.

Table 3.4. Generic description of considered propagation models.

Environment	Propagation Model	Propagation Scenario			Band [GHz]	
		U	SU	R	0.7	3.5
Outdoors	Okumura-Hata	✓	✓	✓	✓	×
	WINNER II	✓	✓	✓	×	✓
Indoors	Experimental Indoors	✓	✓	✓	✓	✓

3.3 Dimensioning Process

The goal of this section is to describe the complete dimensioning process of the cellular network that outputs the estimation for the total number of cells required to cover the target area from a given traffic profile load. This dimensioning process is split into coverage, capacity and cellular levels.

3.3.1 Coverage Planning

Coverage planning is defined by the radio link budget evaluation for both channels, DL and UL, with no specific concern on the capacity or quality of service [Alco17]. From the link budget evaluation, the maximum allowed path loss (MAPL) can be computed based on the required SNR value at the MT, which depend on the reference throughput at the cell edge. With the appropriate propagation model, it is then possible to compute the cell radius and area, and for each municipality, the total number of cells is generated and computed for the global geographical target area.

In the link budget, the essential parameters are related to power (transmission), gains (transmission, reception) and other elements, such as cable or user losses. In the outdoors propagation models the core parameters are the frequency band (0.7 or 3.5 GHz), the propagation scenario (urban, suburban, rural) and the BS/MT antenna heights.

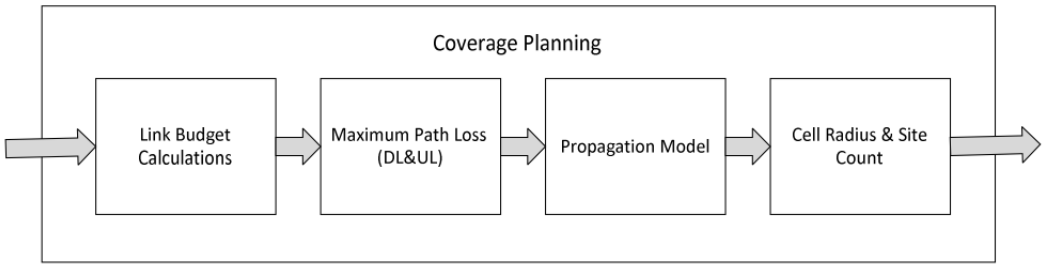

Figure 3.3. General coverage planning process (extracted from [Alco17]).

The different propagation models for the urban, suburban and rural scenarios and the general radio link budget formulations are defined in Annex B.1. Radio Link Budget. Despite the extensive model description in the annexes, the most relevant equations are described in this section. The main formulation of the radio link budget can be expressed as a function of the maximum path loss from the transmitting power, transmitter and receiver gains as well as the receiver power in (2.3). Besides the link budget computation, the received power for coverage estimation is mainly defined by the receiver sensitivity power, which is given by (3.2) having the specific 5G-NR numerology present in the bandwidth per RB:

$$P_{Rx,min_{[\mathrm{dBm}]}} = -174 + 10 \cdot \log(B_{RB_{[\mathrm{Hz}]}}) + F_{N_{[\mathrm{dB}]}} + \rho_{N,min_{[\mathrm{dB}]}} \quad (3.2)$$

where:

- B_{RB}: bandwidth per RB (SCS of 15, 30 or 60 kHz, per subcarrier);
- F_N: noise figure of the receiver;
- $\rho_{N,min}$: SNR requirement for a given throughput;

Assuming a constant noise figure and SNR, the effect on changing the numerology bandwidth is represented by a variation in the sensitivity power, which in turn changes the MAPL, that is to say, as the SCS increases the required minimum sensitivity power increases. Therefore, the numerology that offers the maximum coverage distance is the one that minimises the sensitivity power, which can be achieved with the subcarrier spacing value of 15 kHz (numerology 0).

This is especially important in the throughput at the cell edge evaluation, where a maximum percentage

of RBs allocated to the cell edge is defined to ensure that there is always a nominal throughput available at this region. Since in 5G-NR there can be mixed numerologies within the cell and that each numerology will have a maximum, different, coverage distance (due to the higher sensitivity value), the model assumes the numerology with higher coverage distance to compute the share of RBs, and then estimates if the available throughput level matches the throughput requirement at the cell edge. After selecting the suitable SCS configuration for coverage purposes, the MAPL is computed, and from the appropriate propagation models, the distance from the BS to the cell edge can be obtained from the relationship between the distance, maximum path loss (MAPL) and the propagation model parameters/values. The formulation for the indoors model is given by Table 3.5.

Table 3.5. Model equations for indoors scenarios (0.7 and 3.5 GHz).

Scenario	Experimental Indoors Path Loss
All	$\Delta L_{p_{[\mathrm{dB}]}} = 10\log(A + B \cdot f_{[\mathrm{GHz}]}^2)$

The distance formulation provided by the propagation models concerning outdoors propagation are defined in Table 3.6 and Table 3.7. It should be noted that every distance and path loss equation for every model has its standard deviation and limited range of values, on antenna heights, minimum distances (breakpoint) or others, which are considered in Annex B.

Table 3.6. Model equations for different scenarios for the 0.7 GHz frequency band (outdoors).

Scenario	Okumura-Hata equations
Urban	$L'_{p_{[\mathrm{dB}]}} = 69.55 + 26.16 \cdot \log(f_{[\mathrm{MHz}]}) - 13.83 \cdot \log(h_{BS_{[\mathrm{m}]}}) - \alpha(h_{mt_{[\mathrm{m}]}})$
	$\alpha(h_{m_{[\mathrm{m}]}}) = [1.1 \cdot \log(f_{[\mathrm{MHz}]}) - 0.7] \cdot h_{m_{[\mathrm{m}]}} - [1.56 \cdot \log(f_{[\mathrm{MHz}]}) - 0.8]$
Suburban	$L'_{p_{[\mathrm{dB}]}} = 69.55 + 26.16 \cdot \log(f_{[\mathrm{MHz}]}) - 13.83 \cdot \log(h_{BS_{[\mathrm{m}]}}) - \alpha(h_{mt_{[\mathrm{m}]}}) - 2 \cdot \log\left(\frac{f_{[\mathrm{MHz}]}}{28}\right)^2 - 5.4$
	$\alpha(h_{m_{[\mathrm{m}]}}) = [1.1 \cdot \log(f_{[\mathrm{MHz}]}) - 0.7] \cdot h_{m_{[\mathrm{m}]}} - [1.56 \cdot \log(f_{[\mathrm{MHz}]}) - 0.8]$
Rural	$L'_{p_{[\mathrm{dB}]}} = 69.55 + 26.16 \cdot \log(f_{[\mathrm{MHz}]}) - 13.83 \cdot \log(h_{BS_{[\mathrm{m}]}}) - \alpha(h_{mt_{[\mathrm{m}]}}) - 4.78 \cdot \log(f_{[\mathrm{MHz}]})^2 + 18.33 \cdot \log(f_{[\mathrm{MHz}]}) - 40.98$
	$\alpha(h_{m_{[\mathrm{m}]}}) = [1.1 \cdot \log(f_{[\mathrm{MHz}]}) - 0.7] \cdot h_{m_{[\mathrm{m}]}} - [1.56 \cdot \log(f_{[\mathrm{MHz}]}) - 0.8]$
All	$\alpha_{PD} = \frac{44.90 - 6.55 \cdot \log\left(h_{BS_{[\mathrm{m}]}}\right)}{10}$

One uses:

- h_{BS}: height of base-station;
- h_m: height of mobile terminal;
- f: carrier frequency;

Table 3.7. Model equations for different scenarios for the 3.5 GHz frequency band (outdoors).

Scenario	WINNER II equations
Urban	$L'_{p[\mathrm{dB}]} = 31.46 + 5.83 \cdot \log(h_{BS_{[\mathrm{m}]}}) + 23 \cdot \log(\frac{f_{[\mathrm{GHz}]}}{5})$
	$\alpha_{PD} = \frac{44.9 - 6.55 \cdot \log(h_{BS_{[\mathrm{m}]}})}{10}$
Suburban	$L'_{p[\mathrm{dB}]} = 34.46 + 5.83 \cdot \log(h_{BS_{[\mathrm{m}]}}) + 23 \cdot \log(\frac{f_{[\mathrm{GHz}]}}{5})$
	$\alpha_{PD} = \frac{44.9 - 6.55 \cdot \log(h_{BS_{[\mathrm{m}]}})}{10}$
Rural	$L'_{p[\mathrm{dB}]} = 55.4 - 0.9 \cdot (h_{m_{[\mathrm{m}]}} - 1.5) + 21.3 \cdot \log(\frac{f_{[\mathrm{GHz}]}}{5}) + 0.13 \cdot (h_{BS_{[\mathrm{m}]}} - 25)$
	$\alpha_{PD} = \frac{25.1 - 0.13 \cdot (h_{BS_{[m]}} - 25)}{10}$

Since the considered model for indoors presents only the mean value depending on frequency and a low/high material penetration loss, the values for their standard deviations are approximated from the values considered in [Corr16] for the LTE frequencies of 0.8, 1.8 and 2.6 GHz, in Figure 3.4, for the frequencies of 0.7 and 3.5 GHz. Regarding outdoors, the value is based on [Alco17] with 6 dB for rural and 8 dB for suburban and urban environments. Having defined the mean, standard deviation and coverage probability, the slow fading margin is then computed from the inverse CDF of the Log-Normal Distribution. The standard deviation interpolation from Figure 3.4 is taken as equivalent to the high-loss configuration in the indoors model considered in this thesis, while for the low-loss the same values considered for the outdoors are taken, which are usually much lower.

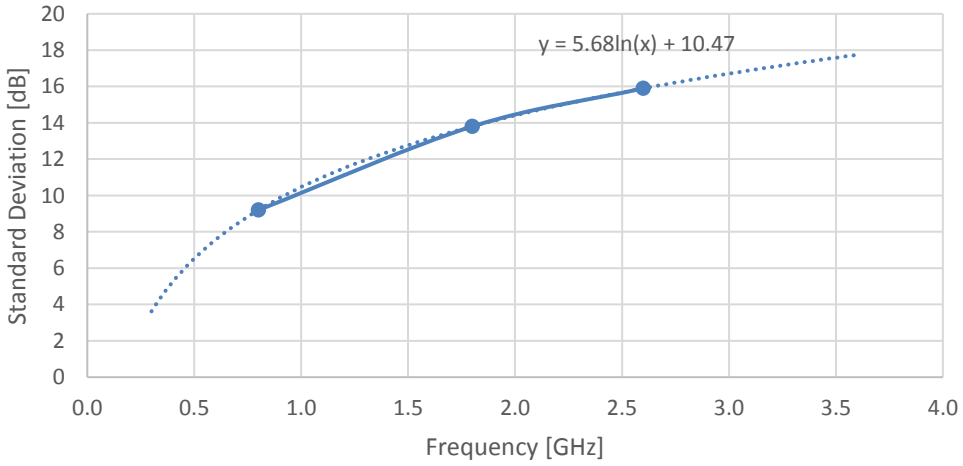

Figure 3.4. Indoor standard deviation interpolation (based on [Corr16]).

Although this interpolation may pose some limitations in terms of validity, in relative terms the standard deviation of path loss value should always be higher in urban/suburban high-loss scenarios than in rural low-loss ones, which is the underlying assumption for the chosen values.

3.3.2 Capacity Planning

After having computed the coverage distance (cell radius/area), capacity evaluation steps in. If the coverage-computed area suffices to fulfil capacity requirements, then no addition is made on planning, otherwise if it does not suffice to deliver the required capacity, the number of cells is re-computed to achieve capacity requirements. From the maximum cell radius, the initial, total, number of users inside the cell can be computed from:

$$N_{users,cell} = \lfloor \eta_{[\text{users/km}^2]} \cdot S_{[\text{km}^2]} \rfloor \quad (3.3)$$

where:

- η: user density in the target area;
- S : total area of coverage;

Capacity dimensioning considers the typical hexagonal shape, but for illustration purposes a uniform circular distribution of users is shown in Figure 3.5. The total number of users in a cell is given by the sum of users served by each modulation (from QPSK to 256-QAM), which fits right if the traffic profile consists strongly of mobile broadband services:

$$N_{users,cell} = \sum_{k=1}^{4} N_{users,area}^{4^k-QAM} \quad (3.4)$$

where:

- $N_{users,area}^{4^k-QAM} = \left\lfloor N_{users,cell} \cdot \frac{A_{4^k-QAM}}{A_{Cell}} \right\rfloor = \left\lfloor N_{users,cell} \cdot \frac{R^2_{4^k-QAM} - R^2_{4^{k+1}-QAM}}{R^2_{QPSK}} \right\rfloor$ (3.5)

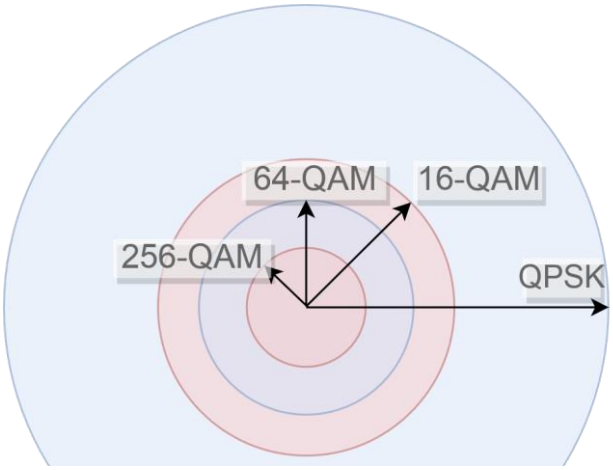

Figure 3.5. Modulation schemes distribution in cell.

The different radii for the different modulations are given by the minimum and maximum SINR values associated to each MCS region through the SNR/throughput relationship, available in Annex A. From these radii the number of users per MCS region is computed through the percentage of area each region has, in relation to the total cell area. By taking user traffic profile requirements into account, some cells are prone to saturate more easily than others. Besides, the traffic profile throughout the day can fluctuate and this is represented in the different mix share for each service based on three environment types, Residential, Office and Mixed (ROM). The capacity planning process estimates then the number of necessary RBs to support the traffic profile with a certain level of QoS.

A novelty factor in 5G-NR capacity planning, relative to LTE, is the concept of numerology, which is related to different subcarrier spacing configurations. The available numerologies for the spectrum considered in this thesis are shown in Table 3.8, where the bandwidth is computed in (3.6).

Table 3.8. Numerology distribution and associated bandwidth (based on [3GPP17a]).

Band [GHz]	μ	RBs		SCS [kHz] (12/carrier)	Bandwidth [MHz]	
		Min	Max		Min	Max
< 6	0	20	275	15	3.6	49.5
	1			30	7.2	99
	2			60	14.4	198

Also, 5G-NR networks are expected to support a mixed numerology configuration in order to present a more efficient RB allocation. However, if one considers a single numerology in the cell, the global cell bandwidth can be defined by (3.6) from [3GPP17c].

$$B_{W_{[\mathrm{MHz}]}} = N_{RBs} \cdot N_C \cdot N_{SCS} \cdot B_{W,SCS_{[\mathrm{MHz}]}} \quad (3.6)$$

where:

- N_{RBs}: number of resource blocks for a given numerology;
- N_C : number of carriers being served to the MT (typically one);
- N_{SCS} : number of subcarriers in 5G-Nr (12);
- $B_{W,SCS}$: subcarrier bandwidth for a given numerology;

There is a specification in Table 3.8 that the maximum number of RBs a cell can handle at the same moment is 275. However, the number of RBs depends on the frequency band, SCS configuration and available bandwidth at the cell, mainly due to the presence of non-static guard bands as the SCS configuration changes or the bandwidth increases. Hence, 3GPP has defined the maximum number of RBs per configuration, present in Table 3.9.

Table 3.9. Valid RB configurations (extracted from [3GPP17c]).

Band [MHz]	SCS [kHz]	Bandwidth [MHz] (max formula / max allowed)								
		5	10	15	20	40	50	60	80	100
700	15	25	52	79	106	(216) [1]	(270) [1]	×	×	×
	30	(11) [1]	24	38	51	(106) [1]	(133) [1]	(162) [1]	(217) [1]	(273) [1]
	60	×	(11) [1]	(18) [1]	(24) [1]	(51) [1]	(65) [1]	(79) [1]	(107) [1]	(135) [1]
3 500	15	×	52	×	106	216	270	×	×	×
	30	(11) [1]	24	(38) [1]	51	106	133	162	217	273
	60	×	11	(18) [1]	24	51	65	79	107	135

[1]maximum RB per SCS configuration can be defined, but bandwidth configuration is not valid according to 3GPP, × : configuration does not exist in 5G-NR according to 3GPP

Despite extensive and comprehensive literature from 3GPP on defining valid and invalid bands plus SCS and bandwidth configurations, two major clarifications can be made at this point. The cells in white with a number of RBs are configurations 3GPP states they can be defined but very unlikely to be

supported in real-life cells, since for example, in the 700 MHz band the total available bandwidth is expected to be around 45 MHz, possibly to be divided amongst different operators. The cells in white with a cross either means that the configuration is not efficient and thus the number of RBs hardly reaches the minimum of 20, or that for the given configuration the maximum number of RBs exceeds the maximum value of 275 RBs per cell. For the other white crossed cells, 3GPP has defined them as not suitable for the moment.

It is important to clarify some effects on using different numerologies. Table 3.10 presents a concise description of the main metrics regarding the SCS considered in this thesis, but it is in the throughput that the most important metric is found and used throughout the work. In Annex A, the throughput per RB is computed and defined for the different modulation schemes (from QPSK to 256-QAM) for the 15 kHz configuration (numerology 0).

Table 3.10. SCS network and propagation main characteristics (based on [ShTe18]).

Metrics	Subcarrier Spacing [kHz]		
	15	30	60
Noise tolerance	Low	Medium	High
Range/distance	**Large/Wide**		**Small / Short**
Spectral efficiency	Higher		Lower
Throughput	**Small**		**High**
Latency	**Higher**		**Lower**

Regarding the throughput per RB for the 30 and 60 kHz options, the increase in throughput is assumed to be theoretically 2, although in practice as the SCS increases the band guards increase, hence it is very much possible the multiplying factor from the 15 to 30 is higher than for the 30 to 60.

The concept of MCS region in this thesis is linked to a region with a minimum and maximum SNR value in which the maximum throughput curve is given by a certain MCS, but where users in this region can also be served with lower order MCS, seeking to maximise the number of allocated users in an efficient manner, e.g., $N_{U,cell\_64QAM}$ means the total number of users in a region in which the maximum throughput is given by the 64-QAM modulation, but users can be served with lower order MCS, such as QPSK.

The cell capacity depends on the available bandwidth and on the bandwidth required to serve the MTs. The higher the available bandwidth, the higher the traffic level the cell can support. Besides, the average throughput per resource block is higher for higher order modulation schemes. This means that 256-QAM requires less RBs than QPSK, for example for the same service and throughput, and thus less bandwidth. The average number of required resource blocks per user, for each service and modulation, is defined in (3.7).

$$\overline{N_{RB,user,k}} = \left\lfloor \frac{\overline{R_{b,user,k_{[\mathrm{Mbit/s}]}}}}{\overline{R^{m}_{b,RB_{[\mathrm{Mbit/s}]}}}} \right\rfloor \tag{3.7}$$

where:

- $\overline{R_{b,user,k}}$: average throughput per user, per service *k*;

- $\overline{R_{b,RB}^{m}}$: average throughput per RB, per modulation *m*;

As it can be observed in Figure 3.5, there is a segmentation of users for each modulation scheme. The number of required RBs per MCS region is naturally different, since both the average throughput per RB and the number of users in each one is different. The number of resource blocks necessary per modulation scheme for a cluster of services can be defined as in:

$$\overline{N_{RB,required}^{m}} = \left\lfloor \sum_{service\ i}^{N} \overline{N_{RB,user,k}} \cdot N_{U,cell}^{m} \cdot P_{u[\%]}^{s} \right\rfloor \tag{3.8}$$

where:

- $\overline{N_{U,cell}}$: number of users served by modulation *m*;
- P_u^s : percentage of users using/subscribing service *s*;

For a single cell, the total number of resource blocks is simply the sum of RBs of each MCS region, defined as in:

$$\overline{N_{RB,required}} = \left\lfloor \sum_{k=1}^{4} \overline{N_{RB}^{4^k-QAM}} \right\rfloor \tag{3.9}$$

where:

- $\overline{N_{RB}^{4^k-QAM}}$: number of RBs required for a given MCS region (QPSK to 256-QAM);

The total number of required RBs to serve a given traffic profile determines if the cell is coverage or capacity-limited, by comparison to the available RBs at the cell. This cell-capacity ratio is defined in (3.10), following the concept from [Alco17].

$$\eta_{cell} = \frac{N_{RB,cell}}{\overline{N_{RB,required}}} \tag{3.10}$$

where:

- $N_{RB,cell}$: number of available RBs in the cell;
- $\overline{N_{RB,required}}$: average number of required RBs in the cell;

The implications at the network capacity level is given by (3.10) and in Table 3.11.

Table 3.11. Cell-capacity ratio implications.

$\eta_{cell} = 0$	$\eta_{cell} < 1$	$\eta_{cell} = 1$	$\eta_{cell} > 1$
No capacity provided in cell	Cell capacity overload	Resource Block balance in cell	Cell capacity in not-overload

The total average throughput per service in the cell can be defined from (3.11) and the percentage of traffic service per cell in (3.12).

$$\overline{R_{b,cell_{[\mathrm{Mbit/s}]}}^{s}} = \sum_{service\ i}^{N} \overline{R_{b,user,s_{[\mathrm{Mbit/s}]}}} \cdot N_u^s \cdot \eta_{cell} \tag{3.11}$$

where:

- N_u^s : number of active users of the service s;

$$\rho_{traffic_s\,[\%]} = \frac{\overline{R_{b,user,s_{[\mathrm{Mbit/s}]}}} \cdot N_u^s \cdot \eta_{cell}}{\overline{R_{b,cell_{[\mathrm{Mbit/s}]}}^{s}}} \tag{3.12}$$

To summarise capacity planning, the flowchart in Figure 3.6 is used as baseline from the works of [Alco17]. A brief explanation is made on the no-successful RB allocation scenario, which is the number of required RBs exceeding the cell capacity. The approach here is to decrease the cell radius by a certain percentage, which will decrease the effective cell area (3.3) and consequently decrease the total number of users in the cell. This leads to decreased intensity in traffic profile demands, which require now fewer resource blocks. The process is iterative until the successful scenario is achieved, by which the cell radius and area are computed, and the total number of cells estimated.

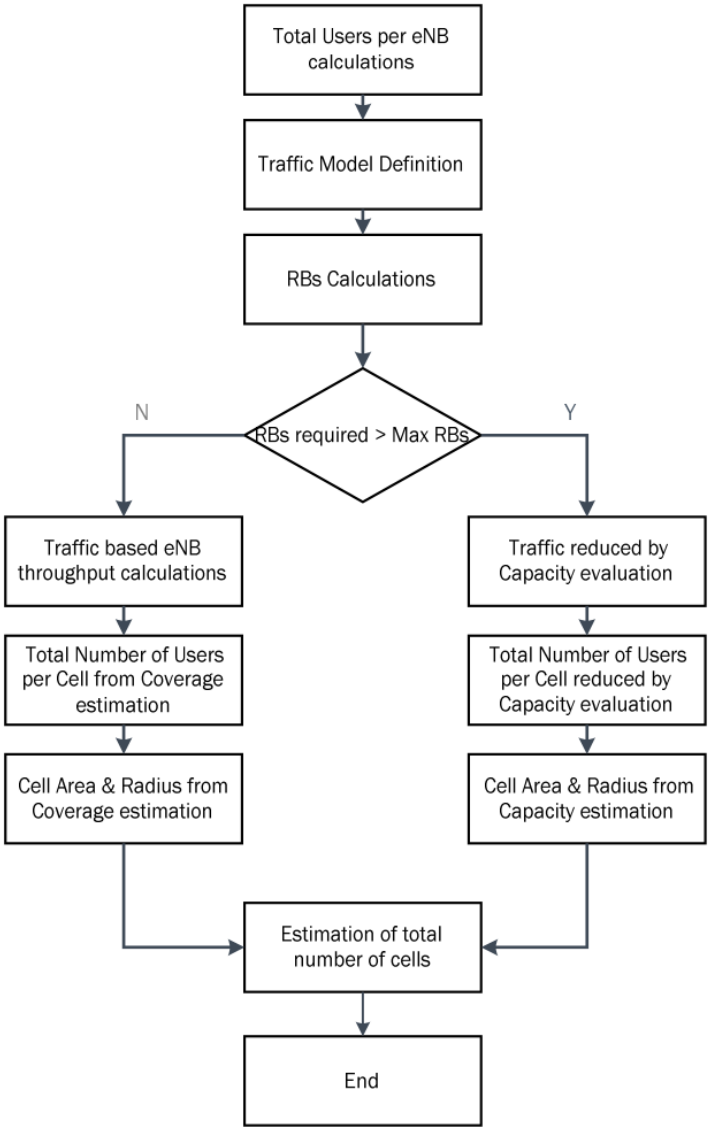

Figure 3.6. Proposed network capacity planning process (extracted from [Alco17]).

3.3.3 Cellular Planning

The main goal of this section is to discuss higher level aspects within the scope of cellular planning, in order to measure and validate the approach taken at this level. To start, a key assumption is that within the coverage area with a specific parameter configuration the cell size is the same, that is to say, it does not take into account two frequencies in use at the same BS site, which could yield different cell radii,

nor the existence of other types of antennas other than macro-cells, which could yield additional coverage area in some specific scenarios, such as pico-cells in shopping malls.

The cell structure is assumed to be hexagonal following the concept of tri-sectorisation in BSs in use in real-life network cell configuration. This is the optimal geometrical shape, since it minimises any overlap or gap given, and on top of this assumption a generic value for handover ratio is defined for any cell size, which finds its limitations if the cell size is too large and thus an approach for absolute handover distance could be considered in a future implementation. The hexagonal cell area can then be computed.

$$A_{cell_{[\mathrm{km}^2]}} = \frac{3}{2} \cdot \sqrt{3} \cdot r_{max\,[\mathrm{km}]}^2 \tag{3.13}$$

where:

- r_{max} : maximum radius (from coverage or capacity estimation)

It is then possible to compute the number of cells within the specific coverage area.

$$N_{sites} = \frac{A_{D_{[\mathrm{km}^2]}}}{A_{cell_{[\mathrm{km}^2]}}} \tag{3.14}$$

where:

- A_D : total target area of deployment;

While it is possible to build an extension to the model to allow a user distribution in the cell by some profile, such as the worst/best case, e.g., all TP intensive services are near the cell edge versus being near the BS, the decision was made to select the random user distribution throughout the cell, since it provides a more realistic insight on how can the network behave if users are moving within the cell.

Figure 3.7 presents a conceptual illustration on what is behind the model. What in real-life are geographically disperse users per MCS region, in the illustration they are all combined in the different MCS region sets. In this case they are distributed on the heavy-load at cell edge profile, where the highest throughput services are associated to the users on the cell edge (QPSK region) and the lowest ones are in the users near the BS (256-QAM).

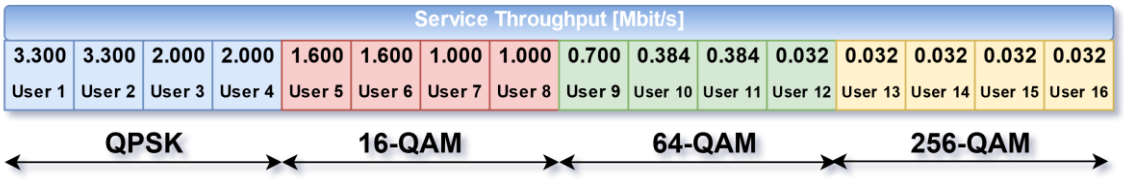

Figure 3.7. Conceptual illustration of the user allocation process per MCS region.

Figure 3.8 illustrates the main model output parameters' variation for a given configuration over 50 simulations. The random process of user allocation places them in different MCS regions. Depending on the mix share per service and the MCS area, there can be a very unequal degree of requirements in terms of network capacity. Since every MCS region has four possible throughput values, corresponding to every MCS, there are at least four possible RB throughput values per MCS region to consider in the allocation.

If the concept of throughput increasing as the distance to the BS reduces is weighted in, the number of required RBs can vary significantly for the same service whether it is on the QPSK region or in the 256-QAM one, thus the importance of running a sufficient number of simulations to find an average and standard deviation value. A higher numerology configuration can take higher throughput values at the expense of more RB bandwidth. Hence, if all numerologies are considered (0, 1, 2) the total number of possible throughput values for every MCS region can reach up to 12 (4 MCS curves and 3 numerologies).

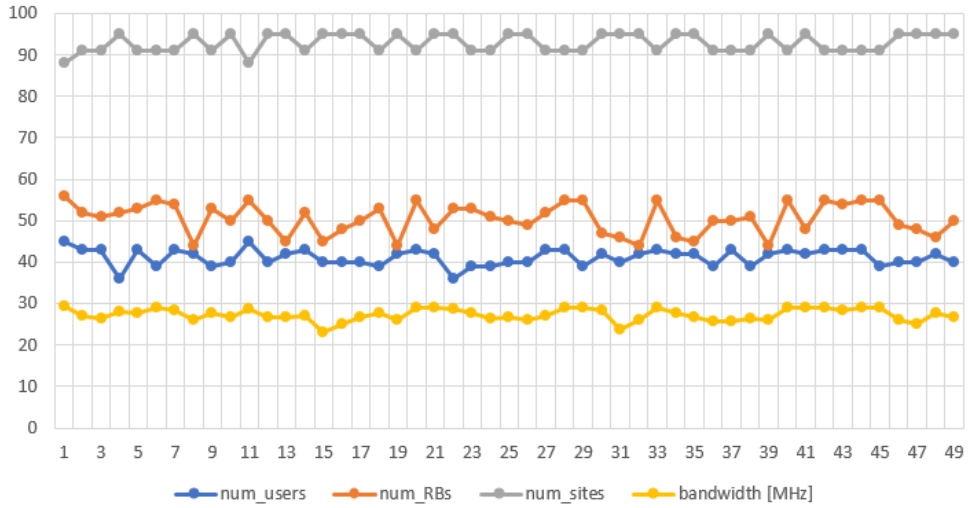

Figure 3.8. Model output parameters variation for *n* = 50 simulations for a given input configuration.

After acknowledging the different throughput curves' configurations within a cell network in 5G-NR, one should define the precise throughput value the model takes in for RB allocation computation, which can be done at the SNR level associated to throughput. While the model never takes a SNR value for throughput lower than the current cycle SNR value associated to distance, in all other cases it needs to have a pre-defined value. This is considered in the input parameters file with the concept of SNR ratio within a given MCS region, which is simply the ratio between the MCS region's minimum and maximum SNRs:

$$\rho_{[\mathrm{dB}]} = \rho_{min\,[\mathrm{dB}]} \cdot (1 - \lambda_{ratio}) + \rho_{max\,[\mathrm{dB}]} \cdot \lambda_{ratio} \quad (3.15)$$

where:

- λ_{ratio} : ratio between the current MCS region's min and maximum SNR value;

Since the SNR boundaries between MCS regions can be defined as static, an example application of the SNR ratio concept is present in Table 3.12.

Table 3.12. SNR index ratio λ (example).

MCS region	ρ_{min} [dB]	ρ_{max} [dB]	λ_{ratio}	ρ [dB]
QPSK	-10	5.5	0.5	-2.3
16-QAM	5.5	12.9	0.5	9.2
64-QAM	12.9	25.5	0.5	19.2
256-QAM	25.5	50	0.5	37.8

A value of 0.0 means the model applies the minimum MCS region's SNR, which in turn produces the lowest throughput values for the region, and as the value increases up to 1.0 the associated RB throughput increases as well. From the moment that the SNR value is defined for the four MCS regions, it is then possible to generate all the possible RB configurations, as it can be seen in Table 3.13.

Table 3.13. Possible RB numerology configurations with λ_{ratio} = {0.50, 0.50, 0.50, 0.50}.

MCS curve	Numerology configuration [kHz]											
	15	30	60	15	30	60	15	30	60	15	30	60
QPSK	0.13	0.26	0.53	0.17	0.33	0.67	0.17	0.33	0.67	0.17	0.33	0.67
16-QAM	0.02	0.05	0.09	0.30	0.60	1.20	0.49	0.99	1.98	0.51	1.02	2.04
64-QAM	0.02	0.03	0.06	0.21	0.42	0.83	0.85	1.70	3.39	1.10	2.20	4.41
256-QAM	0.02	0.03	0.07	0.15	0.29	0.59	0.66	1.33	2.65	1.41	2.82	5.62
MCS region	QPSK			16-QAM			64-QAM			256-QAM		

The standard value considered for throughput evaluation is with the numerology of 15 kHz, from [Alco17]. There are relevant aspects concerning band guards on higher orders of numerology in 5G-NR which can change the multiplying throughput factor from the 15 kHz throughput curve, but for simplicity purposes one assumes a multiplying factor of 2 every time the SCS bandwidth doubles. It should be noted that this approximation may not be suitable for use with much higher orders of numerology (e.g., SCS of 120 or 240 kHz), however since those are not within the scope of this thesis due to it being defined for mm-waves (28 GHz), the factor of 2 is considered in the 15, 30 and 60 kHz throughput curves.

As previously discussed, the model can take any numerology configuration although only the one with highest distance is considered for coverage distance purpose. That is to say, if numerologies 0, 1 and 2 are selected, coverage estimation will always be based on numerology 0 (15 kHz) and consequently the same applies for computing the maximum achievable throughput at the cell edge. Although there is a liberty to pick any numerology configuration, there are certain restrictions imposed by 3GPP. Essentially there are numerologies that are not supported by some pairs of frequency/bandwidth.

In this sense, considering the user population randomly distributed in the cell and the capacity possibilities in terms of throughput from MCS regions and numerologies, the model picks the most efficient RB in use ratio for every service. That is to say, it tries to find the configuration that yields the lowest number of necessary RBs to deliver the user's service:

$$N_{RB,user,k} = min\left\{\frac{\overline{R_{b,user,k_{[\mathrm{Mbit/s}]}}}}{\overline{R^{m,J}_{b,RB_{[\mathrm{Mbit/s}]}}}}\right\} \tag{3.16}$$

where:

- k : user ID with associated requirement in terms of throughput;
- m : MCS curves available at current MCS region (from QPSK to 256-QAM);
- j : throughput corresponding to every numerology (15, 30, 60 kHz);

The process is then done for every user in the cell and continues until the network exceeds either the number of RBs, which in 5G-NR has a maximum value of 275, either the total bandwidth for a given pre-defined cell load ratio, which is composed of the bandwidth allocated at the cell edge and the useful bandwidth allocated to the cell population.

If the process comprises all users and it does not exceed the conditions mentioned above, the cellular design is complete at the specific cellular level, otherwise a re-dimensioning process must take place. The proposed re-dimensioning techniques are essentially in the sense of reducing some parameter of set of parameters that can suffer adjustments, such as reducing the list of services to the ones with highest priority level or reducing the cell size:

- **Reducing list of services:** there are a couple of services that can never be excluded, so this technique works only until a certain point. The idea is to remove one service at a time from the lowest priority and evaluate if the cell avoids capacity overload. The degradation of throughput value is considered for non-essential services such as video-streaming.
- **Reducing cell radius:** this reduction is essentially linked to having less users to be served in the cell and therefore being able to support them with the available cell capacity. This reduction only applies to the cell edge, the remaining MCS region boundaries remain unchanged. It can happen that the cell edge is in a closer MCS region, e.g., 64-QAM regions, but the remaining MCS curves are still available.

At last, due to the increasing number of devices per person (e.g., smartphone, tablet, laptop and IoT sensors) with mobile-network connection capabilities and user-demands, the computation of active user (device) density in 5G takes a device multiplier ratio into account, shown in Figure 3.9.

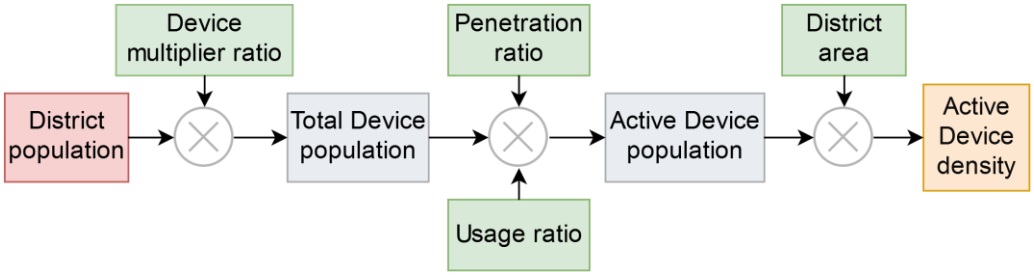

Figure 3.9. Computation of the active device density (model input) from the district population.

The active device population useful for capacity purposes is then computed, applying the penetration and usage ratios to the total device population. The number of inhabitants for each district and respective area are obtained from [Stat16] and [Dire16], respectively, and is factored by the penetration ratio, defined as the percentage of devices with mobile internet access or as the percentage of devices subscribed to the operator, and by the usage ratio, which corresponds to the active users at the present instant of time in study. In the context of this thesis, the default ratios are 15% for penetration and 10% for usage.

3.4 Model Implementation

The models related to coverage and capacity described in the previous sections were implemented into a general purpose 5G-NR network design model/simulator, developed in the programming language of C# (C Sharp) in the Visual Studio 2017 coding environment. It retrieves some common technical aspects from a previous network model implementation (LTE) by [Alco17] and adds the novel aspects concerning 5G-NR current standards to produce a model simulator tool for network dimensioning, covering both coverage and capacity aspects. Its workflow is presented in Figure 3.10

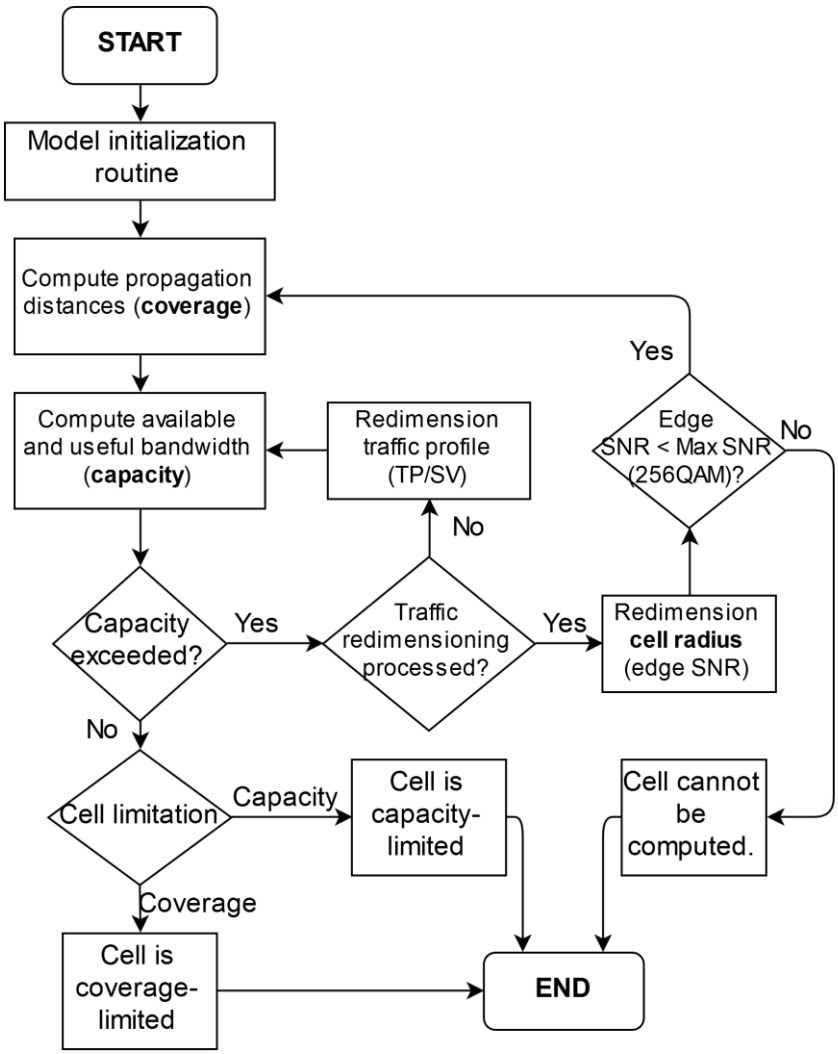

Figure 3.10. Over-the-top generic model workflow.

After computing the cell radius, the algorithm infers how much useful bandwidth is available for capacity evaluation. If it produces a situation of capacity overload the cell re-dimensioning techniques are applied, in a first stage by reducing some services' throughput values, then by removing some services and by reducing the cell radius through the increase of the SNR at the cell edge limit. If there is no capacity overload at a given point, the cell is said to be coverage-limited if no traffic/radius reduction is required, and capacity-limited otherwise. The algorithms behind the secondary routines in the model are described in Annex E Complementary Model Implementation Workflow

Furthermore, every class is defined in a different/specific file to have code readability, and the main methods of every class are present in Figure 3.11.

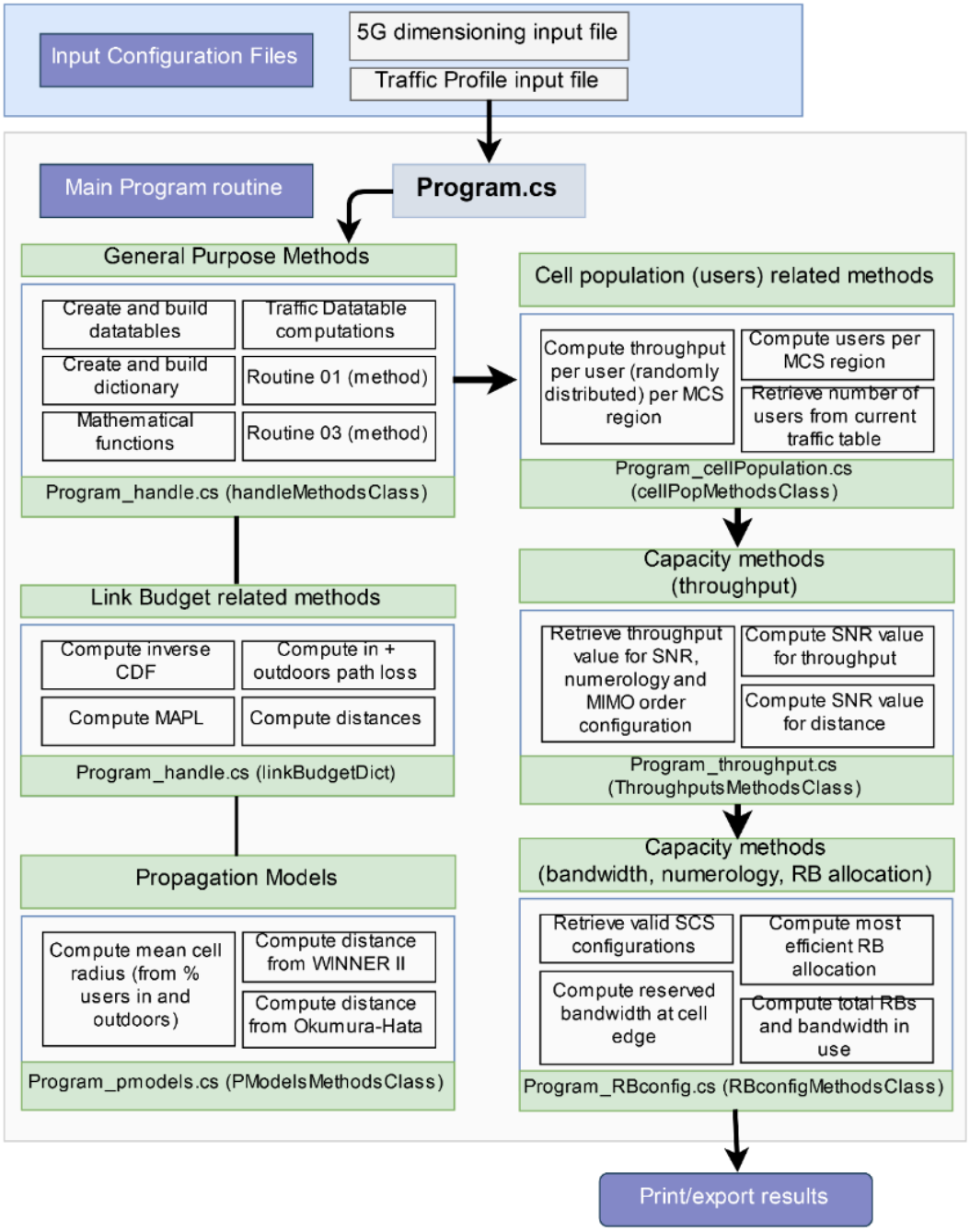

Figure 3.11. Main components of the simulator.

3.5 Model Assessment

To assess the model implementation during its development a list of empirical tests was established to evaluate implementation at the coverage, in Table 3.14, and at the capacity level, in Table 3.15.

Table 3.14. Empirical tests performed to validate the implementation of the coverage model.

Test ID	Element Validation	Example
1	Link budget and propagation models (compare with values obtained from simulator, generate figures).	See Annex D.
2	Cell radius changes in the 2 frequency bands and from different input parameters (e.g., required throughput at cell edge, BS/MT height).	See Annex D.
3	Cell radius decreases with the increase of modulation order and the high/low indoors model.	See Annex D
4	Number of coverage cells increases with the increase of the frequency band.	See Figure 3.12, Figure 3.13

Assuming the standard link budget values later used in Chapter 4, the number of cells for a 150 km^2 geographical target area is computed for both frequency bands in the three propagation scenarios. The impact of the frequency increase is not very significant around the 700 MHz for the target area, but the higher frequencies' number of cells it is at least equal or larger than the lower ones. Moving up in spectrum, the impact of frequency increase is much more noticeable around the 3.5 GHz as it should happen, especially in the urban and suburban scenarios that have a higher degree of obstructions.

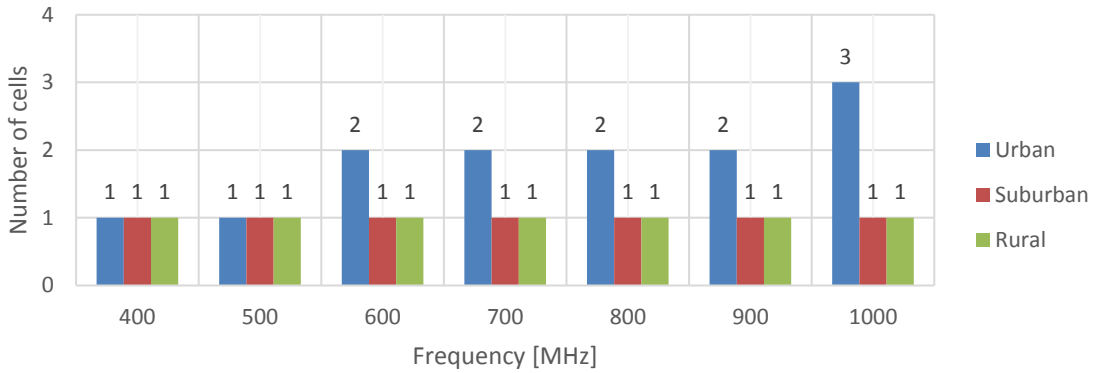

Figure 3.12. Number of cells in 150 km^2 vs frequency (Okumura-Hata).

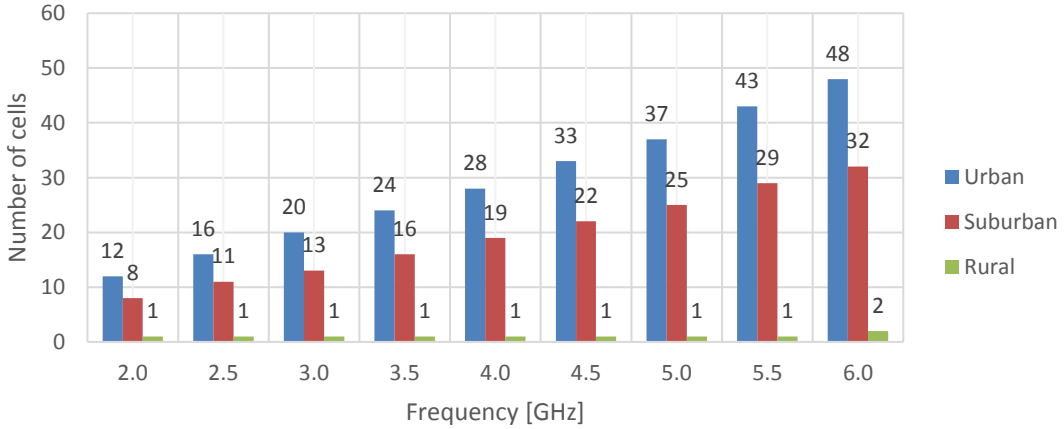

Figure 3.13. Number of cells in 150 km^2 vs frequency (WINNER II).

Table 3.15. Empirical tests performed to validate the implementation of the capacity model.

Test ID	Element Validation	Example
1	Validation of #RBs requested by a user in each service (scientific calculator, excel and model).	-
2	Num. of users per cell increases when user density increases.	See Annex D.
3	Number of allocated RBs and bandwidth increase as the service throughput increases.	See Annex D.
4	Cell radius decreases as the user density increases	Figure 3.14
5	TP at cell edge doubles when reserved bandwidth doubles.	See Annex D.
6	Cell radius with 3 numerologies in use can never be higher than the lowest numerology, nor lower than the highest numerology as the user density increases.	Figure 3.15

An interesting metric to assess the capacity model is whether the cell radius decreases with the increase in user density. This is tested for both frequency bands in the three environment scenarios, and the case for the urban scenario at 3.5 GHz is presented. The cell radius given by a zero-user density corresponds to the maximum coverage radius given in the coverage dimensioning through the link budget and propagation model, and as the user density in the cell starts increasing the capacity dimensioning is active, reducing the cell radius until it can support the traffic profile associated to having that user density value. This metric can also provide an indicator on whether the cell may be coverage or capacity limited, e.g., in the Figure 3.14, until a user density of 100 per km^2, the radius does not decrease and thus can be said to be coverage-limited.

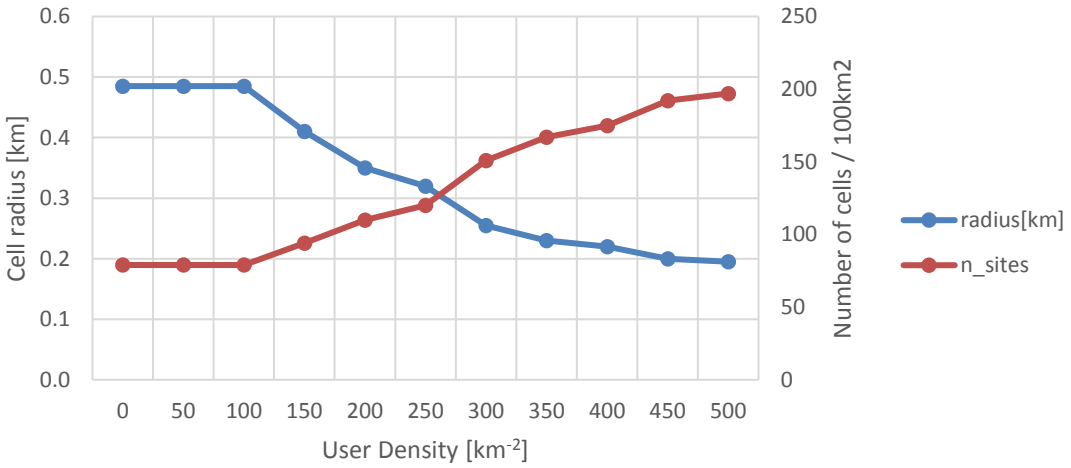

Figure 3.14. Cell radius when increasing user density (urban, 3.5 GHz).

In order to assess the implementation of numerology configurations in the model, two types of results were retrieved, one with a single-numerology in use and another with all numerologies in use (15, 30 and 60 kHz). The goal is to inspect if no single numerology configuration is lower than the higher SCS configuration (15 kHz), nor higher than the lower SCS configuration (60 kHz), for the same user density increase profile. In the first type the distance difference between each numerology configuration curve

is constant, as it should be, since it corresponds to the 3 dB difference in the link budget between SCS bandwidth in the sensitivity power. In the second type, the initial cell radius is given by the lowest numerology configuration of the three, the 15 kHz one, which yields the maximum coverage distance, consisting of the coverage-limited cell situation. As the user density increases the capacity dimensioning proceeds to reduce the cell radius, leading to a capacity-limited cell.

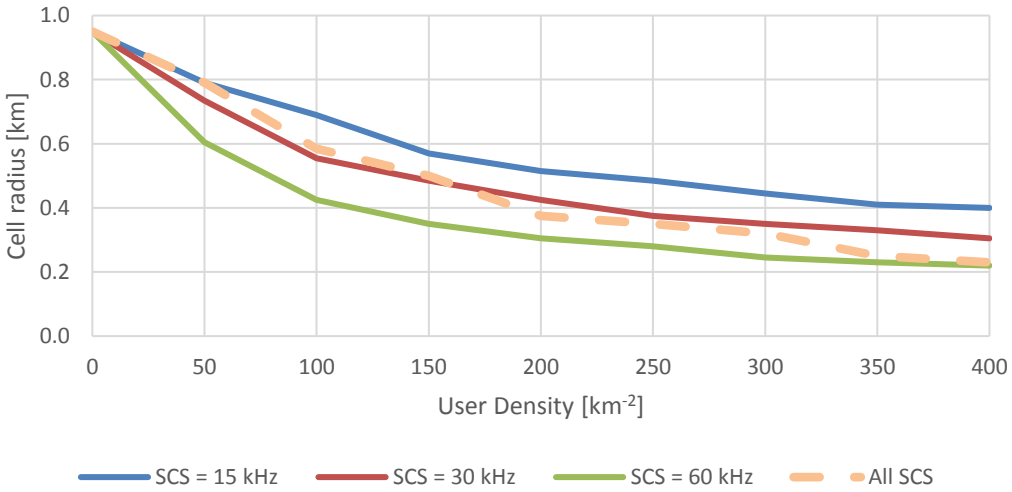

Figure 3.15. Numerologies' impact on cell radius as the user density increases (urban, 3.5 GHz).

Chapter 4

Results Analysis

This chapter is composed of the reference scenario description as well as the simulation results and their respective analysis.

4.1 Scenarios Description

The geographical reference scenario is the city of Lisbon and its northernmost surrounding areas. This scenario has been studied in [Alco17] in the context of an LTE-based network and is thus chosen in the perspective of acquiring comparative measurements regarding 5G deployment. The simulator takes in several input parameters that are dependent on the specific geographical area under study, such as its scenario type (urban, suburban, rural), user density and traffic profile. As such, it is possible to partition the geographical area of coverage into districts based on these parameters, seen in Figure 4.1.

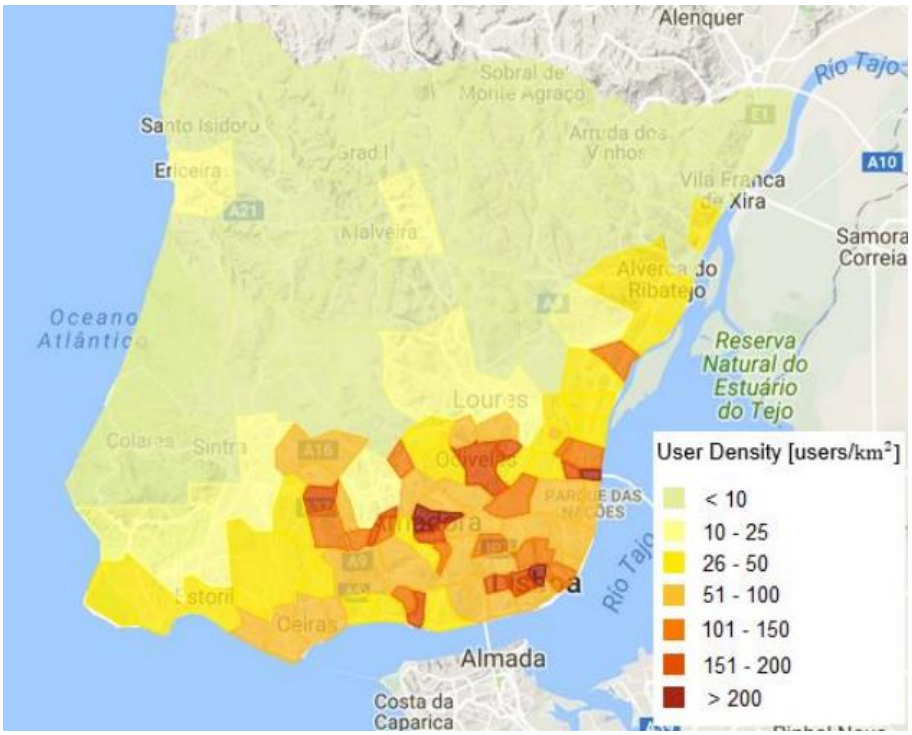

Figure 4.1. Geographical target area in study (extracted from [Alco17]).

The coverage area is approximately 1 500 km^2, where 11% is urban (167 km^2), 26% suburban (385 km^2) and 63% rural (946 km^2). The population density is typically below 50 users/km^2 with the exception of a couple of municipalities in the coverage area, Figure 4.2.

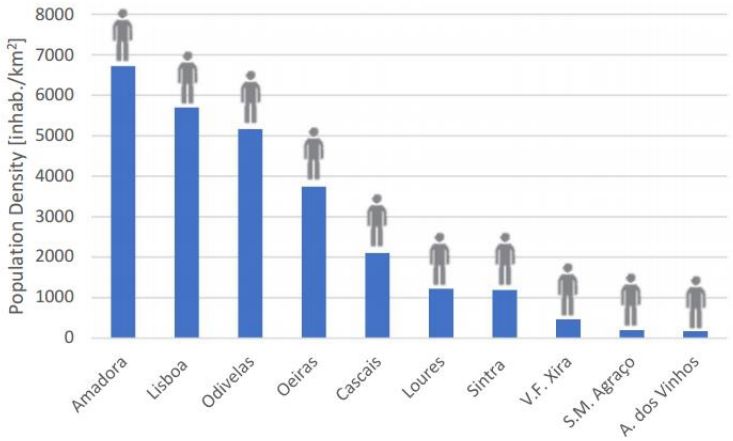

Figure 4.2. Highest population density values in the target area (extracted from [Alco17]).

Due to the natural differences in user density throughout the municipalities one should expect an asymmetric BS distribution for each municipality, as seen in Figure 4.3. Previous works by [Maro15] have performed such computation in the same coverage area for LTE albeit taking the same traffic profile to every municipality.

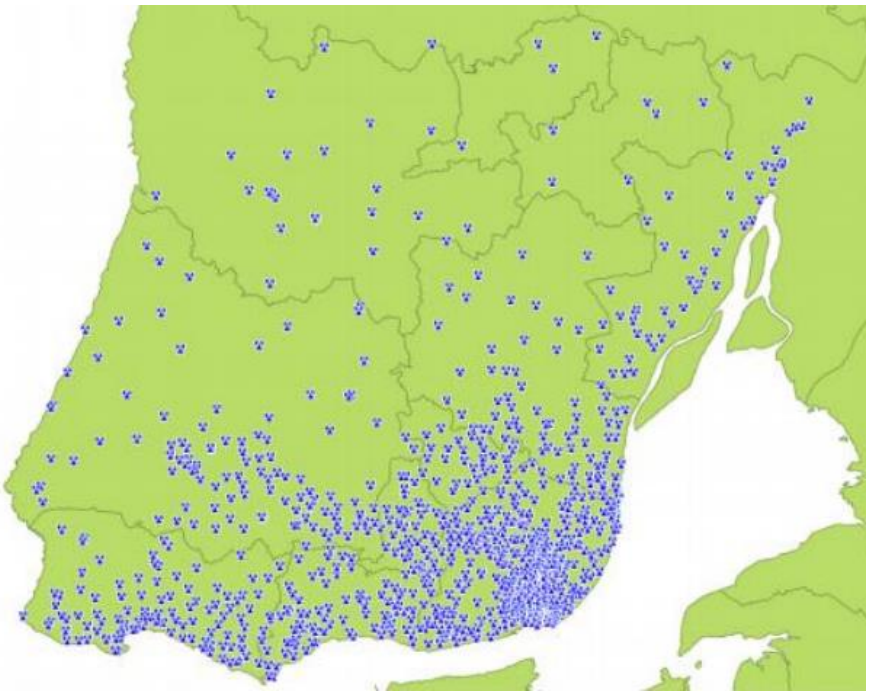

Figure 4.3. Geographical location of BSs based on the works of (extracted from [Maro15]).

Although this thesis presents no geographical BS distribution such as Figure 4.3, some conclusions can be withdrawn from it regardless of the different technology and spectrum aspects from [Maro15] to this thesis. For instance, that in low user-density districts/municipalities the distance between BS is high whereas in high user-density the distance is considerably smaller.

Although a metric for defining the environment (propagation scenario) is established in [Corr16], an approximation is taken based on the density of users per town/city, following the device density histogram computed from [Stat16] in Figure 4.4, assuming an average of 1.5 devices per person/inhabitant. Hence, the areas with higher values of device density are considered to be urban, then suburban, and the lowest are considered to be rural.

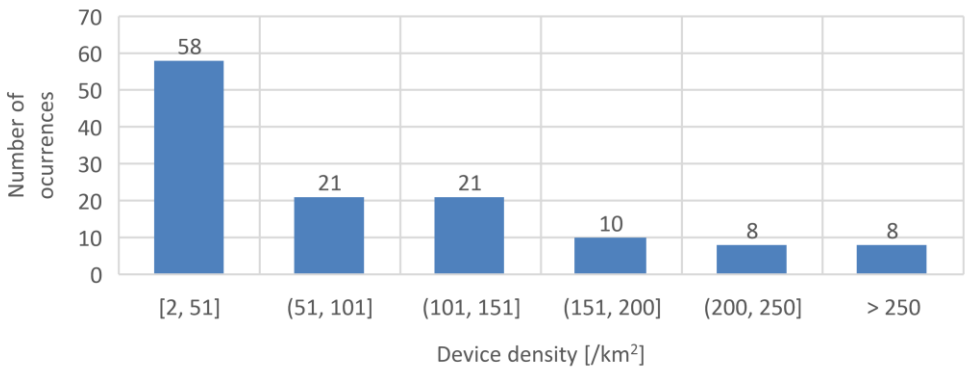

Figure 4.4. Device density histogram (from data in [Stat16]).

Since the path loss computation from the link budget depends, among others, on the coverage probability, it is important to address the mean and standard shadow fading. In indoors, since the indoor model in this thesis presents no estimation on the standard deviation values, an intermediate approach is to decide between the values from [Alco17] and those recommended by [Kris16].

Table 4.1. Indoor mean and standard deviation values. (based on [Alco17] and [Kris16]).

Indoors Model	Frequency Band [GHz]	Mean [dB]	Standard Deviation [dB]	Environment in use
High-Loss	**0.7**	11	8.5	**Urban, suburban**
	3.5	18	17.6	
Low-Loss	**0.7**	7	6	**Rural**
	3.5	7.3	10	

Although the goal of the model is to provide a general-purpose tool for cellular network dimensioning, a model reference scenario is defined with default-valued parameters, present in Table 4.2.

Table 4.2. Model reference scenario parameters.

Parameter Description		Value
Reference Throughput [Mbit/s]		2.0
Maximum dedicated bandwidth at cell edge [%]		10
Coverage Probability [%]	**Indoors**	90.0
	Outdoors	90.0
Slow-Fading standard deviation [dB]	**Indoors**	8.5/17.6
	Outdoors	6.0/10.0
Indoor users [%]		70
Penetration ratio [%]		15
Usage ratio [%]		10
Handover ratio [%]		5
Maximum service TP reduction [%]		40
Maximum allowed cell load [%]		80
Maximum number of services to …	**Reduce TP**	3
	Remove	3
Numerologies in use [kHz]		15, 30, 60

Since the commercial trend has been that more and more devices and users are consuming mobile data inside buildings, whether at home, work or any indoor facility, the percentage of users indoors is considered to be 70% in the model, a value also considered by [Alco17]. The maximum service TP reduction defines how much of service TP reduction can the feasible, while still fulfilling QoS requirements. On the other hand, in cases of capacity overload the model tries to reduce first the lowest priority services' TP, with the maximum number of services to reduce TP, and if unsuccessful it tries to remove services from the lowest priority to highest, with the maximum number of services to remove.

From the valid bandwidth configurations defined by 3GPP. The model simulations were performed for four precise and well-defined spectrum scenarios, Table 4.3.

Table 4.3. Model reference scenario spectrum configuration.

Frequency Band [MHz]	Bandwidth [MHZ]	Available SCS [kHz]			ID
		15	30	60	
700	5	✓	×	×	1
	20	✓	✓	×	2
3 500		✓	✓	✓	3
	100	×	✓	✓	4

The first corresponds the lowest frequency/bandwidth configuration, 700 MHz/5 MHz (1), then the second and third have the same bandwidth, 20 MHz, for 700 (2) and 3 500 MHz (3) bands and the fourth is the highest frequency/bandwidth configuration, 3 500 MHz/100 MHz (4). These simulations are performed both at the DL and UL level, with different traffic profiles and link budget parameters. With this spectrum scenario one can determine the minimum and maximum capacity characteristics of the 5G-NR for the under 6 GHz spectrum, and also compare the effect by having a different frequency for the same bandwidth values (20 MHz). Furthermore, in the link budget, the power and gain default values are taken from [LTEE09] and [ERIC18c] and presented in Table 4.4.

Table 4.4. Link budget reference parameters.

Parameter Description	Channel	
	DL	UL
Transmission power [dBm]	37	10
BS antenna gain [dBi]	18	
UE antenna gain [dBi]	0	
UE losses [dB]	1.0	
Cable losses [dB]	2.0	
Noise Figure [dB]	8.0	5.0
Diversity Gain [dB]	3.0	
Interference Margin [dB]	3.0	
TMA gain [dB]	2.5	
MIMO order	2x2	
Height of BS [m]	25	
Height of MT [m]	1.5	
MCS in use	QPSK, 16QAM, 64QAM, 256QAM	

Regarding the traffic profiles considered in the model, the simulations were performed using an approximate profile for DL and UL, Table 4.5 and Table 4.6 , based on the relative mix share from

previous works, such as [Alco17] and [Guit16]. The throughput values for each service are the average between the minimum and maximum standardised values to provide the service with a satisfying QoS. This allows for throughput reduction in the model in the case of capacity overload without missing the QoS level for the services. Despite the existence of MMTC and URLLC services in 5G-NR, the cellular dimensioning process in this thesis does not take latency profiles into account. Therefore, the decision is taken to only include MMTC services in the traffic profiles in the course of this work. However, in the perspective of future work the dimensioning tool of this thesis could be combined with the algorithms developed by [Silv16], which consider different service latency requirements in a network.

Table 4.5. Traffic profile for UL.

Service name	Service class	Priority	Mix Share [%]	Throughput [Mbit/s]
Voice	Conversational	1	30	0.032
Chat		2	30	0.384
Video conference		3	10	2
Video streaming	Streaming	4	15	5
File sharing	Interactive	5	5	2
MMTC	Background	6	5	0.1
Email		7	5	1

Table 4.6. Traffic profile for DL.

Service name	Service class	Priority	Mix Share [%]	Throughput [Mbit/s]
Voice	Conversational	1	15	0.032
Chat		2	15	0.384
Video conference		3	10	2
Video streaming	Streaming	4	20	5
Music streaming		5	10	0.196
Web browsing	Interactive	6	15	2
File sharing		7	5	2
MMTC	Background	8	5	0.1
Email		9	5	1

4.2 Number of Cells and Cell Radius

Based on the model reference parameters defined in the previous section, two simulations were performed at the 0.7 and 3.5 GHZ bands, with the same bandwidth (20 MHz) and the output results that are under analysis in this section are the total number of cells and cell radius values in the target

geographical area, in each environment and in each municipality. Data is shown both in absolute and relative terms, so empirical inferences can be withdrawn for other cellular scenarios. The first result from the simulation is the absolute number of cells per municipality for both frequencies, which are shown in Figure 4.5.

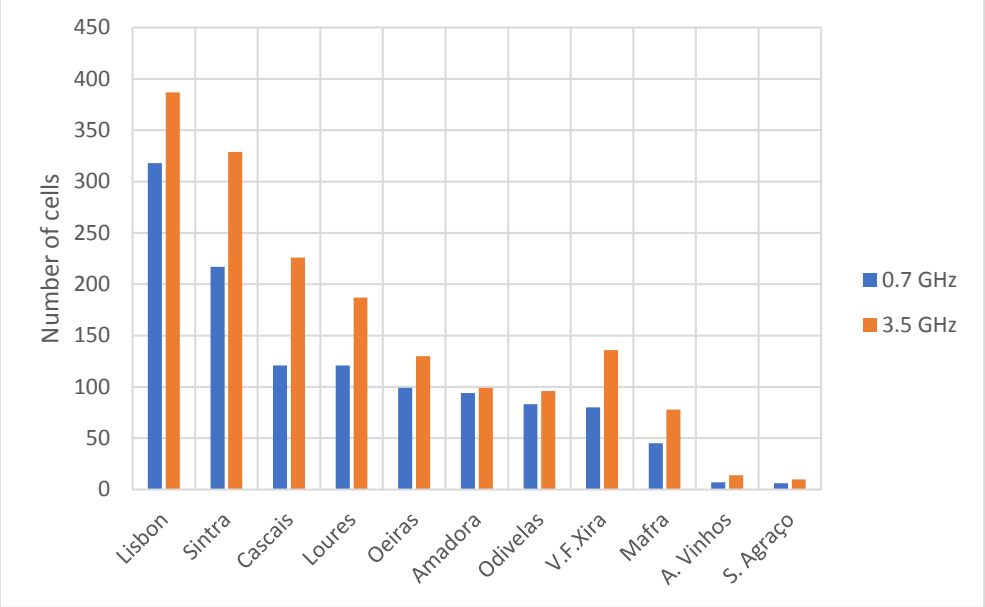

Figure 4.5. Number of cells per municipality (20 MHz bandwidth).

It can be clearly seen that the number of cells increases in general terms, with some municipalities having a larger increase of number of cells than others. For example, Vila Franca de Xira goes from 80 to 136 (+ 70%) while Lisbon only goes from 318 to 387 (+ 22%). Since few municipalities have a single environment (e.g., only urban such as Lisbon), no direct conclusion can be withdrawn from these figures without understanding the environment composition of each municipality.

Regarding the analysis on the number of cells per environment in Figure 4.6, since the total area covered by suburban environment (26%) is higher than the urban one (11%), the total number of cells is a higher in the suburban scenario. Regarding the rural environment, although the corresponding area (63%) is the highest of the three scenarios, the generalised low user-density value leads to it having a much lower total number of cells, compared to the suburban and urban ones.

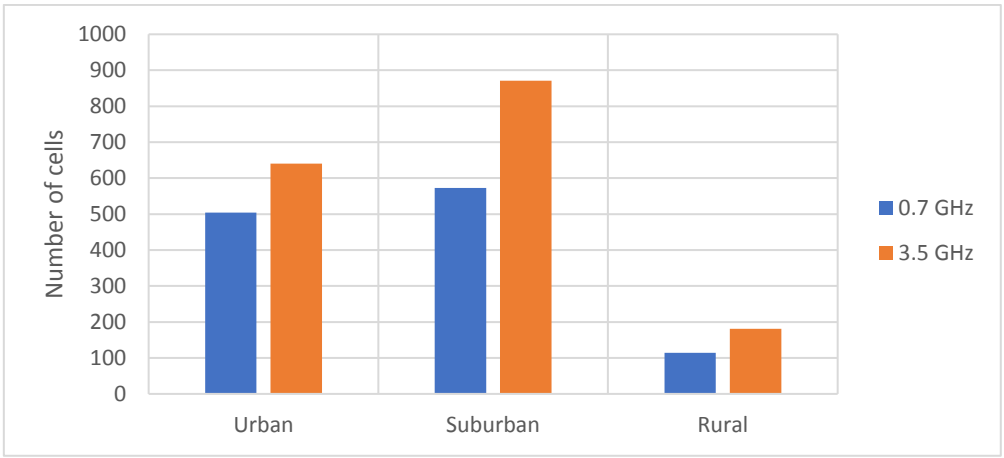

Figure 4.6. Number of cells per environment (20 MHz bandwidth).

Comparing the data in Figure 4.6, when the frequency increases the total number of cells also increases, with a relative increase of 52% in suburban, 27% in urban and 59% In rural. Once again, the higher relative increase in the suburban environment can be explained by it having a larger area than the urban one, but also if one considers that urban municipalities are already quasi-all capacity-limited at 0.7 GHz, and that in the suburban ones there may be more coverage-limited cells, the logical conclusion would be that the increase in the number of cells will be higher in suburban than urban, which is represented in the figure.

As stated before, any conclusion from the total or absolute number of cells can not be directly taken, unless one acknowledges the environment composition per municipality, which is present in Table 4.7. The municipalities with higher percentages of urban environment are unlikely to yield much higher number of cells when the frequency increases due to the predominance of capacity-limited cells, and in Figure 4.6, one sees that could happen to Lisbon and Cascais. On the other hand, municipalities with high levels of suburban or rural environments are more likely to have their number of cells increase by a higher percentage, simply due to them having a larger probability of coverage-limited cells at 0.7 GHz which turn into capacity-limited ones at 3.5 GHz.

Table 4.7. Comparison chart for number of cells evaluation per municipality.

Municipality	Number of cells			Environment type [%]			Mean Device Density [/km2]
	Frequency [GHz]		Increase [%]	U	S	R	
	0.7	3.5					
Lisbon	318	387	22	100	-	-	**153**
Sintra	217	329	52	-	65	35	**85**
Cascais	121	226	87	67	33	-	**70**
Loures	121	187	55	11	58	32	**83**
Oeiras	99	136	37	60	40	-	**39**
Amadora	94	130	38	-	100	-	**181**
Odivelas	83	99	19	29	71	-	**134**
V.F de Xira	80	96	20	-	45	55	**36**
Mafra	45	78	73	-	12	88	**7**
A. dos Vinhos	7	14	100	-	-	100	**4**
S. M. Agraço	6	10	67	-	-	100	**6**
Total	**1 191**	**1 692**	**42**				

In order to grasp the sense of the previous observations, a comprehensive comparison chart for the number of cells per municipality is present in Table 4.7, as well as the relative increase in the number of cells when the frequency increases, the environment type composition and average device density per municipality. Although the total number of cells depends on many different input configuration values, since most of the reference model parameters are based on the ones from [Alco17], by comparing the absolute number of cells, 1285, to the ones obtained in the simulation in this thesis, 1 191

for 0.7 GHz and 1 692 for 3.5 GHz, the order of magnitude is similar.

In order to have a comprehensive perspective on the relative increase of number of cells per municipality and their device density, which is an indicator if the cells in the municipality could lead to capacity-limited cells, Figure 4.7 is presented.

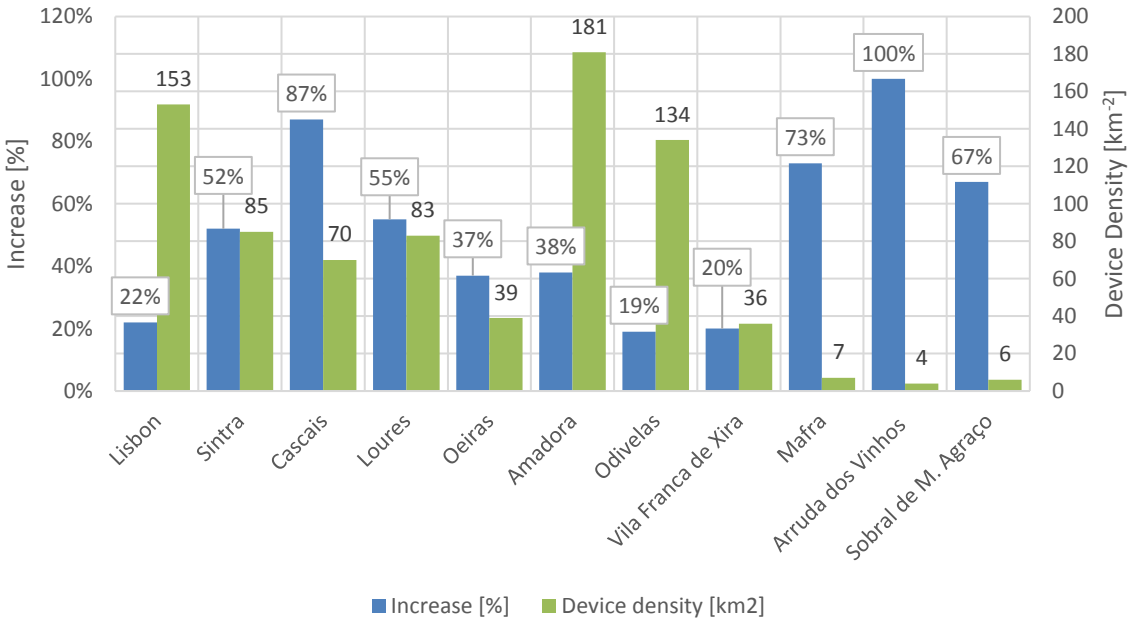

Figure 4.7. Comparison between the average device density per municipality and the relative increase in cell cells from 0.7 to 3.5 GHz.

From Figure 4.7, one can establish that the highest relative number of cells increase happen in the municipalities of Mafra, Arruda dos Vinhos and Sobral de Monte Agraço, which are defined as practically rural. Hence, cells which were formerly coverage-limited due to the higher MAPL values at 0.7 GHz are now mostly capacity-limited at 3.5 GHz, thus yielding a large increase factor.

Furthermore, in the case of Cascais, an urban/suburban scenario, one finds a high relative increase in the number of cells (+ 83%), which does not seem to be in agreement with a similar environment composition municipality, such as the case of Oeiras (67/33% vs 60/40%), with an increase of only 37%. In this case, this may have to do with the threshold user-density value to go from coverage to capacity-limited cells may have been attained in Cascais (70 users/km^2) while in Oeiras the value is almost half, 39 users/km^2. The municipalities with the lowest increase values, 22%, 19% and 20% in Lisbon, Amadora and Odivelas respectively, can be explained by them also having the highest user-density values of all municipalities, 153, 181 and 134 users/km^2, which effortlessly yields capacity-limited cells already in the 0.7 GHz and in 3.5 GHz the case turns stronger.

For the model reference parameters and the default traffic profile for DL and UL, in the target geographical area one can establish the average cell density per environment at both frequency bands. These values in absolute can easily change with any significant difference in the input parameters or in the traffic profile, however the relative different between them does not change. For example, the cell density at 0.7 GHz can never be higher than the one at 3.5 GHz, at most they can be equal if a heavy

traffic profile is considered such that at 0.7 GHz the cells are already all capacity-limited. The average cell density per environment comparison is shown in Figure 4.8.

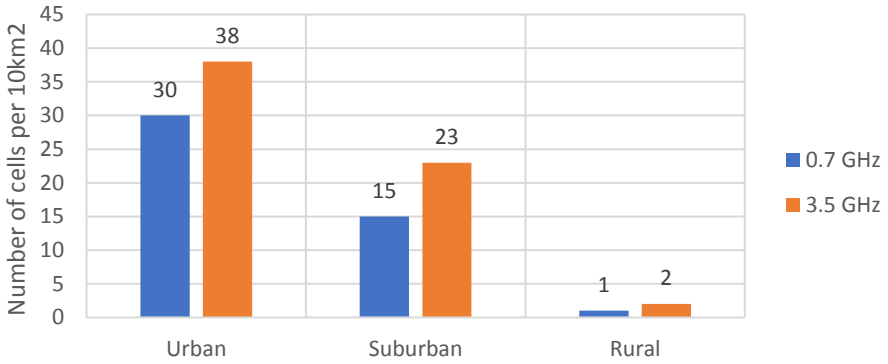

Figure 4.8. Cell density increase per environment and frequency band (20 MHz bandwidth).

In Figure 4.8, one can remark that the increase in cell density in urban environment is the lowest of the three, at 27%, while in suburban is 53% and in rural 100%. Once again, although the precise values of the relative increase can change with any model input change, the relative comparison of these values is not expected to change. Another metric that is interesting to analyse is to compare the frequency of occurrence of specific cell radius value intervals, in Figure 4.9 and Figure 4.10, and compare them when the frequency increases.

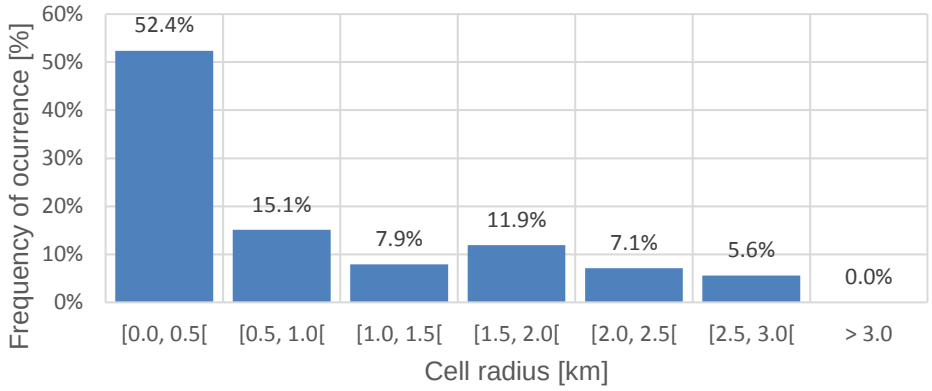

Figure 4.9. Cell radius histogram (0.7 GHz / 20 MHz).

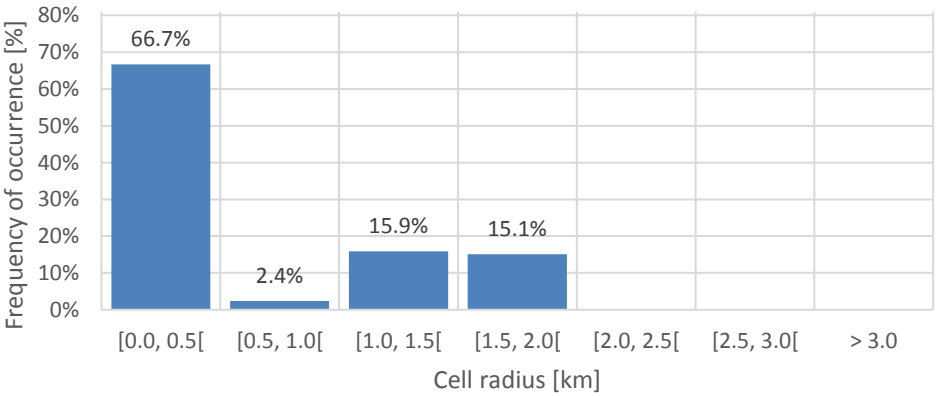

Figure 4.10. Cell radius histogram (3.5 GHz / 20 MHz).

From Figure 4.9 and Figure 4.10, two observations can be made. The first is that the maximum radius decreases considerably from the 2.5 to 3.0 km to the 0.5 to 1.0 km intervals, which is in agreement with the lower maximum distance when frequency increases from 0.7 to 3.5 GHz, the second is that the effect on coverage-limited cells turning into capacity-limited ones can be seen from the total number of cells with a cell radius higher than 1.5 km, which is 24.6% at 0.7 GHz and only 15.1% at 3.5 GHz.

As said before, no direct conclusions can be taken from the absolute number of cells from the simulation output unless one considers, besides the model input, every municipality environment composition. Figure 4.11 and Figure 4.12 are the proof that such direct conclusions can not be taken, through the very different standard cell radius values for the different municipalities, for both frequency bands.

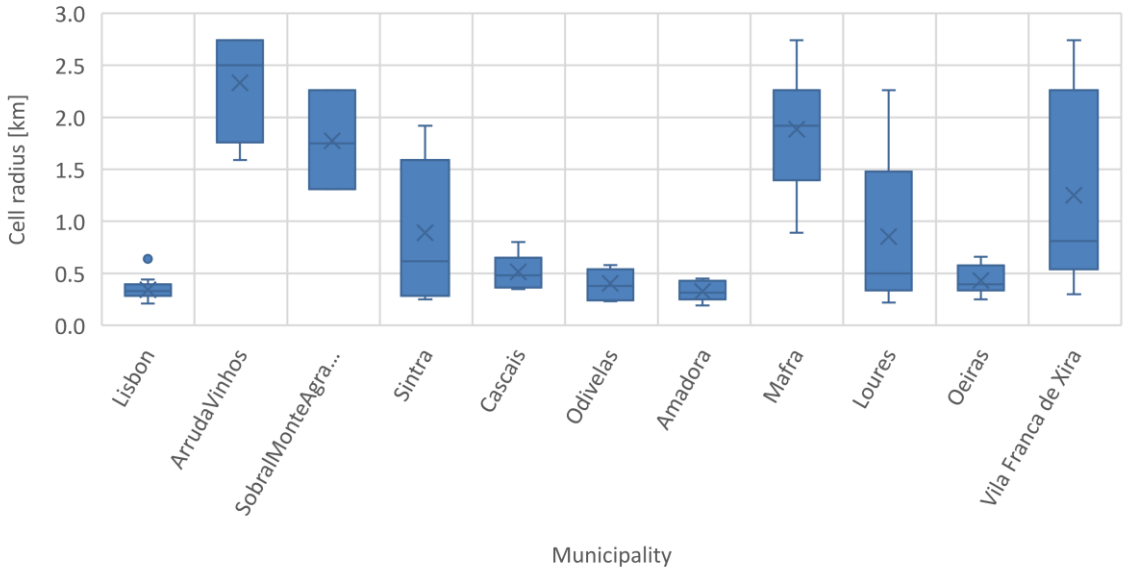

Figure 4.11. Average cell radius for each municipality (0.7 GHz / 20 MHz).

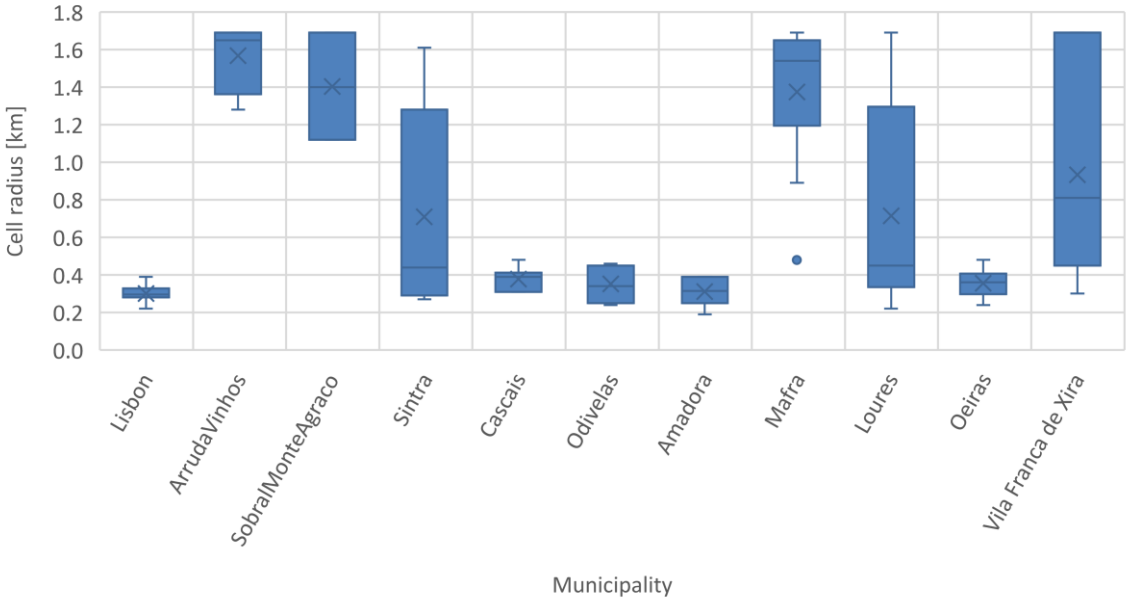

Figure 4.12. Average cell radius for each municipality (3.5 GHz / 20 MHz).

The conclusion is that any municipality whose largest environment type percentage is lower than 70% cannot be expected to have a solid, small standard deviation in terms of cell radius. The largest standard deviation values happen for the municipalities which have a considerable composition of rural environments, 55% for Vila Franca de Xira and 88% for Mafra, but also for municipalities that albeit having the strongest composition in the suburban environment, such as 65% in Sintra and 58% in Loures, they still have sufficient rural locations to yield a wide range of cell radius values.

4.3 Analysis of the Number of Users

Although the population density and the average number of devices per person in a given population can be considered static values, the value considered as model input for device density depends severely on the penetration and usage ratio, combined in the partitioning ratio, in Table 4.8. In the simulation, per default one considers 15% and 10% for the penetration and usage ratio, respectively, and since an increase in device density leads to capacity-limited cells, the site density should not vary significantly from 0.7 to 3.5 GHz. Hence, the simulation is done for the 3.5 GHz band.

Table 4.8. Penetration and Usage ratio for each scenario.

Scenario	Penetration ratio [%]	Usage ratio [%]	Combined ratio [%]
Reference	15	10	1.5
Double	30	20	6.0
Triple	45	30	13.5

The output results for the three configuration scenarios are present in Figure 4.13 and are in relative agreement with the results from [Alco17]. One can visually observe that the cell density seems to increase in the same manner regardless of the environment type, however a more precise analysis is done in Table 4.9.

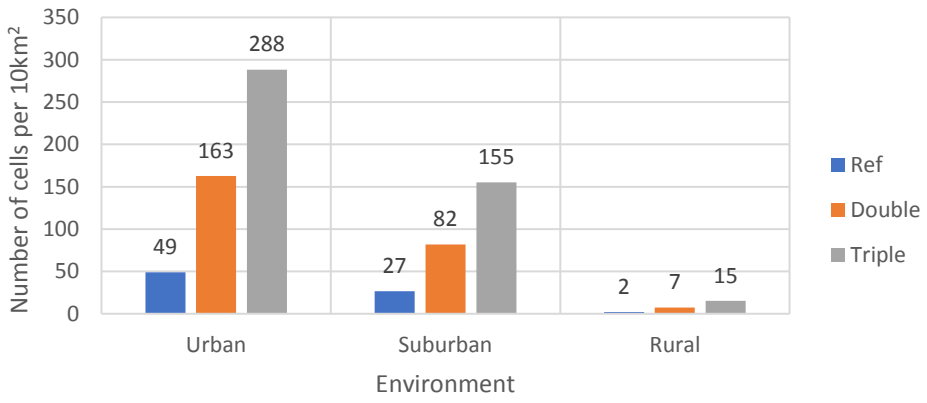

Figure 4.13. Number of cells per 10 km² in different environments and scenarios.

As the active device density increases more resources are required to serve the traffic profile load of the cell device population, which leads to capacity limited cells. In this case, the cell radius can severely be reduced from its original value and increase the number of required cells, which can be noticed in Figure 4.13, when comparing the reference scenario with the double and triple configuration values. On the other hand, the impact of increasing the active device density is heavier as more path losses are included, such as with obstructions, which is the reason the urban scenario requires much more cells than the other scenarios.

Although the increase in the number of cells as the active user density increases has been proven, a convenient metric is to assess if there may be an empirical relationship from these values for a higher increase of device density factor, assuming the same model reference parameters and traffic profile configuration. Hence, for the reference scenario in this thesis an empirical interpolation is derived from Table 4.9 and presented in Figure 4.14, where, for instance, an increase by a factor of 4 in the product between the usage ratio, penetration ratio and device density yields an increase in the number of cells of 3, for the rural environment, and 4 for the urban environment.

Table 4.9. Penetration and Usage ratio for each scenario.

Original Scenario	Target Scenario	Combined ratio increase factor	Number of cells growth factor		
			U	S	R
Reference	Double	4	3	3	4
	Triple	9	6	6	8

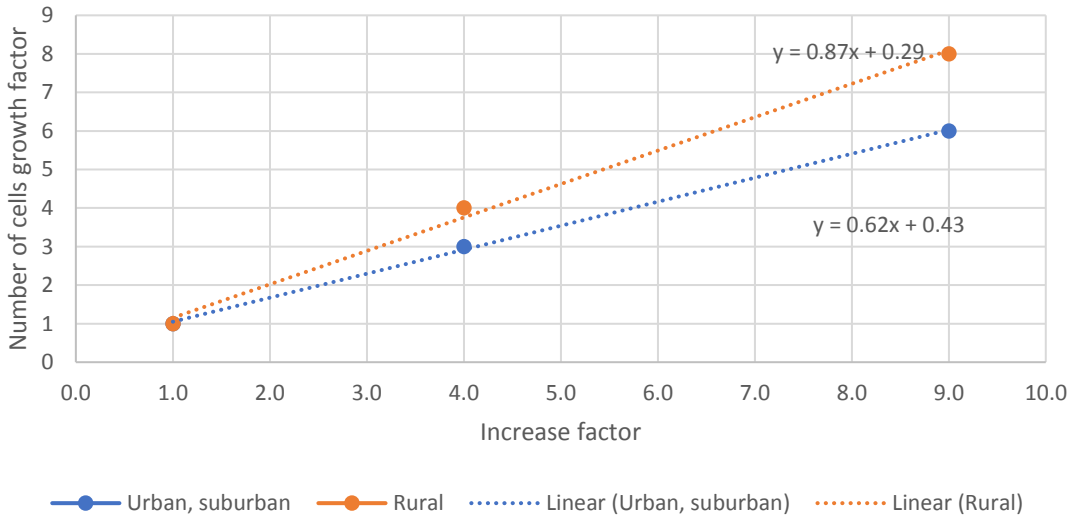

Figure 4.14. Number of cells growth factor for different increase metrics.

This leads to the conclusion that in future 5G deployments, as the number of devices per person is expected to increase considerably, the requirement in terms of cells may also increase significantly, which is a key aspect regarding network dimensioning by an operator. The conclusion is that the usage and penetration ratio in a given target area can severely impact on the number of required cells, but also the average number of devices per person, since some sources project more than 5 devices connected to mobile networks, per person, in a few years.

4.4 Analysis of the Throughput at Cell Edge

The purpose of this analysis is to infer the requirement in terms of percentage of RBs allocated to the cell edge to ensure that there is always a nominal throughput available at this region. For this, it is necessary to establish a maximum percentage of resource blocks associated to the cell edge region, which will define the maximum achievable throughput and then define the cell radius.

In order to understand the impact of numerology on the available throughput at cell edge, one must be aware of yet another cell-radius reduction process in the model. In the dimensioning process, the cell radius can not only be reduced to make it possible to avoid capacity overload, but it can also be reduced to meet the throughput requirement at cell edge. Since as the radius decreases the SNR increases, and thus the available throughput per RB increases, the total available throughput also increases.

This being said, a proper analysis on this process should consider a user density of zero, which sets the threshold for the maximum available throughput, that is to say, it provides a theoretical maximum if the cell is void of users. Any user density different from zero yields a lower throughput at the cell edge. In order to infer the highest throughput value for each configuration, the algorithm computes every hypotheses while the radius is higher than a minimum pre-defined radius value, which for this simulation is 100 m, otherwise in some cases the algorithm would keep reducing the cell radius until a zero distance. Hence, Table 4.10 and Table 4.11 represent the throughput values for a coverage-limited cell.

Table 4.10. Maximum throughput at cell edge with 10% RBs allocated (DL).

Band [MHz]	**SCS [kHz]**	**Maximum Throughput [Mbit/s]**								
		5	**10**	**15**	**20**	**40**	**50**	**60**	**80**	**100**
700	15	**4.4**	**8.8**	**11.8**	**16.2**	×	×	×	×	×
	30	×	**8.8**	**11.7**	**17.7**	×	×	×	×	×
	60	×	×	×	×	×	×	×	×	×
3 500	15	×	**7.6**	×	**13.9**	**27.9**	**35.4**	×	×	×
	30	×	**6.8**	×	**13.6**	**24.9**	**31.8**	**38.6**	**49.9**	**63.5**
	60	×	**4.2**	×	**12.5**	**25.0**	**29.1**	**33.3**	**45.8**	**58.2**

Table 4.11. Maximum throughput at cell edge with 10% RBs allocated (UL).

Band [MHz]	**SCS [kHz]**	**Maximum Throughput [Mbit/s]**								
		5	**10**	**15**	**20**	**40**	**50**	**60**	**80**	**100**
700	15	**4.4**	**8.8**	**11.8**	**16.2**	×	×	×	×	×
	30	×	**8.8**	**11.7**	**17.6**	×	×	×	×	×
	60	×	×	×	×	×	×	×	×	×
3 500	15	×	**6.2**	×	**11.4**	**22.9**	**29.1**	×	×	×
	30	×	**5.5**	×	**10.9**	**20.0**	**25.5**	**30.9**	**40.0**	**50.9**
	60	×	**2.9**	×	**8.6**	**17.3**	**20.2**	**23.0**	**31.7**	**40.3**

The differences between the throughput values at 0.7 and 3.5 GHz for the same bandwidth may have

to do with the fact that the algorithm keeps the cell-radius reducing process while the radius is above 100 m. Since the MAPL for 0.7 GHz is larger than for 3.5 GHz, this results in existing a higher SNR value, which yields a higher throughput per RB at the given cycle/process radius. The same logic can be applied to explain the higher throughput values at DL since the MAPL is higher than at UL, yielding the same logical conclusion of a higher throughput per RB and thus presenting higher TP values for the same frequency and bandwidth configurations.

In the course of the simulations, it has been proved that the throughput value per frequency and bandwidth configuration is proportional to the share percentage of bandwidth allocated to the cell edge, hence if one seeks to find the values for 20% the only necessary step is to multiply Table 4.10 and Table 4.11 throughput values by 2. Figure 4.15 presents a comprehensive perspective on how throughput varies according to the minimum and maximum possible spectrum configurations (0.7 GHz / 5 MHz vs 3.5 MHz / 100 MHz) for both DL and UL, with different cell capacity loads. The percentage of dedicated bandwidth at cell edge is limited to the point of only guaranteeing the required throughput level, which is set to 2 Mbit/s, default value. That is to say, a value of 10% is set, but if that yields a much higher throughput at cell edge than the required, the model reduces this percentage. Hence, the results in Figure 4.15 are taken with this detail into consideration.

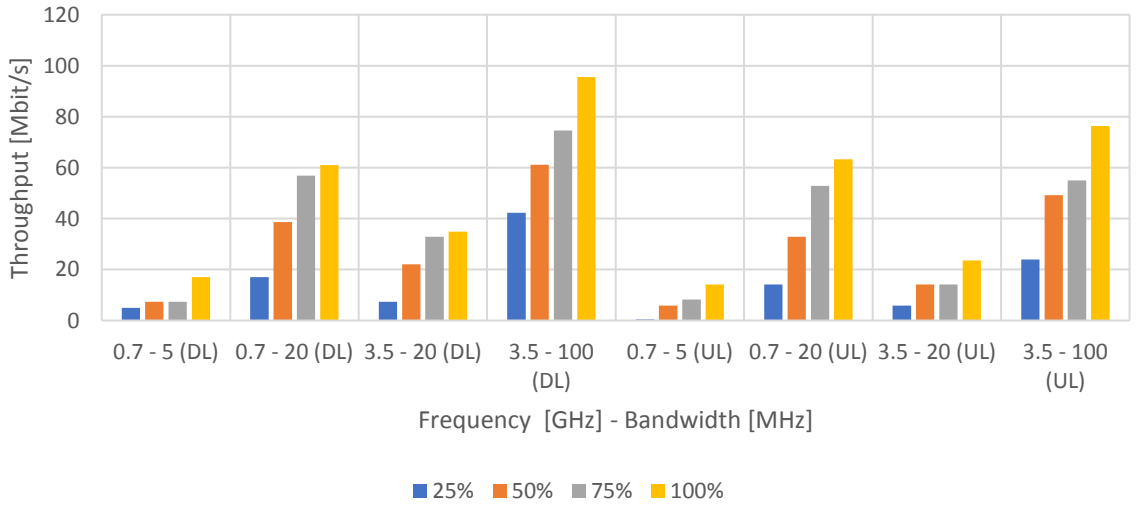

Figure 4.15. Global cell capacity per frequency and bandwidth, for DL and UL, with different cell load percentages.

As it would be expected, the increase in the maximum allowable cell load percentage leads to cells having a much higher global throughput capacity, that is, the sum of every user service's TP. From Figure 4.15, one can notice that the minimum global cell throughput capacity is close to 18 Mbit/s at 0.7 GHz (100% cell load) with a 5 MHz bandwidth and about 96 Mbit/s at 3.5 GHz with a 100 MHz one.

These global cell capacity values are far from the values provided in the literature, both in papers, standards and reports from different entities, i.e., far from the threshold of the several Gbit/s. This happens essentially for two reasons. The first one is that the maximum bandwidth per cell currently defined as valid by 3GPP is 100 MHz without considering yet the perspective of carrier aggregation. The second one is that for the spectrum considered in this thesis the vast majority of devices do not support a MIMO configuration higher than 2x2, hence cell capacity is closer to the values from the

already deployed LTE networks than the ones provisioned for 5G-NR, which typically consider mm-wave spectrum (e.g., 28 GHz) with bandwidths up to 500 MHz and MIMO order up to 64x64 in BSs and 8x8 (smartphones) or 16x16 (tablets), which are the key contributors for the global cell capacity in the Gbit/s.

Also, comparing both frequency bands with a bandwidth of 20 MHz, the total cell capacity is higher at 0.7 than 3.5 GHz, which has to do with the fact there are fewer obstructions limiting the signal at 0.7 GHz and thus larger cell radii, which leads to a higher number of active users per cell and therefore a higher cell capacity throughput. Furthermore, the lower capacity at UL may have to do with the, also, on average, lower cell radius due to a lower MAPL imposed by the model reference parameters.

4.5 Bandwidth and Frequency Band Analysis

The goal of this section is to analyse the impact in terms of spectrum configuration, such as numerology, frequency and bandwidth, in the network in terms of cell radius and in the total number of cells. The cell radius computed from the maximum path loss and the path loss given by the propagation model can vary due to the impact of numerology, which consists of different SCS values. Hence, for example, numerology 0 (15 kHz) will yield a higher distance than numerology 2 (60 kHz) due to the lower required sensitivity power. Simulations are presented for every valid numerology configuration for both frequency bands using the same bandwidth value (20 MHz), as seen in Figure 4.16 and Figure 4.17.

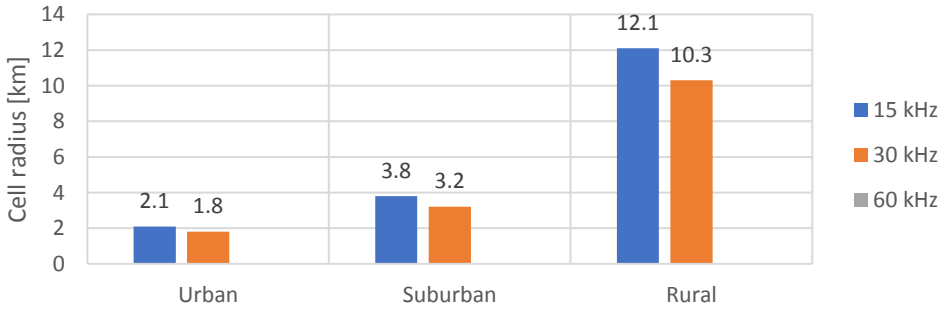

Figure 4.16. Maximum cell radius per numerology (0.7 GHz / 20 MHz).

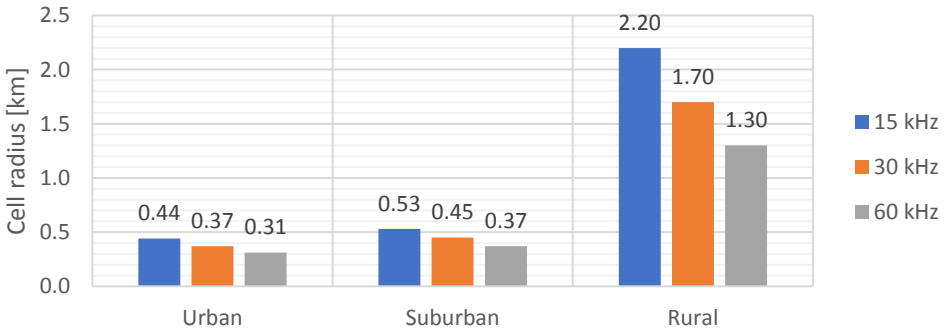

Figure 4.17. Maximum cell radius per numerology (3.5 GHz / 20 MHz).

As it would be expected, within the same environment type the maximum cell radius is higher for the 0.7 GHz band and lower for the 3.5 GHz band, and as the numerology configuration increases the cell radius is reduced. The next analysis consists of comparing the number of required cells for both frequency bands when considering the valid bandwidth values defined by 3GPP, displayed in Figure 4.18. For this analysis, all numerology configurations are considered respecting the limitations imposed by 3GPP, and the total number of cells using the model reference parameters is obtained for each bandwidth value.

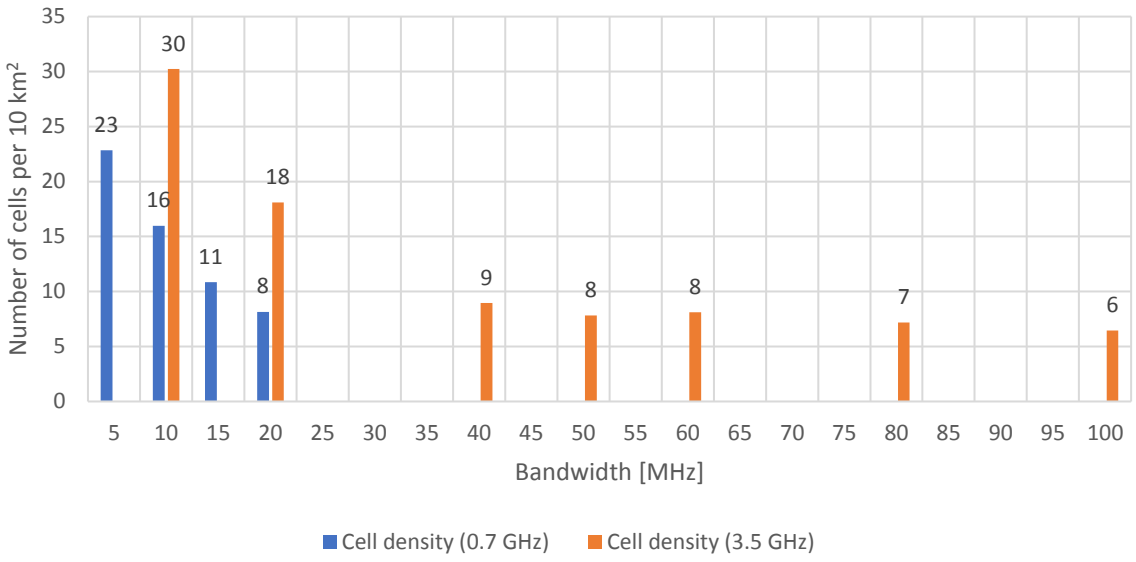

Figure 4.18. Site density for all 3GPP valid spectrum configurations.

In general terms, as the available bandwidth in the cell increases the number of possible users that can be served also increases. This can be seen in Figure 4.18, for both frequency bands, with the decreasing cell density values as the bandwidth increases. Since each cell has a higher capacity it will require less iterations, e.g., cell radius reduction cycles, to find the optimal radius necessary to fulfil both the throughput at the edge requirement and the global capacity requirements.

For the traffic profile considered in this thesis one finds, for the 3.5 GHz band, that increasing the bandwidth serves of no usefulness from a certain threshold value, that is to say from 40 MHz on the difference in cell density is not very significant. This may be an indication that for this traffic profile an operator would not need more than 40 MHz in order to find a compromise between cost in terms of number of cells and of serving their customers. As it would be expected, the number of required cells for the same bandwidth is much higher at the higher frequency (3.5 GHz) than in the lower one (0.7 GHz).

This can be explained by average cell radius at the lower frequency being higher, while serving the same traffic profile as in the higher frequency, due to the lower path loss attenuation, both in outdoor and indoor environments. This metric is an indicator as to why the spectrum at the lower frequency bands is more expensive, since they require fewer cells installed in the same target geographical area.

4.6 Analysis of Coverage Probabilities

The coverage probability in the cellular network dimensioning is essentially a metric matching a certain cell radius to the percentage of signal power being above the threshold to users. It is defined as the slow fading margin and thus as a safety factor to "*determine the probability of successful radio communication"* [Alco17]. A higher coverage probability is related to having a higher chance of receiving the signal with a power above the minimum, and thus the cell radius is shorter.

Two municipalities per propagation scenario are chosen to simulate the effects on changing the coverage probability for both indoors and outdoors, taking the different indoors standard values for the 0.7 and 3.5 GHz. From Table 4.12 and Table 4.13, one can see which are likely to be coverage or capacity limited. If the device density is low, typically in rural settings (ID 125 and 42) the tendency is to have coverage-limited cells, hence there is a considerable decrease in the cell radius as the coverage probability increases, either indoors or outdoors. On the other hand, if the device density is higher, typically in urban settings (e.g., ID 10), the cell is more likely to be capacity-limited and an increase in the probability does not yield a cell radius decrease as big as in the low device density, rural scenarios.

Table 4.12. Cell radius vs coverage probability (0.7 GHz).

ID	District	Type	Cell radius [km]					
			Outdoor coverage probability [%]			Indoor coverage probability [%]		
			85 %	90 %	95 %	85 %	90 %	95 %
10	**Belém**	U	0.53	**0.53**	0.53	0.53	**0.53**	0.52
53	**Cascais**	U	0.52	**0.52**	0.51			
75	**Ericeira**	S	0.89	**0.80**	0.73	0.85	**0.80**	0.75
92	**Loures**	S			0.76			
125	**V.F de Xira**	R	2.77	**2.77**	2.61	3.19	**2.77**	2.77
42	**Terrugem**	R	1.71	**1.71**	1.71	1.73	**1.71**	1.71

Table 4.13. Cell radius vs coverage probability (3.5 GHz).

ID	District	Type	Cell radius [km]					
			Outdoor coverage probability [%]			Indoor coverage probability [%]		
			85	90	95	85	90	95
10	**Belém**	U	0.32	**0.29**	0.24	0.30	**0.29**	0.27
53	**Cascais**	U						
75	**Ericeira**	S	0.39	**0.35**	0.29	0.36	**0.35**	0.33
92	**Loures**	S						
125	**V.F de Xira**	R	1.94	**1.77**	1.36	1.89	**1.77**	1.64
42	**Terrugem**	R	1.35	**1.23**	1.23	1.31	**1.23**	1.19

Therefore, the conclusion is that when cells are limited by capacity the average radius yields a, generally, similar number of cells regardless of the coverage probabilities, assuming the case under study with 85, 90 and 95%. The number of cells per municipality with the different coverage probability values for indoors and outdoors, for both frequency bands, is shown in Figure 4.19 and Figure 4.20.

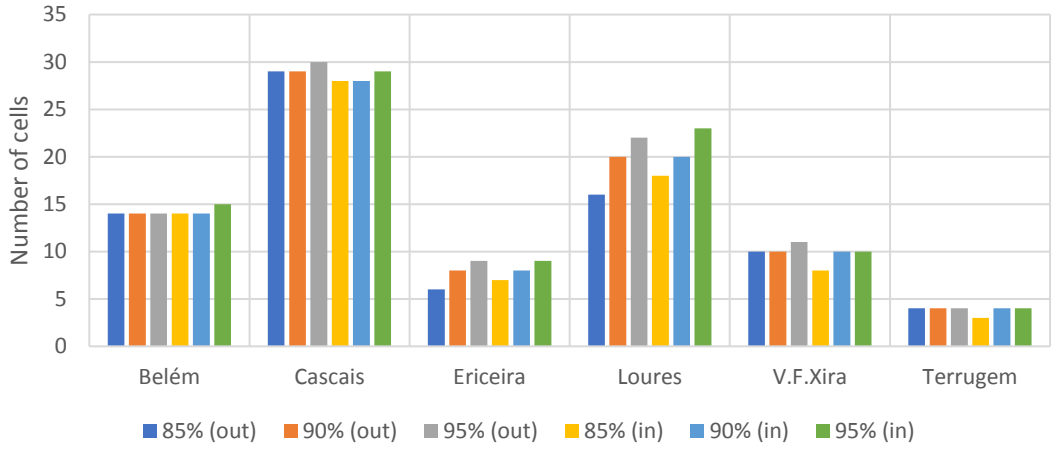

Figure 4.19. Number of cells from different coverage probability values (0.7 GHz / 20 MHz).

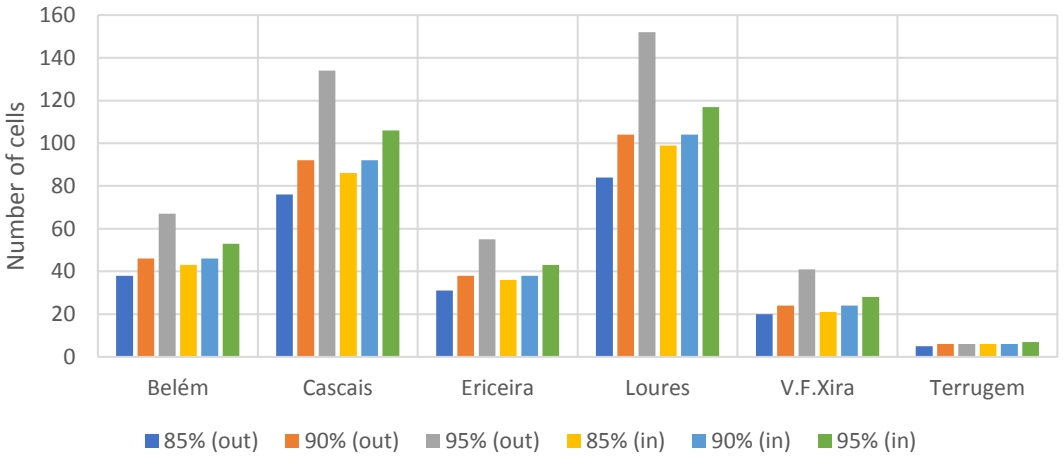

Figure 4.20. Number of cells from different coverage probability values (3.5 GHz / 20 MHz).

The lower the coverage probability the higher the cell radius, which leads to more active users in the current model cycle and to a capacity overload situation. It can be established that the lower the coverage probability the higher chances are of having a capacity limited cell, and in the opposite having coverage limited cells is more likely when the coverage probability increases. Therefore, as the cell radius is higher with a lower coverage percentage, fewer cells are required.

Furthermore, the number of cells in the 0.7 GHz band does not suffer from much increase either changing the indoors or outdoors coverage probabilities, due to the higher signal penetration capability at this band. On the other hand, at 3.5 GHz the increase in the number of cells by changing the probability is much more noticeable. With a higher mean combined path loss (outdoors and indoors) and higher standard deviation values, the signal is much more prone to suffer from obstacles and lose power, which can be seen in Figure 4.20.

4.7 Traffic Profile Analysis

The goal of this section is to analyse the impact of different traffic profile configurations on the average cell radius for each environment, and thus the impact on the total number of required cells. The model reference traffic profile consisted of a list of services and associated mix share for DL and UL, for a residential environment. Now there are two other environments in use, office and mixed.

In order to have a means of comparison, the geographical target area of this section is the urban area of Lisbon, present in Figure 4.21, and the percentages of each environment are the same as given by the reference values in [Alco17]. This share of environment in the user profile has to do with the fact that in real deployments one does not have only residential or only business-like traffic profiles, but that situations a mix of both can exist.

The throughput values per service are the same regardless of the user profile environment, and since the percentage of indoors and outdoors users is also considered to be fixed regardless of the environment, the only varying parameter is the mix share of each service.

Figure 4.21. Municipalities in the urban and city area of Lisbon considered for the current simulation.

In the model reference parameters in use for previous simulations, the traffic profile is split into DL and UL. However, to simplify the analysis in this section one considers the profile for DL as the same for UL, shown in Table 4.14, with the service throughput values those defined in the model reference parameters in Section 4.1. The mix share values are not the same as those defined in the work of [Alco17] due to the inclusion of new services such as MMTC,

Table 4.14. Traffic profile values for Residential, Office and Mixed (based on [Alco17]).

Service name	Service mix per scenario [%]		
	R	O	M
Voice	15	20	17.5
Chat	15	10	12.5
Video conference	10	20	15.0
Video streaming	20	5	12.5
Music streaming	10	5	7.5
Web browsing	15	20	17.5
MMTC	5	7	6.0
File sharing	5	6	5.5
Email	5	7	6.0

The simulations were made with the 3.5 GHz band and a bandwidth of 20 MHz. The number of cells for each scenario partition configuration is given in Table 4.15.

Table 4.15. Number of cells for each scenario partition, with different traffic profiles.

Traffic profile environment	Number of cells	Scenario partition [%]		Number of cells	
		Reference	ROM	Reference	ROM
Residential	605	100	60	605	363
Office	583	0	30	0	175
Mixed	596	0	10	0	60
Total		**100**	**100**	**605**	**598**

The number of cells from the ROM configuration in Table 4.15 is assumed to be the reference in this analysis, which can be compared with some service-centric scenarios. In this case, these are the video-centric and voice-centric scenarios where the services' mix share is much higher than the one in the reference ROM configuration. They are defined in Table 4.16 from the reference values of [Alco17]. Then, the total number of cells in the video and voice-centric traffic profiles are present in Table 4.17 and Table 4.18 for the reference and ROM scenario partition values, and are represented in Figure 4.22.

In Figure 4.22, the impact of video-centric scenario's highest throughput and mix share for the video services can be noticed, since it leads to the highest cell density, while in the voice-centric scenario the low throughput values of this service, even with high service mix share, produces a cell density value just slightly below the average value found in the default/reference configuration. Furthermore, using the reference mix share from the model traffic profile reference parameters, the analysis on the impact of each service throughput value on the number of cells can be observed in the values from Table 4.19, which are based on those from [Alco17] and some of the reference values in Section 2.4.

Table 4.16. Service mix scenarios (based on [Alco17]).

Service name	Service mix per scenario [%]					
	Video-centric			Voice-centric		
	R	O	M	R	O	M
Voice	5	20	12.5	47	40	43.5
Chat	5	5	5	5	5	5
Video conference	7	10	8.5	5	7.5	6.25
Video streaming	40	20	30	18	10	14
Music streaming	8	10	9	5	7.5	6.25
Web browsing	22	20	21	5	15	10
MMTC	5	5	5	5	5	5
File sharing	4	5	4.5	5	5	5
Email	4	5	4.5	5	5	5

Table 4.17. Number of cells for each scenario partition with video-centric traffic profile.

Traffic profile environment	Number of cells	Scenario partition [%]		Number of cells	
		Reference	ROM	Reference	ROM
Residential	703	100	60	703	422
Office	634	0	30	0	191
Mixed	678	0	10	0	68
Total		100	100	703	681

Table 4.18. Number of cells for each scenario partition with voice-centric traffic profile.

Traffic profile environment	Number of cells	Scenario partition [%]		Number of cells	
		Reference	ROM	Reference	ROM
Residential	591	100	60	591	355
Office	556	0	30	0	167
Mixed	561	0	10	0	57
Total		100	100	591	579

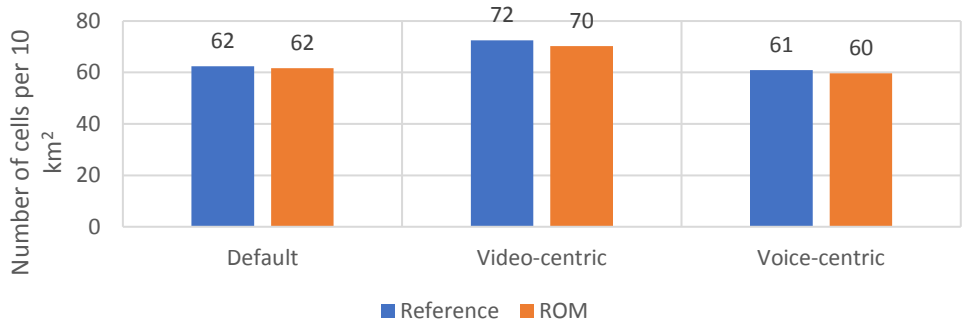

Figure 4.22. Cell density per traffic profile scenario (3.5 GHz / 20 MHz).

Table 4.19. Throughput-varying scenarios (based on [Alco17]).

Service name	Throughput [Mbit/s]		
	Min	Ref.	Max
Voice	0.009	0.032	0.036
Chat	0.231	0.384	0.422
Video conference	1	2	4
Video streaming	2	5	10
Music streaming	0.176	0.196	0.294
Web browsing	1	2	4
File sharing	1	2	4
MMTC	0.05	0.1	1
Email	0.819	1	1.5
Number of cells	**530**	**638**	**757**

The cell density for each throughput configuration with the default traffic profile is shown in Figure 4.23.

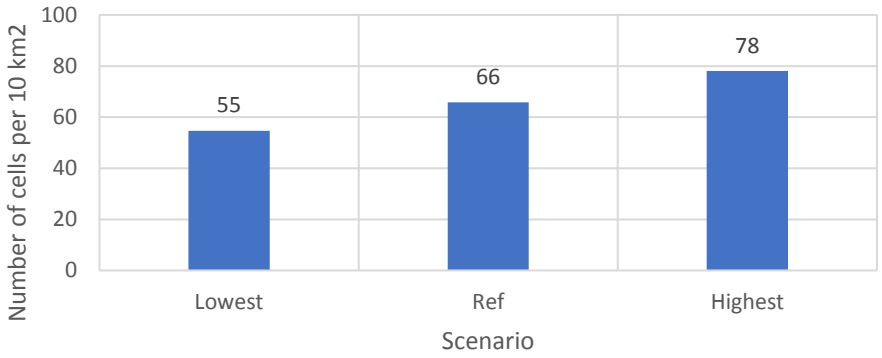

Figure 4.23. Cell density per throughput configuration (3.5 GHz / 20 MHz).

The increase in the average throughput per service leads to a higher number of cells, as it would be expected, since the increase of necessary RBs to serve the traffic profile leads to lower cell radii and higher cell densities. Hence, the difference in the number of cells between the lowest and highest throughput scenarios is about 40%. However, using other spectrum configurations, such as the highest throughput scenario with a 5 MHz bands could lead to an increase of much more than 40%, while with a 100 MHz band the difference could be lower than 40%.

Chapter 5

Conclusions

This chapter summarises all the carried-out work by presenting the main topics related to the model development and results. In the end, a few recommendations for future work are presented.

The main goal of this thesis was to develop a dimensioning and cellular network planning tool for the near-future and early 5G-NR deployments over several propagation scenarios and different input scenarios, in order to understand the impact on the number of required cells in the network. To assess this impact on the number of cells, a model was developed, and some simulations were done to provide an overview on the impact on network performance of different user densities, municipality areas, spectrum options in terms of frequency and bandwidth, as well the impact of numerologies in the allocation of RBs in 5G-NR. Furthermore, some variations in the context of traffic profile are performed, in terms of service throughput, service share percentages and different traffic profile configuration shares in some municipalities.

The northern part of the metropolitan region of Lisbon was chosen as the reference scenario for two reasons. The first that it presents a diverse enough deployment area with very different values of user density and area per municipality, and the second is that it would serve as a measure of comparison to works of [Alco17] with LTE in some of the simulation results. Although the simulations were done taken for the northern Lisbon database of 125 municipalities, the model is able to accept any municipality database as long as the format is the same, e.g., with municipality area, user and device density. Besides the model is also able to accept any traffic profile configuration with any number of services, as long as the priority, mix share and throughput values are defined.

Chapter 1 presents a generic and brief description of the mobile communications panorama and the current standards in terms of 5G-NR deployment from different entities, manufacturers and operators, followed by a short description of the motivation and contents that compose the core of this thesis. In Chapter 2, a transversal and theoretical description is made on the fundamental aspects of 5G-NR, regarding network architecture, radio interface, coverage and capacity characteristics, and at last the services and applications (use cases) that are expected to be supported, generically, in 5G networks as the deployment phases advance time-wise. The chapter ends with a description on the state of the art concerning some of the available elements that relate to the core study of this thesis, coverage and capacity elements, and are divided into academic theses, industry reports and official papers from telecommunications entities.

Chapter 3 is composed of the description and implementation of the most relevant and important assumptions, equations and models for the simulator development. The simulator has the purpose of providing a generic dimensioning tool with a certain degree of abstraction, i.e., a number of assumptions are considered in order to reduce the overall model complexity, such as assuming that users are uniformly distributed in the cell or that all numerologies in the model input configuration are always available for capacity processing independently of user location and distance to the BS, while the sensitivity power restricts the use of some numerologies to a certain distance. An user uniform distribution in the cell assumption is limited in one aspect. The area corresponding to the MCS region of QPSK is always higher than the others, e.g., 16-QAM, which leads to having a much higher number of users within the MCS region of QPSK and since it is the farthest MCS region from the BS, the SNR value is much lower, which requires much more RBs to serve these users. The consequence of this

assumption is that the number of RBs computed in the model is tendentially considerably higher than the ones in real-life cells, and with lower cell radii due to cell reduction iterations (traffic or radius wise) this means the number of cells outputted by any simulation may very likely be higher than the one for a real-life scenario.

The expressions for the throughput calculation from the user's SNR are given in Annex A based on the works of [Belc18] and [Alco17]. Some basic features from the traffic load calculation are retrieved from the works of [Alco17], however the inclusion of numerologies due to the novelty network elements of 5G-NR add a completely new layer in the capacity related algorithms in the model. The model performs an evaluation for both DL and UL, with respective different link budget parameters and different traffic profile configurations, then for each simulation or municipality, it picks the worst case, i.e., the channel with lowest cell radius, or with highest number of cells. Furthermore, Chapter 3 includes the model implementation where a description on the most relevant and important routines in the model are done, finishing with the model assessment, where a battery of tests were performed to verify the coverage and capacity models independently as the model was being developed.

The coverage assessment has started with the verification of the path loss and propagation distance results between the manual computation, in Excel, and the results provided by the simulator. Then, the cell radius did change as the frequency band increased for both propagation models and from different input parameters, such as the required throughput at cell edge, the BS and the MT heights. Besides, the cell radius did decrease with the increase of the MCS (from QPSK to 256-QAM) and also decreased more when applying the high-loss indoor pathloss than the low-loss indoor path loss model, as it would be expected. The final output is the number of cells did increase while the frequency band increased.

The capacity assessment has started with the verification of the uniqueness process of randomly allocating users in each MCS region and the number of RBs required by each user given its throughput requirement and available throughput configurations in terms of numerologies and MCS curves, through means of scientific calculator, Excel and model results comparison. The number of users per cell increased generically when the user density increased, and the number of allocated RBs and bandwidth increased as the overall service throughput values increased. Furthermore, the cell radius is seen to decrease as the user density increased, which represents the cell radius reduction routine, and the throughput at the cell edge doubles when the reserved bandwidth doubles, as it would be expected. At last, the cell radius is never higher than the distance given by using only the lowest numerology configuration, which yields the highest distance, and the cell radius is never lower than the distance given by only using the highest numerology configuration, which yields the lowest distance, which is an expected result.

In Chapter 4, the reference scenario is described, which is divided into the model reference parameters, such as the link budget, numerologies in use, share of bandwidth at cell edge, among others, and the external references, such as the municipality database and the traffic profile configuration for both DL and UL. The results presented in the chapter are computed with the 0.7 and 3.5 GHz bands into consideration, except in the traffic profile analysis where only the 3.5 GHz band is considered in order

to compare the results with those from [Alco17] on some of the traffic profile configurations. The dual frequency band comparison is also considered to investigate the consequences on different path loss values either in outdoors either in indoors and on different bandwidth and numerology configurations, with different possible achievable capacities. Contrary to the work of [Alco17] where each frequency band has an associated bandwidth value, in this thesis the analysis is done at a higher and more transversal view, assuming all valid spectrum configurations from 3GPP in terms of frequency band, bandwidth and numerologies in use.

To start with, in Section 4.2 the number of cells is computed for every municipality and every environment, with the analysis being complemented with data such as the propagation environment share per municipality. The comparison of the number of cells between both frequency bands is done, using the same bandwidth value of 20 MHz, with different environment types and device densities and compared with the number of cells obtained in the simulator developed by [Alco17]. The main conclusion one can take is that no solid conclusion can be made by only considering the number of cells per municipality in both frequency bands. Hence, one should take other factors into consideration, such as the environment composition per municipality, the average number of devices per user or the set of mean and standard deviation values for the cell radius for all municipalities.

Cell limitation by coverage or capacity is an important concept that makes some results clearer. For instance, municipalities with strongly composed of urban environments do not suffer a much relative increase in the number of cells, since they are already mostly capacity limited at the lower frequency band, while municipalities strongly composed of suburban or rural environments are much more prone to suffering larger relative increase values in the number of cells. User and device densities are also another metric that can strongly influence the number of cells within a specific propagation environment, e.g., the municipality of Cascais and Oeiras have similar environment composition, but where the former has an 83% increase in the number of cells, while increasing the frequency the latter only has 37%, and this is because Cascais has almost the double device density compared to Oeiras. On the other hand, the municipalities with highest device density values, such as Lisbon, Amadora and Odivelas, are less likely to increase severely the number of cells when increasing frequency, the increase is merely around 20%.

Furthermore, the cell radius histogram for both frequency bands shows a clear shift to lower cell radius values when the frequency increases, as well as the relative percentage of cell radii lower than 500 m which increases from 52.4% to 66.7% as the frequency increases. At last, with the purpose of validating the results from the simulator, a brief comparison is made between the results obtained from [Alco17] at 2.6 GHz and the results from Section 4.3 at 3.5 GHz. The traffic profile is the same, as well as the bandwidth, with some minor changes such as numerologies. Nevertheless, the number of cells per 10 km^2 in LTE's 2.6 GHz is 32, 16 and 1 in the urban, suburban and rural scenarios, while for 5G-NR's 3.5 GHz the number of cells is 38, 23 and 2 per 10 km^2, which is in agreement with the increase in the number of cells as the frequency increases.

In Section 4.3, the impact of active device density on the number of required cells is studied. The

reference scenario is a penetration ratio of 15%, an usage ratio of 10% and an average device per user of 1.5. The product of these metrics produces the reference percentage for how much of the population density is active in the network, and the impact of increasing this product on the number of extra required cells is studied through the number of cells growth factor. For a bandwidth value of 20 MHz an empirical relationship is obtained, where an increase factor of 2, 4 and 8 from the reference produces an increase factor of 2, 4 (all propagation scenarios) and 5.5 (rural) / 7.3 (urban, suburban), respectively, are retrieved. Still, regardless of the precise interpolation values, the expected increase on the number of cells is approximately linear with the increase from the reference scenario.

In Section 4.4, the analysis on the throughput at the cell edge is done for both frequency bands for all valid spectrum configurations defined by 3GPP, for both channels (DL/UL), defining the minimum possible cell radius as 100 m. Furthermore, the impact of different imposed maximum cell load ratios in the global cell capacity, measured in Mbit/s, is studied for the minimum, average and maximum spectrum configurations, i.e., lowest frequency band with the lowest bandwidth, the lowest and highest frequency bands with the same bandwidth, and the highest frequency band with the highest bandwidth, for both channels. The impact of bandwidth in the achievable throughput is measured, where for instance, to achieve a throughput at cell edge of 20 Mbit/s one would need a bandwidth of at least 40 MHz at either frequency band.

In Section 4.5, the analysis is centred on the impact of different frequency bands, bandwidth and numerology configurations on the maximum cell radii distances by assuming a fixed bandwidth of 20 MHz for a certain user density. As it would be expected, the distance values at 0.7 GHz are much higher than the ones at 3.5 GHz mainly due to higher losses at the latter, and also the increase of numerology configuration, and thus in the SCS, leads to a requirement for higher sensitivity power (every doubling of SCS corresponds to more 3 dB) which reduces the overall cell radius, e.g., the decrease from 0.53 to 0.37 km in the suburban environment scenario at 3.5 GHz. Furthermore, assuming the model reference parameters and the reference traffic profile, the site density is computed for every valid 3GPP spectrum configuration. The number of cells at 0.7 GHz is much lower than 3.5 GHz for the same bandwidth values, which is essentially explained by the higher losses at the latter. For the remaining values, the cell density keeps decreasing until the bandwidth of 100 MHz, but at a much slower pace than from 5 to 40 MHz. This can be an indicator on the maximum required bandwidth to fulfil not only the current model reference parameters but also the reference traffic profile, e.g., if many more services are added or the average throughput increases considerably and the maximum deployment site density, for reasons of cost, is 9 cells per 10 km^2, in order to achieve this with the increase on the traffic load the required bandwidth could increase from 40 to 80 or 100 MHz.

In Section 4.6, the focus is on the analysis on the impact of some coverage probabilities, 85, 90 and 95%. This study is done for each environment type for both frequency bands using the same bandwidth value of 20 MHz. When the probability increases the cell radius decreases, due to the requirement for more users to be covered. The traffic profile is the same for every municipality in this section, thus the increase on the probability leads indirectly to a higher number of cells. In some cases, the increase of

the probability does not decrease the cell radius, which is an indicator that the cell is capacity-limited, while on the other hand if the cell radius decreases considerably, it is an indicator the cell is coverage-limited.

Lastly, Section 4.7 studies the impact on some changes on the traffic profile configurations in Lisbon. The change in the service mix share yields different traffic profiles (reference, video-centric, voice-centric) and the change in the throughput (minimum, reference, maximum) produce an estimation on the required cell density for each traffic profile configuration. The simulations provided the absolute number of cells to be lowest for the voice-centric scenario, with 579 cells, the reference with 598 and the video-centric with 681 cells with ROM. The higher mix share of the low-throughput voice-service leads to a lower capacity demand, which translates into fewer required cells, while a high throughput service leads to a significant increase in the number of cells (video-centric).

The traffic profile in this section is similar to the one from [Alco17], but some of the throughput values were increased to match the literature overview on higher throughput demands for some of the services. The impact of this increase can be seen on the number of cells per 10 km^2 in the reference, video and voice-centric scenarios in this thesis, {62, 70, 60} and in [Alco17] with {34, 44, 30}. In both results the density is higher for the video-centric, and for the varying throughput scenario, the same number of cells per 10km^2 is outputted for the lowest, reference and highest throughput cases with {55, 66, 78} in this thesis and {20, 33, 62} in [Alco17], which shows a similar increase when the throughput increases.

As a matter of future work, some recommendations that can be applied to this work are an algorithm that could pick the most efficient spectrum configuration for the characteristics for some specific sets of municipalities, since the available bandwidth each operator has may not be the same throughout the whole country, as well as the inclusion of other services or classes of services, such as, e.g., vehicular, which would require specific propagation models such as the vehicular WINNER II, or latency critical applications (URLLC) which would require an extra model layer, which would deal with the number of cells, distances and propagation times, which is somewhat similar to the works of [Silv16].

Additionally, some topics have been simplified in this thesis, such as the throughput and SNR relationship and the assumption that every numerology is available for capacity regardless of their maximum coverage distance from their different power sensitivity and other topics, which have not been covered at all, such as the issue of interference, carrier aggregation that could provide interesting results with the higher bandwidths available for the 3.5 GHz band, or the exclusion of some of the services expected to be included in future deployments but which are not yet confirmed to be released and commercially available in first 5G network deployments.

Annex A

SNR versus Throughput

This annex provides a description and overview on the formulas related to SINR and throughput in 5G for a given set of system configurations.

The relationship between SINR and throughput is established in this annex for different modulation scheme configurations. For QPSK, 16-QAM and 64-QAM, each one is associated with the median value of the coding rates (CRs) obtained from the Channel Quality Indicator (CQI) reported by the MT.

Regarding 256-QAM, the experimental relationship from [LLRP14] defines a 256/64-QAM gain of 23.1%, which is in a good level of agreement with [SKYW17] gain of 4/3 due to a different inferior to 10%. Hence, the 256-QAM expression is extrapolated from the 64-QAM in [Alco17] with the lower gain value of 23.1% from [LLRP14]. The coding rates and channel models for these MCS are defined in Table A.1.

Table A.1. MCS related parameters (extracted from [Alco17], [3GPP11], [LLRP14] and [SKYW17]).

Parameters	Modulation Scheme			
	QPSK	16-QAM	64-QAM	256-QAM
Coding Rate	1/3	1/2	3/4	[0.7; 0.9]
Channel Model	EPA5			EPA10

The relationship between the throughput per RB and its SINR, on a MIMO 2x2 configuration and with the coding rates of Table A.1 is defined by the equations:

For QPSK:

$$R_{b,QPSK[\text{bit/s}]} = \frac{2.34201 \cdot 10^6}{14.0051 + e^{-0.577897 \cdot \rho_{IN[\text{dB}]}}} \quad \text{(A.1)}$$

$$\rho_{IN,QPSK[\text{dB}]} = -\frac{1}{0.577897} \cdot \ln\left(\frac{2.34201 \cdot 10^6}{R_{b[\text{bit/s}]}} - 14.0051\right) \quad \text{(A.2)}$$

For 16-QAM:

$$R_{b,16QAM[\text{bit/s}]} = \frac{47613.1}{0.0926275 + e^{-0.295838 \cdot \rho_{IN[\text{dB}]}}} \quad \text{(A.3)}$$

$$\rho_{IN,16QAM[\text{dB}]} = -\frac{1}{0.295838} \cdot \ln\left(\frac{47613.1}{R_{b[\text{bit/s}]}} - 0.0926275\right) \quad \text{(A.4)}$$

For 64-QAM:

$$R_{b,64QAM[\text{bit/s}]} = \frac{26405.8}{0.0220186 + e^{-0.24491 \cdot \rho_{IN[\text{dB}]}}} \quad \text{(A.5)}$$

$$\rho_{IN,64QAM[\text{dB}]} = -\frac{1}{0.24491} \cdot \ln\left(\frac{26405.8}{R_{b[\text{bit/s}]}} - 0.0220186\right) \quad \text{(A.6)}$$

For 256-QAM:

$$R_{b,256QAM[\text{bit/s}]} = \frac{26407.1}{0.0178868 + e^{-0.198952 \cdot \rho_{IN[\text{dB}]}}} \quad \text{(A.7)}$$

$$\rho_{IN,256QAM[\text{dB}]} = -\frac{1}{0.198952} \cdot ln\left(\frac{26407.1}{R_{b[\text{bit/s}]}} - 0.0178868\right) \quad \text{(A.8)}$$

The equations are defined for MIMO 2x2 configuration. However, it may be useful to analyse the throughput-per-RB variation as the MIMO order increases due to it being a likely case for future 5G deployments. The SINR versus throughput relationship per RB in this annex is given for the numerology

0 configuration, with a subcarrier spacing of 15 kHz on a total RB bandwidth of 180 kHz. For other numerology configurations the relationship should be at maximum the same value as the ratio between the higher SCS and the standard of 15 kHz.

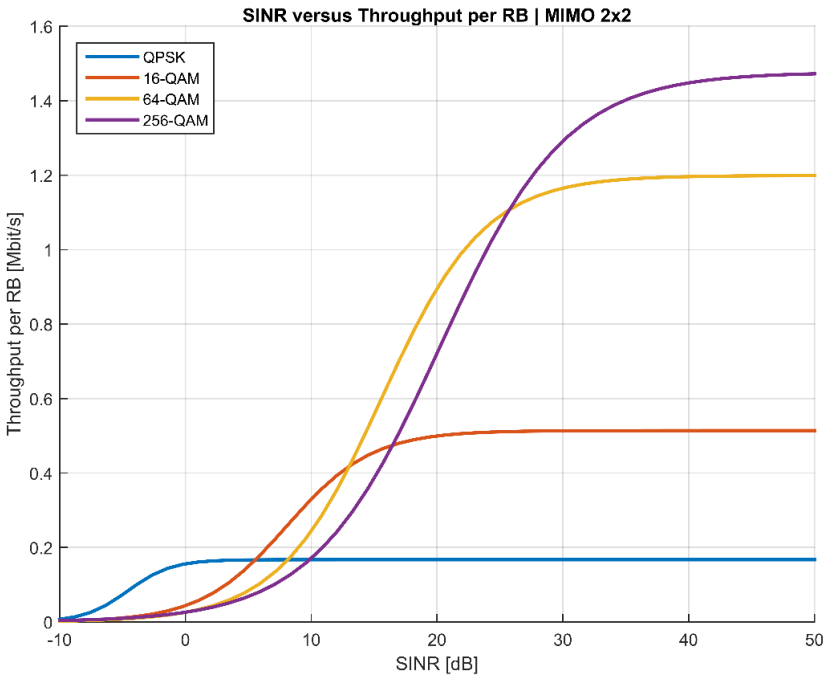

Figure A.1. SINR versus throughput per RB for MIMO 2x2

The maximum throughput per modulation scheme is established for the different MCS regions:

$$R_{b,max[\text{bit/s}]} = \begin{cases} \dfrac{2.34201 \cdot 10^6}{14.0051 + e^{-0.577897 \cdot \rho_{IN[\text{dB}]}}}, & \rho_{IN} < 5.5 \text{ dB} \\ \dfrac{47613.1}{0.0926275 + e^{-0.295838 \cdot \rho_{IN[\text{dB}]}}}, & 5.5\ dB \leq \rho_{IN} < 12.9 \text{ dB} \\ \dfrac{26405.8}{0.0220186 + e^{-0.24491 \cdot \rho_{IN[\text{dB}]}}}, & 12.9\ dB \leq \rho_{IN} < 25.5 \text{ dB} \\ \dfrac{26407.1}{0.0178868 + e^{-0.198952 \cdot \rho_{IN[\text{dB}]}}}, & 25.5\ dB \leq \rho_{IN} \end{cases} \quad \text{(A.9)}$$

The average SINR value per modulation scheme region is defined in Table A.2.

Table A.2. Average throughput per RB per modulation and SCS.

	QPSK	16-QAM	64-QAM	256-QAM
$\boldsymbol{\rho_{min}}$ **[dB]**	**-10**	**5.5**	**12.9**	**25.5**
$\boldsymbol{\rho_{max}}$ **[dB]**	**5.5**	**12.9**	**25.5**	**45**
$\boldsymbol{\overline{\rho_{[\text{dB}]}}}$	**-1.3**	**9.2**	**19.2**	**35.3**

Annex B

Propagation Models

This annex provides a description and overview on the propagation models used in the context of this thesis.

B.1. Radio Link Budget

The general formulation of the radio link budget and its parameters are described in this annex, based on the formulation from [Corr16].

$$P_{r_{[\mathrm{dBm}]}} = P_{t_{[\mathrm{dBm}]}} + G_{r_{[\mathrm{dBi}]}} + G_{t_{[\mathrm{dBi}]}} - L_{p,max_{[\mathrm{dB}]}} \quad \text{(B.1)}$$

where:

- P_t: power fed to the transmitting antenna
- G_r: gain of the receiving antenna
- G_t: gain of the transmitting antenna
- $L_{p,max}$: maximum path loss

The power fed to the antenna is defined by:

$$P_{t_{[\mathrm{dBm}]}} = P_{Tx_{[\mathrm{dBm}]}} - L_{t_{[\mathrm{dB}]}} \quad \text{(B.2)}$$

where:

- P_{Tx}: transmitter output power;
- G_r: gain of the receiving antenna;
- L_t: cable losses (between Tx and Rx, UL) or loss in the MT;

While the antenna received power is given by:

$$P_{r_{[\mathrm{dBm}]}} = P_{Rx_{[\mathrm{dBm}]}} - L_{r_{[\mathrm{dB}]}} \quad \text{(B.3)}$$

where:

- P_{Rx}: transmitter output power;
- G_r: gain of the receiving antenna;
- L_r: cable losses (between Tx and Rx, DL) or loss in the MT;

Therefore, the radio link budget can be expressed as:

$$L_{p,max_{[\mathrm{dB}]}} = P_{Tx_{[\mathrm{dBm}]}} - L_{t_{[\mathrm{dB}]}} - P_{Rx,min_{[\mathrm{dBm}]}} - L_{r_{[\mathrm{dB}]}} + G_{r_{[\mathrm{dBi}]}} + G_{t_{[\mathrm{dBi}]}} - I_{m_{[\mathrm{dB}]}} + G_{t_{[\mathrm{dBi}]}} + G_{Tx_{[\mathrm{dBi}]}} + G_{TMA_{[\mathrm{dBi}]}} \quad \text{(B.4)}$$

where:

- I_m: interference margin;
- G_{Tx}: diversity gain (MIMO order);
- G_{TMA}: Tower Mounted Amplifier;

The parameter in the radio link budget directly accounting for interference is the interference margin (I_m). Its value ranges from 2 to 4 dB in coverage-limited cells and 4 to 7 dB in capacity-limited cells [Alco17]. A Tower Mounted Amplifier (TMA) can reduce the BS figure noise (F_N) and compensate for cable losses at the cost of an insertion loss of 0.5 dB, typically, in DL.

Through the computation of maximum allowed propagation path loss for DL and UL and the use of appropriate propagation models, along with the SNR-throughput relationship, it is possible to calculate the maximum distance between the BS and the MT having a given throughput reference. Then, this

distance (cell radius) is used to determine the number of required cells to cover the desired coverage area. The mean cell-radius is defined as dependent on the share of indoors and outdoors users in B.5:

$$\overline{r_{cell_{[\mathrm{km}]}}} = p_{indoor_{[\%]}} \cdot \overline{r_{indoor_{[\mathrm{km}]}}} + p_{outdoor_{[\%]}} \cdot \overline{r_{outdoor_{[\mathrm{km}]}}} \quad \text{(B.5)}$$

where:

- p_{indoor}: percentage of users in indoors;
- $\overline{r_{indoor}}$: maximum/mean indoor radius;
- $p_{outdoor}$: percentage of users in outdoors;
- $\overline{r_{outdoor}}$: maximum/mean outdoors radius;

The percentage of users in indoors and outdoors is defined for the specific scenario in analysis. This means that depending on the scenario, it may not always be useful to compute its indoor or outdoor path loss.

B.2. Propagation Model - Okumura-Hata

The path-loss experienced by a signal between the BS and the MT in urban, suburban and rural scenarios at the 700 MHz band can be described by Okumura's original experimentation values.

$$L_{p_{[\mathrm{dB}]}} = L_{A_{[\mathrm{dB}]}} + L_{B_{[\mathrm{dB}]}} \cdot \log(d_{[\mathrm{km}]}) + L_{C_{[\mathrm{dB}]}} \quad \text{(B.6)}$$

$$d_{max,[\mathrm{km}]} = 10^{\frac{L_{p,max_{[\mathrm{dB}]}} - L_{A_{[\mathrm{dB}]}} - L_{C_{[\mathrm{dB}]}}}{L_{B_{[\mathrm{dB}]}}}} \quad \text{(B.7)}$$

where:

- L_A : correction factor related to the frequency, BS and UE antenna height, dependent on the propagation scenario;
- L_B : correction factor related to the BS antenna height;
- L_C : propagation scenario correction factor;

In which:

- $L_{A_{[\mathrm{dB}]}} = 69.55 + 26.16 \cdot \log(f_{[\mathrm{MHz}]}) - 13.83 \cdot \log(h_{BS_{[\mathrm{m}]}}) - \alpha(h_{mt_{[\mathrm{m}]}})$ (B.8)
- $L_{B_{[\mathrm{dB}]}} = 44.90 - 6.55 \cdot \log\left(h_{BS_{[\mathrm{m}]}}\right)$ (B.9)

where:

Urban	$\alpha(h_{m_{[\mathrm{m}]}}) = [1.1 \cdot \log(f_{[\mathrm{MHz}]}) - 0.7] \cdot h_{m_{[\mathrm{m}]}} - [1.56 \cdot \log(f_{[\mathrm{MHz}]}) - 0.8]$	(B.10)
	$L_{C_{[\mathrm{dB}]}} = 0$	(B.11)
Suburban	$\alpha(h_{m_{[\mathrm{m}]}}) = [1.1 \cdot \log(f_{[\mathrm{MHz}]}) - 0.7] \cdot h_{m_{[\mathrm{m}]}} - [1.56 \cdot \log(f_{[\mathrm{MHz}]}) - 0.8]$	(B.12)
	$L_{C_{[\mathrm{dB}]}} = -2 \cdot \log\left(\frac{f_{[\mathrm{MHz}]}}{28}\right)^2 - 5.4$	(B.13)
Rural	$\alpha(h_{m_{[\mathrm{m}]}}) = [1.1 \cdot \log(f_{[\mathrm{MHz}]}) - 0.7] \cdot h_{m_{[\mathrm{m}]}} - [1.56 \cdot \log(f_{[\mathrm{MHz}]}) - 0.8]$	(B.14)
	$L_{C_{[\mathrm{dB}]}} = -4.78 \cdot \log\left(f_{[\mathrm{MHz}]}\right)^2 + 18.33 \cdot \log(f_{[\mathrm{MHz}]}) - 40.98$	(B.15)

B.3. Propagation Model – WINNER II

The path-loss experienced by a signal travelling between the BS and the UE can be calculated from the WINNER II model, with a valid frequency from 2 to 6 GHz, according to [WINN07]. The model parameters have been developed from measurements carrier both from WINNER and from open literature results. It is valid for different antenna heights.

$$L_{p_{[\mathrm{dB}]}} = \mathrm{A}\log(d_{[\mathrm{m}]}) + B + C\log(\frac{f_{[\mathrm{GHz}]}}{5.0}) \quad \text{(B.16)}$$

where:

- A : path loss exponent;
- B : intercept parameter;
- C : path loss frequency dependence;

This model accounts for penetration losses in some propagation scenarios. The summary table of the WINNER II propagation model parameters is defined in Table B.1 (path-loss), Table B.2 (distance) and Table B.3 (path-loss). The breakpoint distance is defined, which can be formulated by:

$$d_{BP_{[\mathrm{m}]}} = 4 \cdot h_{m_{[\mathrm{m}]}} \cdot h_{BS_{[\mathrm{m}]}} \cdot \frac{f_{[\mathrm{Hz}]}}{c_{[\mathrm{m/s}]}} = \frac{40}{3} \cdot h_{m_{[\mathrm{m}]}} \cdot h_{BS_{[\mathrm{m}]}} \cdot f_{[\mathrm{GHz}]} \quad \text{(B.17)}$$

$$d'_{BP_{[\mathrm{m}]}} = 4 \cdot (h_{m_{[\mathrm{m}]}} - 1) \cdot (h_{BS_{[\mathrm{m}]}} - 1) \cdot \frac{f_{[\mathrm{Hz}]}}{c_{[\mathrm{m/s}]}} = \frac{40}{3} \cdot (h_{m_{[\mathrm{m}]}} - 1) \cdot (h_{BS_{[\mathrm{m}]}} - 1) \cdot f_{[\mathrm{GHz}]} \quad \text{(B.18)}$$

Table B.1. WINNER II path-loss equations (extracted from [WINN07]).

Scenario		**Path Loss [dB]**	$\sigma_{[dB]}$	**Validity Range / Default Values**
C1 – Suburban (macro-cell)	**LOS**	$A = 23.8$, $B = 41.2$, $C = 20$	4	$30\ \mathrm{m} < \mathrm{d}_{[\mathrm{m}]} < d_{BP_{[\mathrm{m}]}}$
		$L_{p_{[\mathrm{dB}]}} = 40 \cdot \log(d_{[\mathrm{m}]}) + 11.65 - 16.2 \cdot \log(h_{BS_{[\mathrm{m}]}}) - 16.2 \cdot \log(h_{m_{[\mathrm{m}]}}) + 3.8 \cdot \log(\frac{f_{[\mathrm{GHz}]}}{5})$	6	$d_{BP_{[\mathrm{m}]}} < \mathrm{d}_{[\mathrm{m}]} < 5\ \mathrm{km}$
				$h_{BS} = 25\ \mathrm{m}$, $h_m = 1.5\ \mathrm{m}$
	NLOS	$L_{p_{[\mathrm{dB}]}} = [44.9 - 6.55 \cdot \log(h_{BS_{[\mathrm{m}]}})] \cdot \log(d_{[\mathrm{m}]}) + 31.46 + 5.83 \cdot \log(h_{BS_{[\mathrm{m}]}}) + 23 \cdot \log(\frac{f_{[\mathrm{GHz}]}}{5})$	8	$50\ \mathrm{m} < \mathrm{d}_{[\mathrm{m}]} < 5\ \mathrm{km}$
				$h_{BS} = 25\ \mathrm{m}$, $h_m = 1.5\ \mathrm{m}$
C2 – Urban (macro-cell)	**LOS**	$A = 26$, $B = 39$, $C = 20$	4	$10\ \mathrm{m} < \mathrm{d}_{[\mathrm{m}]} < d'_{BP_{[\mathrm{m}]}}$
		$L_{p_{[\mathrm{dB}]}} = 40.0 \cdot \log(d_{[\mathrm{m}]}) + 13.47 - 14 \cdot \log(h_{BS_{[\mathrm{m}]}} - 1) - 14 \cdot \log(h_{m_{[\mathrm{m}]}} - 1) + 6 \cdot \log(\frac{f_{[\mathrm{GHz}]}}{5})$	6	$d'_{BP_{[\mathrm{m}]}} < \mathrm{d}_{[\mathrm{m}]} < 5\ \mathrm{km}$
				$h_{BS} = 25\ \mathrm{m}$, $h_m = 1.5\ \mathrm{m}$
	NLOS	$L_{p_{[\mathrm{dB}]}} = [44.9 - 6.55 \cdot \log(h_{BS_{[\mathrm{m}]}})] \cdot \log(d_{[\mathrm{m}]}) + 34.46 + 5.83 \cdot \log(h_{BS_{[\mathrm{m}]}}) + 23 \cdot \log(\frac{f_{[\mathrm{GHz}]}}{5})$	8	$50\ \mathrm{m} < \mathrm{d}_{[\mathrm{m}]} < 5\ \mathrm{km}$
				$h_{BS} = 25\ \mathrm{m}$, $h_m = 1.5\ \mathrm{m}$

Table B.2. WINNER II distance equations (extracted from [WINN07]).

Scenario		Distance [km]	$\sigma_{[dB]}$	Validity Range / Default Values
C1 – Suburban (macro-cell)	LOS	$d_{max\,[\mathrm{m}]} = 10^{\frac{L_{p,max_{[\mathrm{dB}]}} - 41.2 - 20\log(\frac{f_{[\mathrm{GHz}]}}{5.0}) - X_{sc[\mathrm{dB}]}}{23.8}}$	4	$30\ \mathrm{m} < \mathrm{d}_{[m]} < d_{BP_{[\mathrm{m}]}}$
		$10^{\frac{L_{p,max_{[\mathrm{dB}]}} - [11.65 - 16.2\cdot\log(h_{BS_{[\mathrm{m}]}}) - 16.2\cdot\log(h_{m_{[\mathrm{m}]}}) + 3.8\cdot\log(\frac{f_{[\mathrm{GHz}]}}{5})]}{40}}$	6	$d_{BP_{[\mathrm{m}]}} < \mathrm{d}_{[\mathrm{m}]} < 5\ \mathrm{km}$
				$h_{BS} = 25\ \mathrm{m},\ h_m = 1.5\ \mathrm{m}$
	NLOS	$d_{max\,[\mathrm{m}]} = 10^{\frac{L_{p,max_{[\mathrm{dB}]}} - [31.46 + 5.83\cdot\log(h_{BS_{[\mathrm{m}]}}) + 23\cdot\log(\frac{f_{[\mathrm{GHz}]}}{5})]}{44.9 - 6.55\cdot\log(h_{BS_{[\mathrm{m}]}})}}$	8	$50\ \mathrm{m} < \mathrm{d}_{[m]} < 5\ \mathrm{km}$
				$h_{BS} = 25\ \mathrm{m},\ h_m = 1.5\ \mathrm{m}$
C2 – Urban (macro-cell)	LOS	$d_{max\,[\mathrm{m}]} = 10^{\frac{L_{p,max_{[\mathrm{dB}]}} - 39 - 20\log(\frac{f_{[\mathrm{GHz}]}}{5.0})}{26}}$	4	$10\ \mathrm{m} < \mathrm{d}_{[\mathrm{m}]} < d'_{BP_{[\mathrm{m}]}}$
		$10^{\frac{L_{p,max_{[\mathrm{dB}]}} - [13.47 - 14\cdot\log(h_{BS_{[\mathrm{m}]}} - 1) - 14\cdot\log(h_{m_{[\mathrm{m}]}} - 1) + 6\cdot\log(\frac{f_{[\mathrm{GHz}]}}{5})}{40.0}}$	6	$d'_{BP_{[\mathrm{m}]}} < \mathrm{d}_{[\mathrm{m}]} < 5\ \mathrm{km}$
				$h_{BS} = 25\ \mathrm{m},\ h_m = 1.5\ \mathrm{m}$
	NLOS	$d_{max\,[\mathrm{m}]} = 10^{\frac{L_{p,max_{[\mathrm{dB}]}} - [34.46 + 5.83\cdot\log(h_{BS_{[\mathrm{m}]}}) + 23\cdot\log(\frac{f_{[\mathrm{GHz}]}}{5})]}{44.9 - 6.55\cdot\log(h_{BS_{[\mathrm{m}]}})}}$	8	$50\ \mathrm{m} < \mathrm{d}_{[\mathrm{m}]} < 5\ \mathrm{km}$
				$h_{BS} = 25\ \mathrm{m},\ h_m = 1.5\ \mathrm{m}$

The C1 and C2 model configuration assume macro-cells located above the rooftops to allow a wide coverage area and mobile users to be outdoors at street level:

- The **C1 configuration assume** buildings are typically low residential detached houses top two floors or blocks of flats with a few floors. The environment is moderately open, with open areas such as parks or playgrounds, and vegetation is modest.
- **The C2 Configuration** assumes obstructed line of sight is a common case since street level is often reached by a single diffraction over the rooftop. The building blocks can form either a regular Manhattan type of grid or have more irregular patterns. Typical building heights are over 4 floors, with height and density mostly homogeneous.

Furthermore, the D1 configuration (rural macro-cell) configuration consists of radio propagation in large areas (up to 10 km) with low building density. The height of the base station is in the range of 20 to 70 m, above the average surrounding building height, leading to good LOS conditions. The model parameters and distance validity range are shown in Table B.3.

Table B.3. WINNER II path-loss equations (extracted from [WINN07]).

Scenario		Path Loss [dB]	$\sigma_{[\mathrm{dB}]}$	Validity Range
D1 – Rural (macro-cell)	LOS	$d_{max\,[\mathrm{m}]} = 10^{\frac{L_{p,max_{[\mathrm{dB}]}} - 44.2 - 20\log(\frac{f_{[\mathrm{GHz}]}}{5.0})}{21.5}}$	4	$10\ \mathrm{m} < \mathrm{d}_{[m]} < d_{BP_{[m]}}$
		$d_{max\,[\mathrm{m}]} = 10^{\frac{L_{p,max_{[\mathrm{dB}]}} - [10.5 - 18.5\cdot\log(h_{BS_{[\mathrm{m}]}}) - 18.5\cdot\log(h_{m_{[\mathrm{m}]}}) + 1.5\cdot\log(\frac{f_{[\mathrm{GHz}]}}{5})]}{40.0}}$	6	$d_{BP_{[m]}} < \mathrm{d}_{[m]} < 10\ km$
				$h_{BS} = 32\ m,\ h_m = 1.5\ m$
	NLOS	$d_{max\,[m]} = 10^{\frac{L_{p,max_{[\mathrm{dB}]}} - [55.4 - 0.9\cdot(h_{m_{[\mathrm{m}]}} - 1.5) + 21.3\cdot\log(\frac{f_{[\mathrm{GHz}]}}{5}) - 0.26\cdot(h_{BS_{[\mathrm{m}]}} - 25)]}{25.1 - 0.13\cdot(h_{BS_{[\mathrm{m}]}} - 25)}}$		$50\ \mathrm{m} < \mathrm{d}_{[m]} < 5\ km$
				$h_{BS} = 32\ m,\ h_m = 1.5\ m$

B.4. Propagation Model – Experimental Indoors

This model is retrieved from [HTZA16] and it is based on field tests from Samsung and Nokia, consisting on an approximate for estimating this penetration loss on the premise of low and high-loss buildings, given by the presence of strongly reflective surfaces, e.g., glass walls, for both frequency bands. Its path loss is given by (B.19).

$$L_{p,indoor_{[\mathrm{dB}]}} = 10\log(A + B\cdot f_{[\mathrm{GHz}]}^2) \quad \text{(B.19)}$$

where:

- A: 5 for low-loss buildings, 10 for high-loss buildings;
- B: 0.03 for low-loss buildings, 5 for high-loss buildings;

Annex C

Districts

This annex provides the description of the municipality data used in this thesis, consisting of 125 locations in the northernmost metropolitan area of Lisbon.

In this thesis, the number of cells, is obtained for each district taking into account the values presented in the tables below, the area is obtained in [Dire16] and the number of inhabitants in [Stat16].

Table C.1. District characteristics in the municipality of Lisbon, A. dos Vinhos and S. M. Agraço.

ID	Location	Scenario	Area [km^2]	Inhabitants	Population Density [km^{-2}]	Municipality
1	Ajuda	U	3	15 584	5 195	Lisbon
2	Alcântara		4	13 943	3 486	Lisbon
3	Alvalade		5	31 813	6 363	Lisbon
4	Beato		2	12 429	6 215	Lisbon
5	Benfica		8	36 821	4 603	Lisbon
6	Campolide		3	15 460	5 153	Lisbon
7	Carnide		4	23 316	5 829	Lisbon
8	Penha de França		3	27 967	9 322	Lisbon
9	Parque das Nações		5	21 025	4 205	Lisbon
10	Estrela		5	20 128	4 026	Lisbon
11	Belém		10	16 528	1 653	Lisbon
12	Lumiar		6	41 163	6 861	Lisbon
13	Marvila		7	38 102	5 443	Lisbon
14	S.D. Benfica		4	33 745	8 436	Lisbon
15	São Vicente		2	15 339	7 670	Lisbon
16	Santo António		1	11 836	1 186	Lisbon
17	S.M. Maior		3	12 822	4 274	Lisbon
18	Santa Clara		3	22 480	7 493	Lisbon
19	Olivais		8	33 788	4 224	Lisbon
20	Misericórdia		2	13 044	6 522	Lisbon
21	Av. Novas		3	21 625	7 208	Lisbon
22	Arroios		2	31 653	15 827	Lisbon
23	Areeiro		2	20 131	10 061	Lisbon
24	Campo Ourique		2	22 120	11 060	Lisbon
25	Arruda dos Vinhos	R	34	8 656	255	A. Dos Vinhos
26	Arranhó		22	2 381	108	A. Dos Vinhos
27	Cardosas		6	836	139	A. Dos Vinhos
28	Santiago dos Velhos		16	1 518	95	A. Dos Vinhos
29	Sobral de M. Agraço	R	9	3 406	378	S. M. Agraço
30	Sapataria		14	3 044	217	S. M. Agraço
31	Santo Quintino		29	3 706	128	S. M. Agraço

Table C.2. District characteristics in the municipality of Sintra, Odivelas and Amadora.

ID	Location	Scenario	Area [km^2]	Inhabitants	Population Density [km^{-2}]	Municipality
32	Algueirão M. Martins	S	16	66 250	4 141	Sintra
33	Alargem Bispo	R	37	8 983	243	Sintra
34	Belas	S	22	26 087	1 186	Sintra
35	Colares	R	33	7 628	231	Sintra
36	Montelavar	R	12	3 559	297	Sintra
37	Queluz	S	3	26 248	8 749	Sintra
38	Rio de Mouro	S	16	47 311	2 957	Sintra
39	Santa Maria and Sao Miguel	S	12	9 364	780	Sintra
40	S.J. Lampas	R	57	11 392	200	Sintra
41	Sintra (Sº Martinho)	R	24	6 226	259	Sintra
42	Sao Pedro de Penaferrim	S	27	14 001	519	Sintra
43	Terrugem	R	23	5 113	222	Sintra
44	Pero Pinheiro	R	16	4 246	265	Sintra
45	Casal de Cambra	S	2	12 701	6 351	Sintra
46	Massamá	S	3	28 112	9 371	Sintra
47	Monte Abrãao	S	2	20 809	10 405	Sintra
48	Agualva	S	8	35 824	4 478	Sintra
49	Cacém	S	2	21 289	10 645	Sintra
50	Mira Sintra	S	1	5 280	5 280	Sintra
51	S. Marcos	S	2	17 412	8 706	Sintra
52	Alcabideche	S	40	42 162	1 054	Cascais
53	Carcavelos	U	5	23 347	4 669	Cascais
54	Cascais		20	35 409	1 770	Cascais
55	Estoril		9	26 399	2 933	Cascais
56	Parede		4	21 660	5 415	Cascais
57	S.D Rana	S	20	57 502	2 875	Cascais
58	Canecas		6	12 324	2 054	Odivelas
59	Famoes		5	11 095	2 219	Odivelas
60	Odivelas	U	5	59 559	11 912	Odivelas
61	O. Basto	S	2	5 812	2 906	Odivelas
62	Pontinha	U	5	23 041	4 608	Odivelas

Table C.2 (cont). District characteristics in the municipality of Sintra, Odivelas and Amadora.

ID	Location	Scenario	Area [km^2]	Inhabitants	Population Density [km^{-2}]	Municipality
63	P.S Adriao	S	1	13 069	13 069	Odivelas
64	Ramada		4	19 657	4 914	Odivelas
65	Alfragide		3	9 904	3 301	Amadora
66	Aguas Livres		2	37 426	18 713	Amadora
67	Encosta do Sol		3	28 261	9 420	Amadora
68	Falagueira - V. N		3	23 186	7 729	Amadora
69	Mina de Agua		8	43 927	5 491	Amadora
70	Venteira		5	18 539	3 708	Amadora

Table C.3. District characteristics in the municipality of Mafra and Oeiras.

ID	Location	Scenario	Area [km^2]	Inhabitants	Population Density [km^{-2}]	Municipality
71	Azueira	R	15	3 164	211	Mafra
72	Carvoeira		8	2 155	269	Mafra
73	Cheleiros		12	1 347	112	Mafra
74	Encarnacao		29	4 798	165	Mafra
75	E.Bispo		18	1 740	97	Mafra
76	Ericeira	S	12	10 260	855	Mafra
77	Gradil	R	8	1 226	153	Mafra
78	Igreja Nova		26	3 037	117	Mafra
79	Mafra		48	17 986	375	Mafra
80	Malveira		10	6 493	649	Mafra
81	Milharado		24	7 023	293	Mafra
82	S.E. Gales		18	1 709	95	Mafra
83	S. Isidoro		25	3 814	153	Mafra
84	Sobral A.		16	1 152	72	Mafra
85	V.F Rosário		6	871	145	Mafra
86	Venda Pinheiro	S	12	8 146	679	Mafra
87	S.M Alcainça	R	7	1 764	252	Mafra
106	Barcarena	S	9	13 869	1 541	Oeiras
107	Carnaxide	S	7	25 911	3 702	Oeiras
108	Oeiras	U	7	33 827	4 832	Oeiras
109	Paco de Arcos		3	15 315	5 105	Oeiras
110	Alges		2	22 273	11 137	Oeiras

Table C.3 (cont). District characteristics in the municipality of Mafra and Oeiras.

ID	Location	Scenario	Area [km^2]	Inhabitants	Population Density [km^{-2}]	Municipality
111	Cruz Quebrada	U	3	6 393	2 131	Oeiras
112	Linda-a-Velha		2	19 999	10 000	Oeiras

Table C.4. District characteristics in the municipality of Loures and V.F de Xira

ID	Location	Scenario	Area [km^2]	Inhabitants	Population Density [km^{-2}]	Municipality
88	Apelacao	S	1	5 647	5 647	Loures
89	Bucelas	R	34	4 663	137	Loures
90	Camarate	S	6	19 789	3 298	Loures
91	Fanhoes	R	12	2 801	233	Loures
92	Frielas		5	2 171	434	Loures
93	Loures	S	33	27 362	829	Loures
94	Lousa	R	17	3 169	186	Loures
95	Moscavide	U	1	14 266	14 266	Loures
96	Sacavem	S	4	18 469	4 617	Loures
97	S.I. Azoia	S	8	18 240	2 280	Loures
98	S.A. Tojal	R	15	4 216	281	Loures
99	S.J. Talha	S	6	17 252	2 875	Loures
101	S.J. Tojal	R	13	3 837	295	Loures
102	Unhos	S	4	9 507	2 377	Loures
103	Portela	U	1	11 809	11 809	Loures
104	Bobadela	S	3	8 839	2 946	Loures
105	P. Velho		1	7 136	7 136	Loures
116	Alhandra		2	6 047	3 024	V.F de Xira
117	Alverca Ribatejo		18	31 070	1 726	V.F de Xira
118	Cachoeiras	R	10	766	77	V.F de Xira
119	Calhandriz		7	801	114	V.F de Xira
120	C. Ribatejo		15	7 500	500	V.F de Xira
121	P.S. Iria	S	4	29 348	7 337	V.F de Xira
122	S.J Montes	R	18	6 018	334	V.F de Xira
123	Vialonga	S	18	21 033	1 169	V.F de Xira
124	Sobralinho	R	5	5 050	1 010	V.F de Xira
125	Forte Casa	S	5	11 056	2 211	V.F de Xira
126	Vila Franca de Xira	R	193	18 197	94	V.F de Xira

Annex D

Complementary Model Assessment Data

This annex provides a description and overview the auxiliary parameter relationships regarding the model assessment coverage and capacity wise.

This annex provides complementary data within the coverage and capacity model assessment.

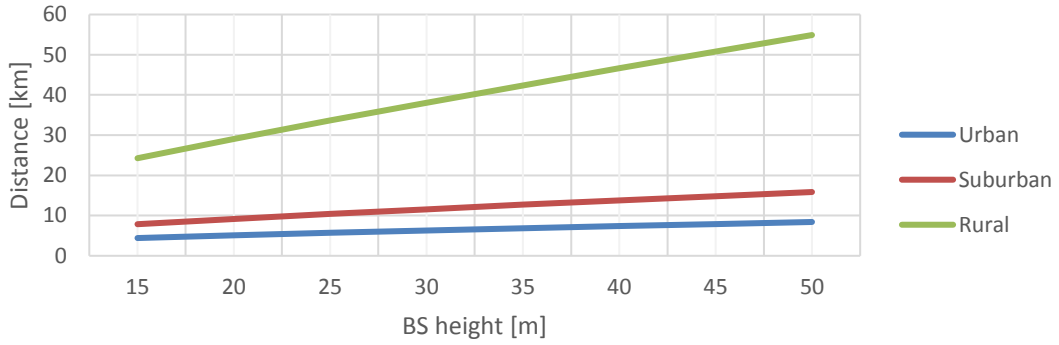

Figure D.1. Distance versus BS height (Okumura-Hata, 0.7 GHz).

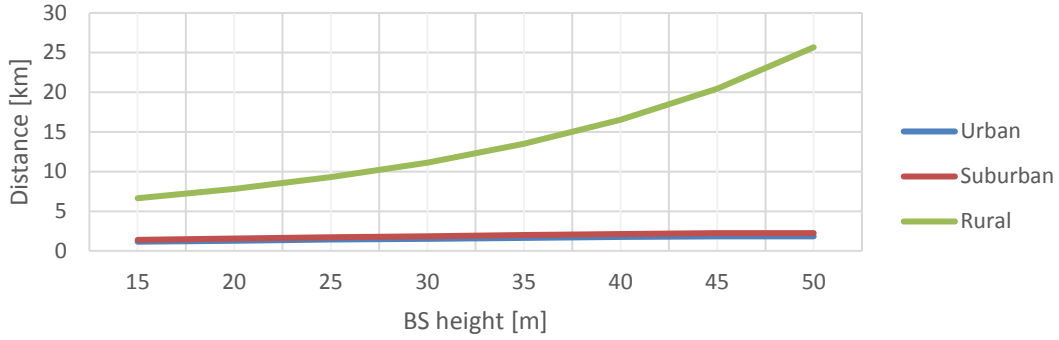

Figure D.2. Distance versus BS height (WINNER II, 3.5 GHz).

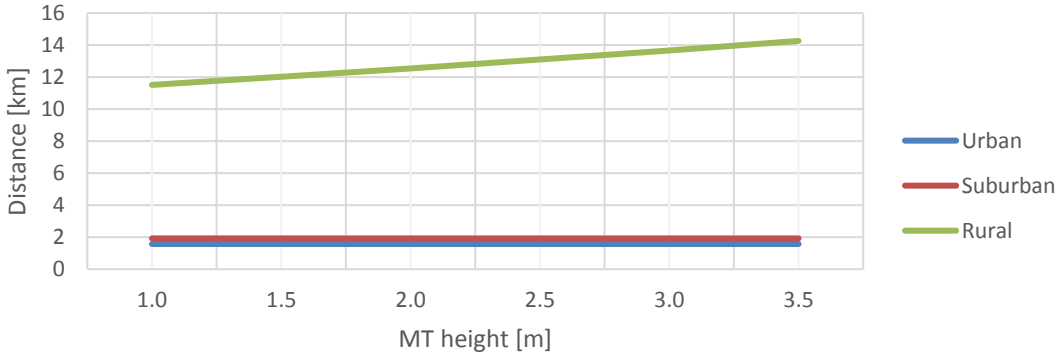

Figure D.3. Propagation distance versus MT height (Okumura-Hata, 0.7 GHz).

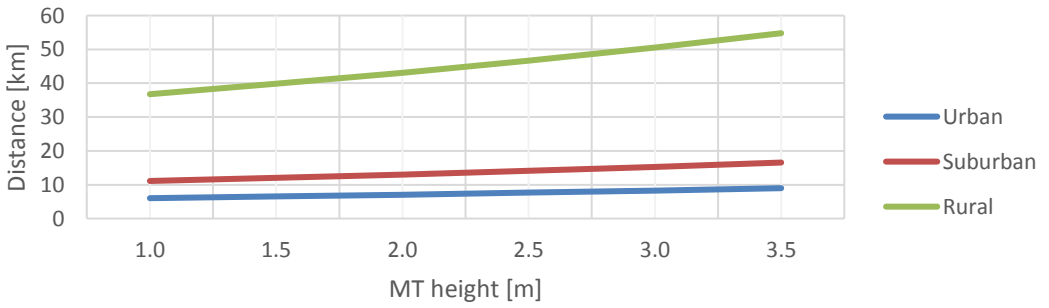

Figure D.4. Propagation distance versus MT height (WINNER II, 3.5 GHz).

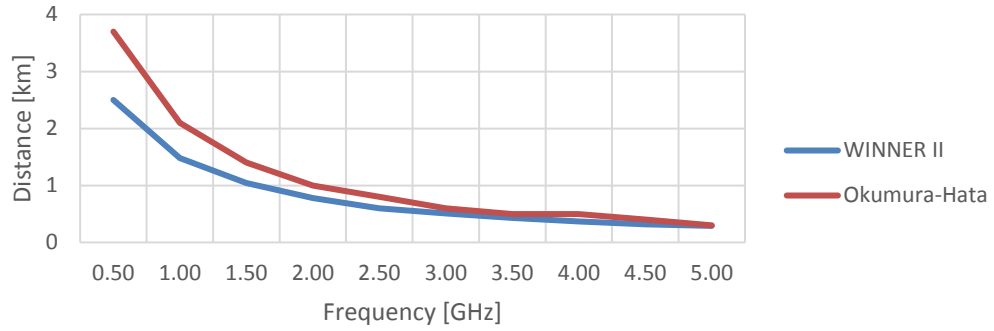

Figure D.5. Propagation model distance comparison (urban).

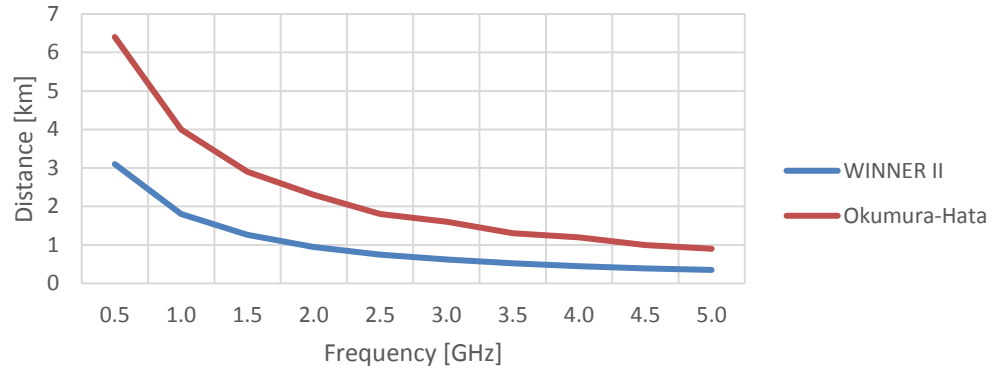

Figure D.6. Propagation model distance comparison (suburban).

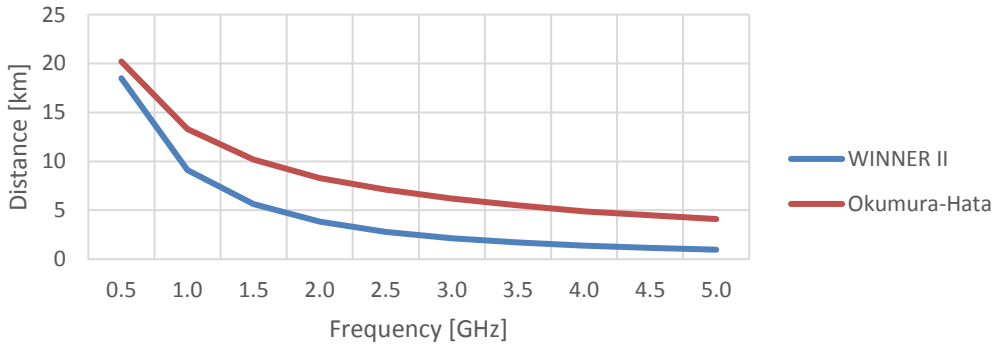

Figure D.7. Propagation model distance comparison (rural).

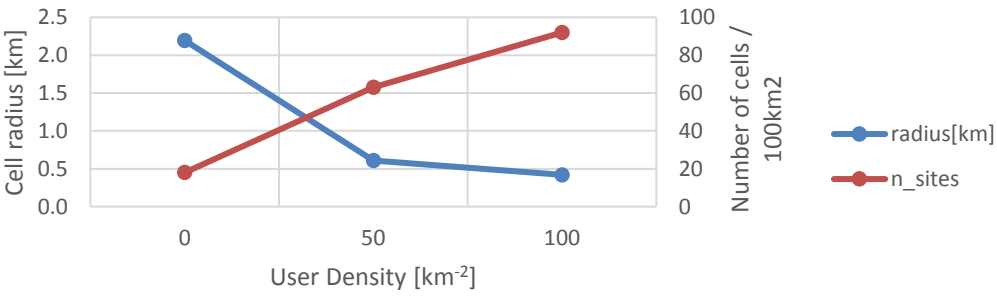

Figure D.8. Cell radius when increasing user density (rural, 3.5 GHz).

Concerning the addition of indoor pathloss to the path loss given by the propagation models, the tests are performed considering the cell radius for every MCS region border and different indoor configuration (none, low-loss, high-loss). The BS height is set to 25 m and the MT height to 1.5 m.

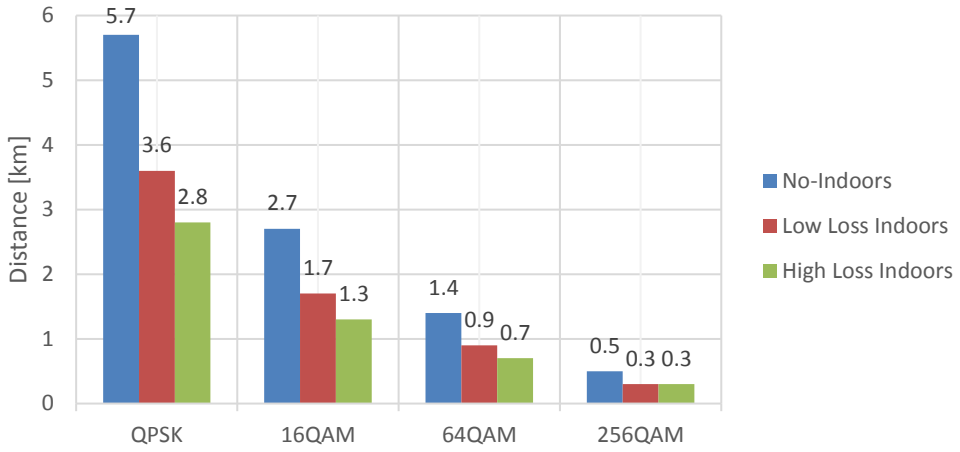

Figure D.9. Propagation distances with indoors (urban, 0.7 GHz).

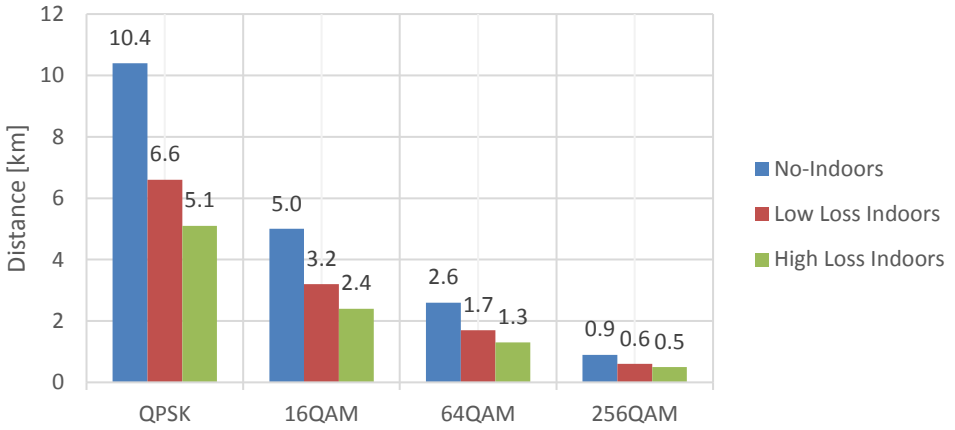

Figure D.10. Propagation distances with indoors (suburban, 0.7 GHz).

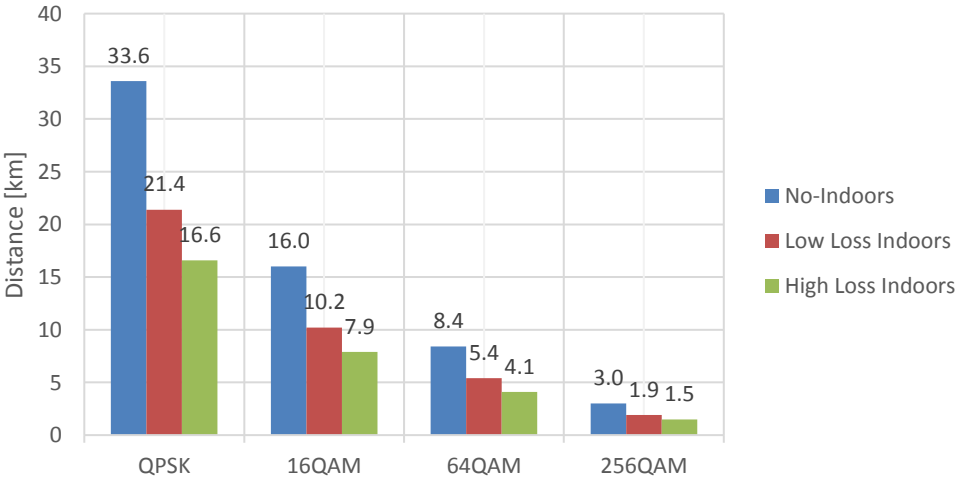

Figure D.11. Propagation distances with indoors (rural, 0.7 GHz).

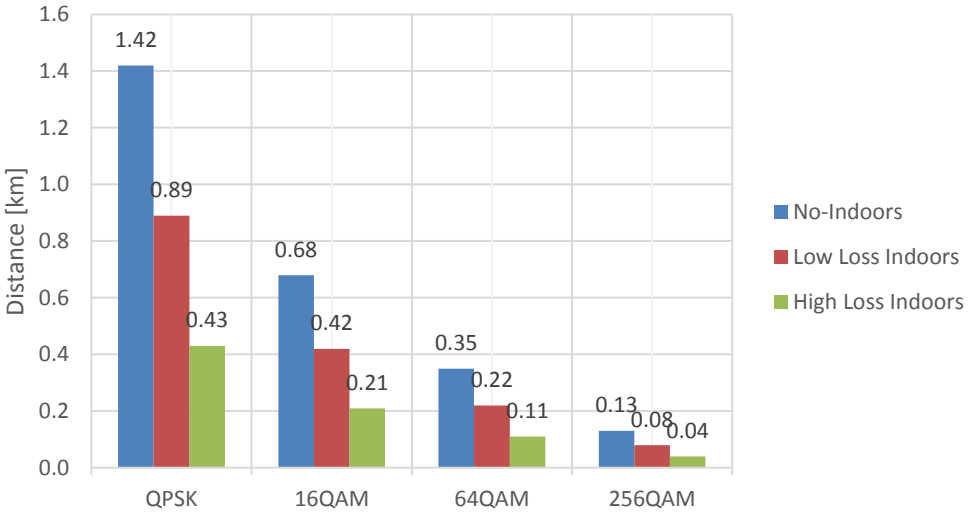

Figure D.12. Propagation distances with indoors (urban, 3.5 GHz).

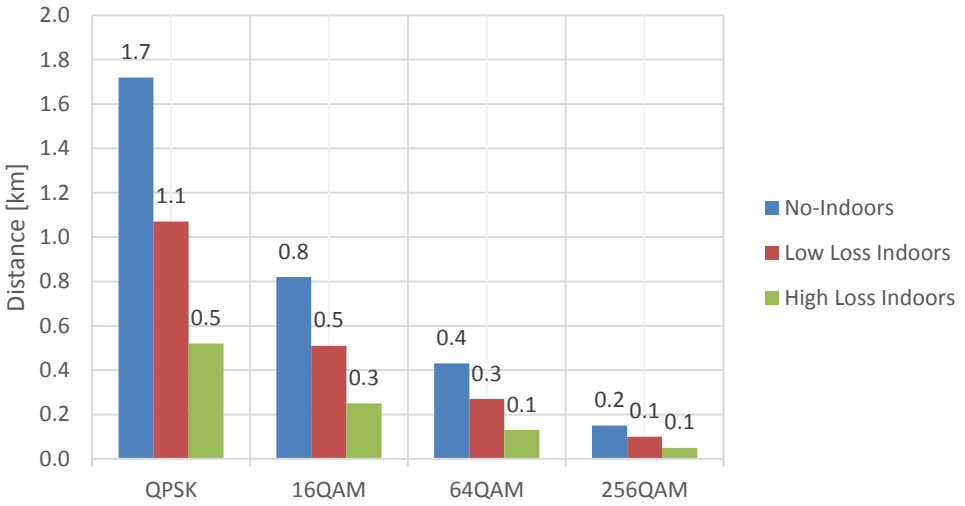

Figure D.13. Propagation distances with indoors (suburban, 3.5 GHz).

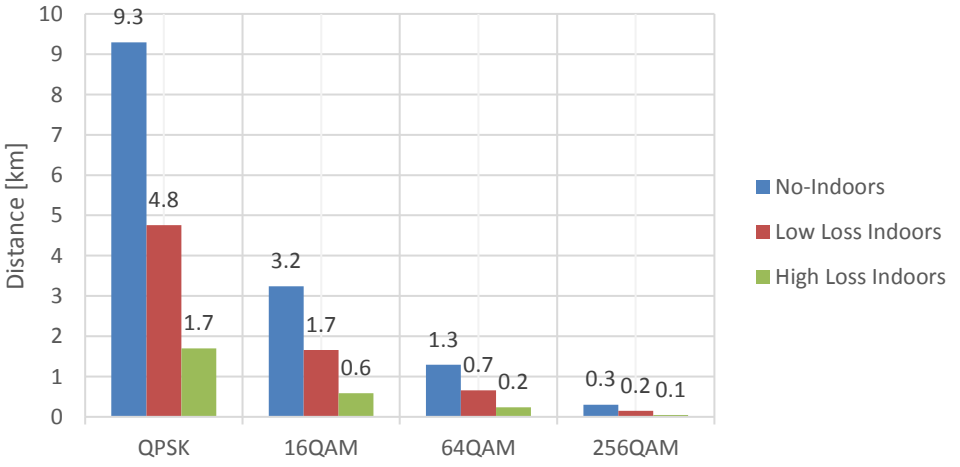

Figure D.14. Propagation distances with indoors (rural, 3.5 GHz).

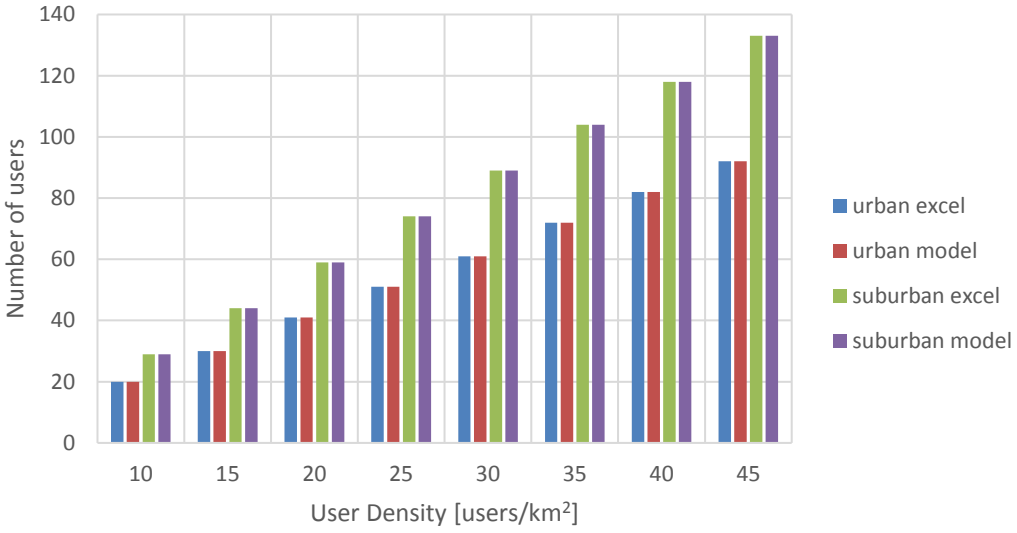

Figure D.15. Number of users versus user density verification (urban, suburban).

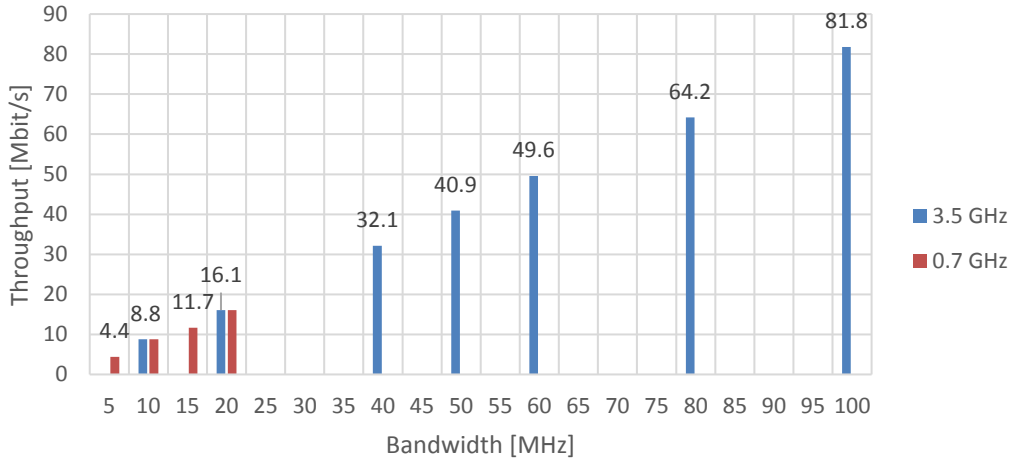

Figure D.16. Achievable throughput values by reserving 10% bandwidth at cell edge.

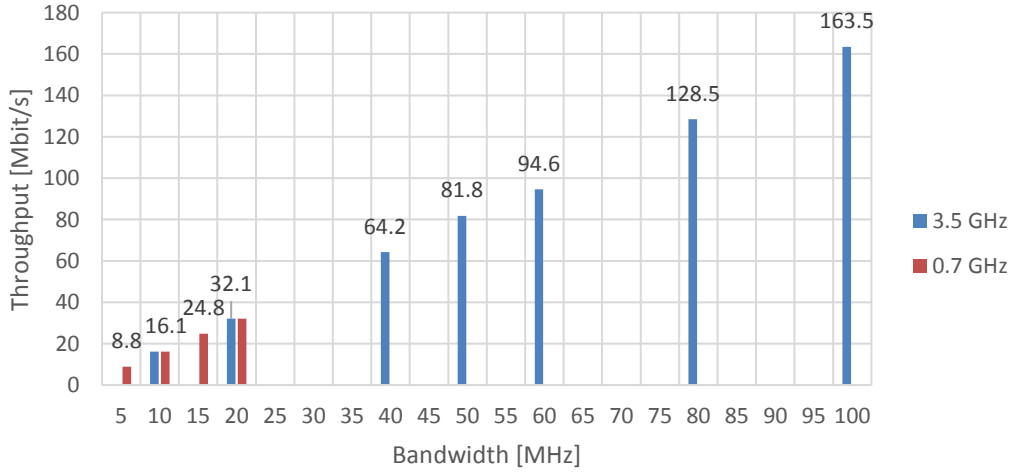

Figure D.17. Achievable throughput values by reserving 20% bandwidth at cell edge.

Annex E

Complementary Model Implementation Workflow

This annex provides a more comprehensive and detailed description of the key routines regarding the coverage and capacity dimensioning models involved in this thesis.

The secondary routines concerning the model workflow are presented in this annex. In the beginning model loads the configuration file into a dictionary to avoid creating variables in the code, making it possible a dynamic variable inclusion/removal in the code in Table E.1. The distance computation workflow is present in Figure E.1, where the propagation models are the Okumura-Hata for 0.7 GHz and WINNER II for 3.5 GHz, and the inputs are defined in Table E.2.

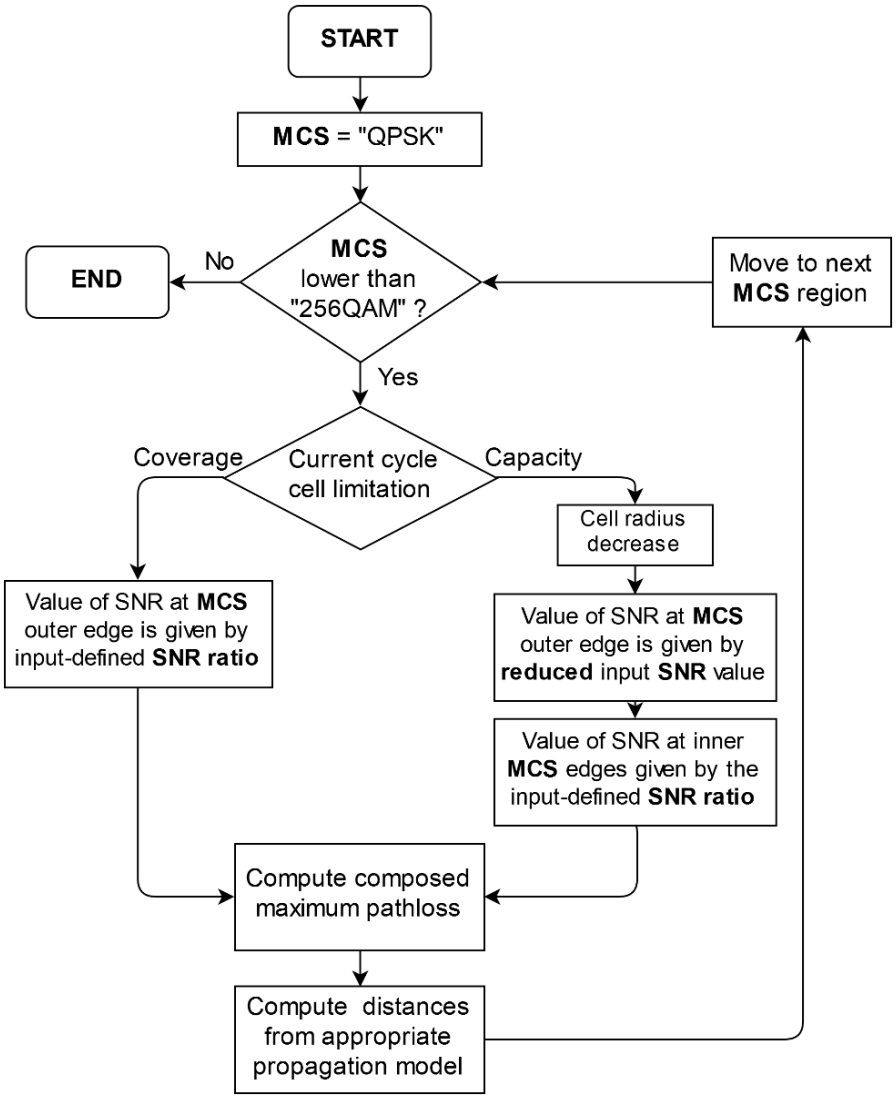

Figure E.1. Propagation distance computation workflow.

The link budget computation gives the MAPL which in its turn produces the minimum SNR value at the cell, which corresponds to the MCS region of QPSK. Hence, the propagation distance routine starts by this region and depending if the current cell limitation is by coverage or capacity, the algorithm picks the distance SNR ratio defined in the input file which defines the start and end of each MCS region.

For example, if the 16-QAM region goes from 5.5 to 12.9 dB and the SNR ratio is 0, it means the algorithm considers the 5.5 dB value as the starting point for this MCS region, if the ratio is 0.5 the starting point will be given by 9.2 dB, which then defines the maximum range of each MCS region and will later yield in the total area per MCS region. In the case of capacity-limited the edge cell SNR is reduced by a fixed margin, and this value will yield the new maximum and reduced cell radius through

a higher SNR value, since by getting closer to the antenna the SNR value increases. After obtaining the edge SNR value the new MAPL is then computed and the propagation distances for each MCS region are generated.

Table E.1. List of main input parameters for model initialisation.

Type	Description	Variable name
Dictionary	Generate dictionary with input parameters from external configuration file	*inputParams_dict*
Datatable	Generate datatable with traffic profile from external configuration file	*trafficProfile_table*
Datatable	Generate datatable with maximum RBs configuration (defined by 3GPP)	*maxRB_table*
Int []	Retrieve valid SCS configurations for frequency/bandwidth	*Valid_SCS*

Table E.2. List of main input parameters for propagation distance computation.

Type	Description	Variable name
Int	Lowest MCS region in current cycle	MCS_min
Int	Number of users in current scenario/cycle	*numUsers_perScenario*
Dictionary	Generate dictionary with input parameters from external configuration file	*inputParams_dict*
String []	Formal definition of MCS regions	*MCSregion*
Int []	Retrieve valid SCS configurations for frequency/bandwidth	*Valid_SCS*
Double	Maximum SNR value at current cell edge distance	*Edge_snrVal_out*
Boolean	Indication if method is to be used in primary capacity mode or not;	*primaryCapacity*

A key metric in cellular design is having a guaranteed throughput at the cell edge regardless of the conditions in the cell in terms of capacity traffic or load. Two parameters are defined, one is the required global available throughput at cell edge and the other is the maximum percentage of bandwidth the operator is willing to spend at the cell edge, and the workflow is represented by Figure E.2 and its inputs are shown in Table E.3.

The fulfilment of this condition is critical to obtaining a valid number of cells or cell radius, that is to say, even if at the current cycle the cell capacity is not in overload the algorithm does not stop until the throughput at cell edge requirement is achieved. On the other hand, if the cell radius is reduced to a point that the share of dedicated bandwidth produces a much higher throughput at cell edge than the required, the model reduces that percentage until the available throughput is just above the required, about 1 Mbit/s. For example, if with 10% of dedicated bandwidth at the current cycle and cell radius the algorithm yields a throughput at cell edge of 50 Mbit/s and the required is only 5 Mbit/s, the model

reduces the percentage by 0.5% until the available throughput is just above that level (5 Mbit/s).

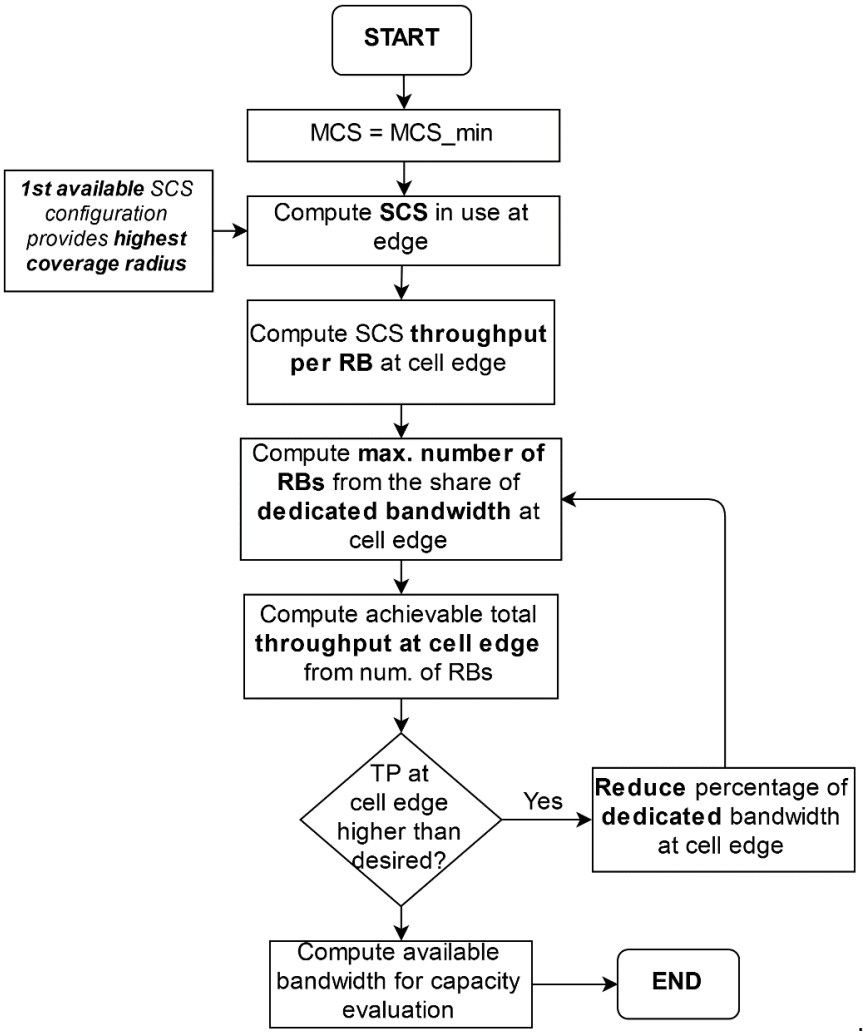

Figure E.2. Computation of reserved bandwidth at cell edge and available bandwidth for capacity evaluation workflow.

Since this metric is given at the cell edge, the model assumes the numerology in use the one with lower bandwidth which can be served with a lower sensitivity value and thus served in a higher distance than higher-bandwidth numerologies.

Table E.3. List of main input parameters for the computation of reserved bandwidth at cell edge and available bandwidth for capacity evaluation.

Type	Description	Variable name
Dictionary	Generate dictionary with input parameters from external configuration file	*inputParams_dict*
Datatable	Generate datatable with maximum RBs configuration (defined by 3GPP)	*maxRB_table*
Int	Lowest MCS region in current cycle	MCS_min
Int []	Retrieve valid SCS configurations for frequency/bandwidth	*Valid_SCS*

For example, if the numerologies of 15, 30 and 60 kHz are defined as active in the input configuration file, the model will consider numerology of 15 kHz. From the current cycle cell's minimum SNR value (maximum distance) the average throughput per RB of 15 kHz is computed. Then, from the reserved bandwidth value at cell edge at the current cycle the RB bandwidth is factored in and produces the maximum number of 15 kHz RBs passible of being used. The total throughput at cell edge is then computed by multiplying the number of 15 kHz RBs by the associated throughput previously computed.

The next algorithm is the cornerstone of the whole capacity evaluation in the model. It accepts the traffic profile, which contains the number of services, their mix share and average throughput values, the available bandwidth to capacity purposes, which is capped at a pre-defined maximum cell load ratio, and the maximum distances of each existing MCS regions, which can be inferior to 4 if the cell radius reduction produces a SNR value such that one quits having a certain MCS region. The area of each MCS region is computed from the maximum distance per region and from the input user density the number of users in the current cell is generated. Since the maximum number of RBs in 5G-NR per cell is 275, and that the minimum RB allocation per user is 1, the maximum theoretical number of users per cell is 275. Hence, if the number of users in the current cell is higher than this value the algorithm does not go into capacity considerations, it keeps reducing the maximum cell radius until it yields a value around 275. Only then it starts analysing the cell capacity load.

From the traffic profile mix share per service the number of users per service is computed, and through the use of random sorting algorithm, these users are randomly allocated in the cell by means of a seed value which is dependent on the current system time, to generate as non-unique user allocation profiles as possible. The number of random user allocations is defined to one per simulation, if more is required one only needs to change the number of simulations value in the input file. Then these users are split into each MCS region by the percentage which corresponds to their share of total area. It is possible at this point to know the user population per MCS region and their associated throughput requirements. As seen previously, there are four MCS curves per numerology per MCS region, in a total of 12 possible RB throughput values per MCS region if all three numerologies are considered.

The algorithm now reads each user's throughput requirement and from the user's MCS region it traverses all throughput RB configurations until it finds the optimal one. For the current service's MCS region the algorithm traverses each MCS curve's TP values in increasing value of numerology configuration and computes the required TP vs available TP ratio. For example, for a service TP of 1.2 Mbit/s, from Annex A the Table E.4 and Table E.5 are produced.

On the other hand, then there are throughput values per RB higher than the required service throughput the model picks the RB configuration with lowest bandwidth. For instance, in Table E.5, the first value yielding the minimum ratio is 16-QAM with 60 kHz by using a 1.98 Mbit/s RB to serve a 1.2 Mbit/s service. However, and since the model reads each line from the left to the right and then moves to the next MCS curve (line in the table), one sees more configurations yielding the same minimum ratio of 1.

In this case, the model searches for any RB configuration which yields the same minimum and previously obtained ratio of 1 but minimising the bandwidth, which is possible by considering the 64-QAM 30 kHz RB with 1.70 Mbit/s. If there are no other configuration yielding the same ratio with an even smaller bandwidth, such as 15 kHz, the RB is allocated to the service.

Table E.4. RB allocation – case 1.

MCS curve	Numerology [kHz]					
	15	30	60	15	30	60
	RB throughput [Mbit/s]			Number of RBs		
QPSK	0.13	0.26	0.53	10	5	**3**
16-QAM	0.02	0.05	0.09	60	24	13
64-QAM	0.02	0.03	0.06	60	40	20
256-QAM	0.02	0.03	0.07	60	40	17
MCS region	**QPSK**					

Table E.5. RB allocation – case 2.

MCS curve	Numerology [kHz]					
	15	30	60	15	30	60
	RB throughput [Mbit/s]			Number of RBs		
QPSK	0.17	0.33	0.67	8	4	2
16-QAM	0.49	0.99	1.98	3	2	1
64-QAM	0.85	1.70	3.39	2	1	1
256-QAM	0.66	1.33	2.65	2	1	1
MCS region	**64-QAM**					

Since this computation is likely the model element consuming more running time in the simulation since this is done for every user/service in the cell, several times if the cell is continuously reduced to fulfil the input requirements, which can be seen in Debugging mode of Visual Studio, no further algorithms were developed in the RB allocation process. However, one could find improvement points, such as computing the throughput excess and minimising it, for example, if two equally optimal values of 1.70 and 1.33 Mbit/s are obtained within the same bandwidth for the service's TP of 1.2 Mbit/s, minimising would be picking the minimum of (1.70 – 1.20 = 0.5) and (1.33 – 1.20 = 0.13).

This process is done for every user/service and the total number of RBs and the total accumulated bandwidth is compared to the maximum limits. The total number of RBs is limited to the 3GPP defined maximum values for every spectrum configuration and the bandwidth is limited by the end-user inputted bandwidth value, in concordance with the valid configurations also specified by 3GPP. If there is an excess in any of those, the cell is considered to be in overload and cell re-dimensioning techniques are applied.

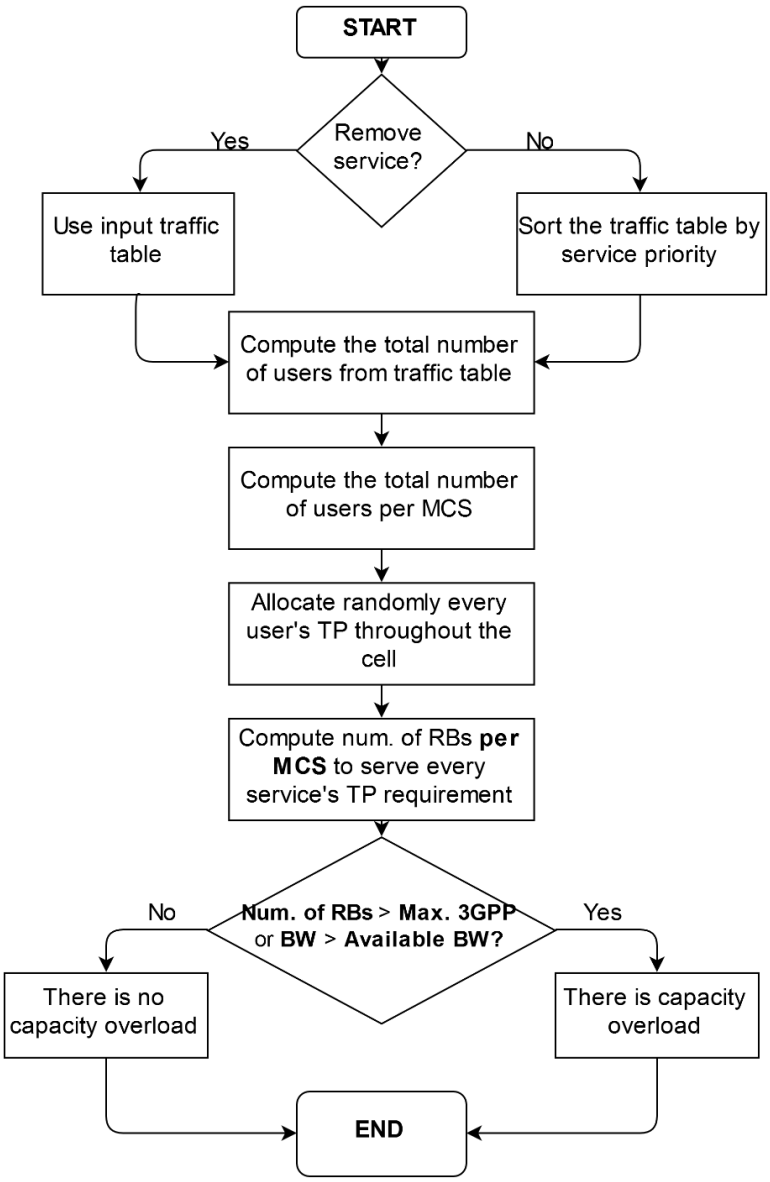

Figure E.3. Evaluation of capacity overload workflow.

Table E.6 Main input parameters for capacity overload evaluation.

Type	Description	Variable name
Int	Number of users in current scenario/cycle	*numUsers_perScenario*
Dictionary	Generate dictionary with input parameters from external configuration file	*inputParams_dict*
Datatable	Generate datatable with traffic profile from external configuration file	*trafficProfile_table*
Datatable	Previously generated table of propagation distances per MCS region	*distTable*
Double	Available bandwidth for capacity evaluation	*AvailableBW_atCapacity*
Int	Lowest MCS region in current cycle	MCS_min
Double	SNR value at cell edge	*Edge_snrVal*

Table E.6 (cont). Main input parameters for capacity overload evaluation.

Type	Description	Variable name
Boolean	Whether the method is to work under the throughput reduction routine	*serviceThroughputReductionRoutine*
Boolean	Whether the method is to work under the service removal routine	*serviceRemovalRoutine*

If there is a capacity overload the approach is to reduce the requirements in the network. This can be achieved by either reducing the throughput of the services with less priority or by removing some services until a given threshold, that is to say the maximum number of services whose throughput can be reduced of the maximum number of services which could be removed if necessary, which can be defined in the input file. The workflow logic of this routine is present in Figure E.4.

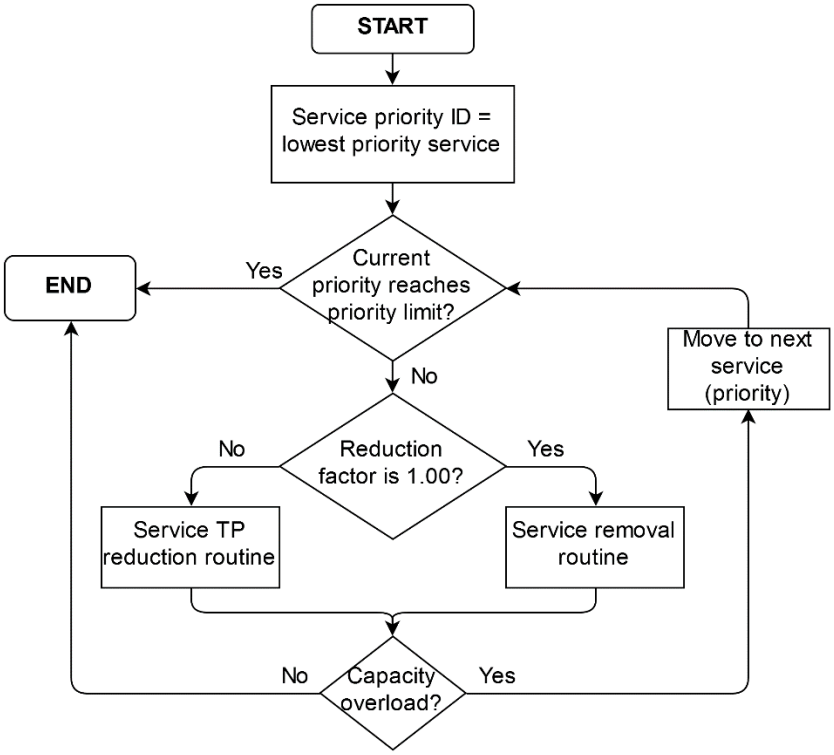

Figure E.4. Reduction of service throughput or removal workflow.

Table E.7 Main input parameters for reduction of service throughput or removal routine.

Type	Description	Variable name
Int	Current (last) service priority to remove	*lowestPrr*
Dictionary	Generate dictionary with input parameters from external configuration file	*inputParams_dict*
Datatable	Datatable with current cycle traffic	*trafficProfile_table*
Datatable	Previously generated table of propagation distances per MCS region	*distTable*
Double	Service throughput reduction ratio	*reduceTP_perc*

Although this model was developed for the variables present in the input configuration file, it is possible to add or remove any variable due to the usage of the dictionary. In the model initialisation stage, the dictionary imports all parameters and values from the input file, which are considered to be:

- **Spectrum parameters:** frequency, bandwidth, share of reserved bandwidth at cell edge;
- **Link Budget:** coverage probability and standard deviation (indoors, outdoors), antenna power, gains, noise figures, cable losses, interference margins, MIMO order, share of indoor users;
- **Propagation/distances:** Okumura-Hata, WINNER II, height of BS, height of MT, high/low loss indoors propagation model;
- **5G-NR:** numerologies in use;
- **Others:** number of simulations, user density, SNR minimum value for distance, SNR value for corresponding throughput value, throughput requirement at cell edge, deployment area;

The main input parameters for services in the traffic profile configuration are their name (identification), priority, mix and average throughput. Both configuration files are received as input in CSV format. Concerning the simulation times for the model reference parameters, the expected results are shown in Figure E.5 for both frequency bands for the 125 municipalities, for a workstation with an Intel i7-4500 1.80 GHz processor, 8 GB RAM and Windows 8 (64 bits) operating system.

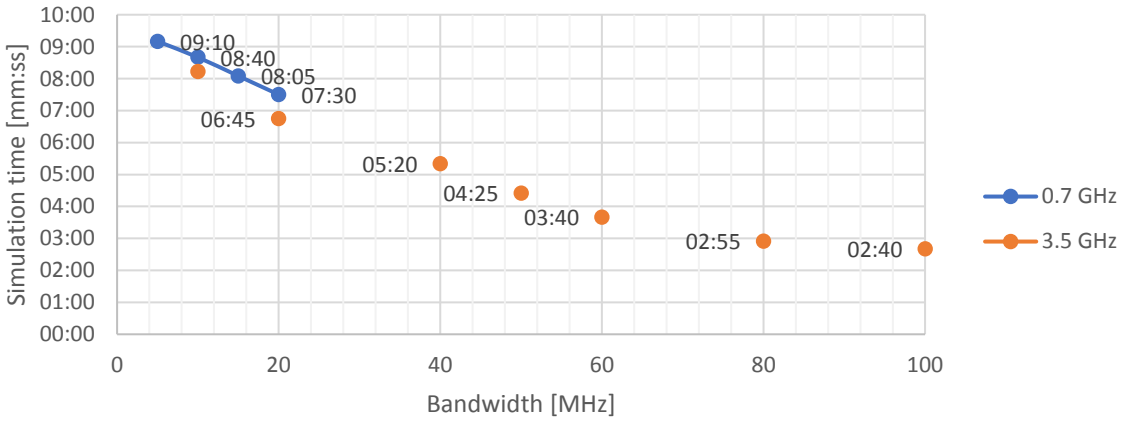

Figure E.5. Simulation times for both frequency bands for the 125 municipalities.

The simulation time per municipality essentially depends on the propagation environment, user density and bandwidth, where the number of iterations is defined as the number of iterations where after computing the cell radius (or reduced cell radius) the model computes if there is capacity overload:

- **Propagation environment:** responsible for defining the initial cell radius. A higher initial cell radius may lead to a higher number of iterations in order to achieve the optimal cell radius which can satisfy the traffic profile requirements, and a higher simulation run time.
- **User density:** responsible for defining the number of active users per cell. A high value may force the cell to shrink in terms of cell radius, requiring more iterations and running time.
- **Cell bandwidth:** responsible for defining how much bandwidth can the cell allocate to its active users. A high value is related to having more active users in the cell, and thus requires less iterations to find the optimal cell radius value, and less simulation run time.

References

[3GPP15] 3GPP, *Digital cellular telecommunications system (Phase 2+); Universal Mobile Telecommunications System (UMTS); LTE; Quality of Service (QoS) concept and architecture (Release 13)*, ETSI TS, No. 23.107, Ver. 13.0.0, Dec. 2015 (http://www.3gpp.org).

[3GPP17a] 3GPP, *Physical channels and modulation,* TS 38.211, Release 15 Version 1.2.0, Nov. 2017. (http://www.tech-invite.com/3m38/tinv-3gpp-38-211.html).

[3GPP17b] 3GPP, *Technical Specification Group RAN - Study on channel model for frequencies from 0.5 to 100 GHz*,TR38.901 V14.1.1 Release 14, July 2017. (https://goo.gl/LpsGZE).

[3GPP17c] 3GPP, *Technical Specification Group – User Equipment (UE) radio transmission and reception*; TR38.101-1 V1.0.0 Release 15, Dec. 2017. (https://goo.gl/hLmhBN).

[5GCO18] 5G in the U.K, "5G UK Auction", https://5g.co.uk/guides/5g-uk-auction/, June. 2018.

[5GPP17] 5G-PPP, *View on 5G Architecture*, Report, V 2.0, July 2017. (https://goo.gl/oYdYCz).

[ADRA17] R.K. Al-Dabbagh, H.S. Al-Raweshidy and N.A. Al-Aboody, "*Performance Comparison of Exploiting Different Milimetre-Wave Bands in 5G Cellular Networks"* in International Conference on Performance Evaluation and Modeling in Wired and Wireless Networks (PEMWN), Nov. 2017. (https://ieeexplore.ieee.org/document/8308031/).

[Alco17] B. Alcobia, *LTE radio network deployment design in urban environments under different traffic scenarios,* M.Sc. Thesis, Instituto Superior Técnico, May 2017. (https://goo.gl/VmYT7J).

[AM5G16] 5G Americas, *Network Slicing for 5G Networks & Services*, Report, Nov. 2016. (https://goo.gl/GHnmtg).

[AM5G17] 5G Americas, *5G Spectrum Recommendations,* Report, April 2017. (https://goo.gl/7eW8Wi).

[ANAC18] ANACOM Portugal, "ANACOM makes way for 5th Mobile Generation", *https://www.anacom.pt/render.jsp?contentId=1431845&languageId=1,* June. 2018.

[ANDR17] Android Central, "*How much mobile data does streaming media use?",* https://goo.gl/TyKdg5, Mar. 2018.

[AnJa15] T. Anttalainen. and V. Jaaskelainen, *Introduction to Communication Networks*, Artech House, London, UK, 2015.

[Anni17] S. Annisa, *Analysis of 5G Mobile Broadband Solutions in Rural and Remote Areas: A Case Study of Banten, Indonesia*, MSc. Thesis, KTH Royal Institute of Technology, Aug. 2017. (https://goo.gl/XvgR9N).

[AVID16] Analytics Vidhya, "*10 Real World Applications of Internet of Things (IoT)",*

https://goo.gl/jyRMJE , Mar. 2018.

[BEEC14] BEECube, *Challenges and Solutions in Prototyping 5G Radio Access Network,* White Paper, Dec. 2014. (http://usdatavault.com/library/5gwhitepaper.pdf).

[Belc18] I. Belchior, *Evaluation of 5G Cellular Network Implementation over an Existing LTE One*, M.Sc. Thesis, Instituto Superior Técnico, Universidade de Lisboa, Nov. 2018.

[BSCW16] Y.L Ban, C.-Y. -D. Sim, C. Li, K. -L. Wong, *"4G/5G Multiple Antennas for Future Multi-Mode Smartphone Applications"*, IEEE Access, Volume 4 1-1, Jan. 2016. (https://ieeexplore.ieee.org/document/7496871/).

[CARS15] 5G-PPP, *5G Automotive Vision*, Report, Oct. 2015 (https://5g-ppp.eu/wp-content/uploads/2014/02/5G-PPP-White-Paper-on-Automotive-Vertical-Sectors.pdf)

[Chan16] L. Chang, *MIMO Heterogeneous and Small Cell Networks for 5G Systems*, Ph.D. Thesis, Hong Kong University of Science and Technology, March 2016. (http://repository.ust.hk/ir/Record/1783.1-82364).

[Corr16] L. M. Correia, *Mobile Communication Systems*, Lecture Notes, Instituto Superior Técnico, Lisbon, Portugal, 2016. (https://goo.gl/ZydmpV).

[DEVA17] Device Atlas, "*The most used smartphone screen resolutions in 2017",* https://goo.gl/z3Q9tp, Mar. 2018.

[DGDR18] D. Demmer, R. Gerzaguet, J.B. Doré and D.L. Ruyet, *"Analytical study of 5G NR eMBB co-existence"*, CoRR, May. 2018. (https://arxiv.org/pdf/1805.05591.pdf).

[Dire16] Directorate-General for Territorial Planning of Portugal, *Official Administrative Map of Portugal 2016* (in Portuguese), https://goo.gl/a6v8vK , Oct.2016.

[DTUG16] P. Demestichas, K. Tsagkaris, S. Vassaki, A. Georgakopoulos, V. Kosmatos, *"Service Classification in 5G networks"* in Network Machine Learning Research Group (NMLRG) 5th Meeting, Nov. 2016. (https://goo.gl/NKNP5b).

[ERIC15] Ericsson, *Massive Beamforming in 5G Radio Access,* Mar 2015 (https://www.ericsson.com/research-blog/massive-beamforming-in-5g-radio-access/).

[ERIC16] Ericsson, *5G Radio Access – Capabilities and Technologies,* Rev C, April 2016. (https://goo.gl/BmFf1T).

[ERIC17] Ericsson, *The 5G Business Potential – Industry digitalisation and the untapped opportunities for operators,* 2nd Edition, June 2017. (https://goo.gl/En2fk8).

[ERIC18a] Ericsson, *5G New Radio: Unveiling the Essentials of the Next Generation Wireless Access Technology*, Report, June. 2018. (https://arxiv.org/abs/1806.06898).

[ERIC18b] Ericsson, *Technology Milestones: showcasing 5G NR interoperability*, Report, June. 2018. (https://goo.gl/aojPGj).

[ERIC18c] B. Halvarsson, A. Simonsson, A Elgcrona, R Chana, P Machado and H. Asplund, *"5G NR Testbed 3.5 GHz Coverage Results"*, Ericsson, IEEE 87th Vehicular Technology Conference, June. 2018. (https://goo.gl/TwSY85).

[GOBR18] GoBrolly, *"Data & Bandwidth Requirements for Internet Applications", https://gobrolly.com/summary-data-bandwidth-requirements/ ,* July. 2018.

[GSMA17] GSMA IoT, "*What is Mobile IoT?",* https://www.gsma.com/iot/mobile-iot/, Mar. 2018.

[Guit16] J. Guita., *Balancing the load in LTE urban networks via inter-frequency handovers*, M.Sc. Thesis, Instituto Superior Técnico, Lisbon, Portugal, Aug. 2016. (https://goo.gl/x1NRFX).

[HTZA16] Katsuyuki Haneda, Lei Tian, Yi Zheng, Henrik Asplund, J. Li, Y. Wang, D. Steer, C. Li,T. Balercia, S. Lee, Y. Kim, A. Ghosh, T. ThomasT. Nakamura,Y. Kakishima, T. Imai, H. Papadopoulas, T. S. Rappaport, G. MacCartney Jr., M. K. Samimi, S. Sun, O. Koymen, S. Hur, J. Park, C. Zhang, E. Mellios, A. F. Molisch, S. S. Ghassamzadeh, and Arun Ghosh, "*5G 3GPP-like Channel Models for Outdoor Urban Microcellular and Macrocellular Environments",* in IEEE 83rd Vehicular Technology Conference (VTC Spring), May 2016. (https://arxiv.org/pdf/1602.07533.pdf).

[Hish16] E. Hisham, *Decoupled Cell Association Towards Device-Centric 5G Cellular Networks*, Ph.D Thesis, King's College London, Nov. 2016. (https://goo.gl/NCbfrs).

[HUAW16] HUAWEI, "*Up in the Air with 5G",* http://www.huawei.com/en/about-huawei/publications/communicate/80/up-in-the-air-with-5g , Mar. 2018.

[ITU17a] ITU-R, *Propagation data and prediction methods for the planning of indoor radiocommunication systems and radio local area networks in the frequency range 300 MHz to 100 GHz*, Recommendation ITU-R P.1238-9, P Series, June 2017. (https://goo.gl/tH4b38).

[ITUn17] ITU News, *Forging Paths to 5G,* Feb. 2017. (https://www.itu.int/en/itunews/Documents/2017/2017-02/2017_ITUNews02-en.pdf).

[Jan16] J. Jan, *Measurement-Based Milimeter-Wave Radio Channel Simulations and Modeling*, Ph.D. Thesis, Aalto University, Sept. 2016. (https://goo.gl/zcr2TG).

[Jian15] Q. Jian, *Enabling Milimeter Wave Communication for 5G Cellular Networks: MAC-layer Perspective*, Ph. D. Thesis, University of Waterloo, April 2015. (https://uwspace.uwaterloo.ca/handle/10012/9243).

[Kris16] P. Krishnamurth, *Large Scale Fading and Network Deployment,* Lecture Notes, University of Pittsburgh, U.S.A, 2016.

[LETM14] E. Larsson, O. Edfors, F. Tufvesson and T. Marzetta, *"Massive MIMO for Next Generation Wireless Systems",* in IEEE Communications Magazine, Feb. 2014. (https://ieeexplore.ieee.org/document/6736761/).

[LIBE12] Libelium, "*50 Sensor Applications for a Smarter World",* http://www.libelium.com/resources/ , Mar. 2018.

[LIBE18] Libelium, "Waspmote Plug & Sense!", a general-purpose sensor device, http://www.libelium.com/products/plug-sense/technical-overview/ , May. 2018.

[LiSL18] Y. Li, C.Y.D Sim, Y. Luo, *"Multiband 10-Antenna Array for Sub-6 GHz MIMO Applications in 5-G Smartphones"*, in IEEE Access, Volume 6, May 2018. (https://ieeexplore.ieee.org/document/8361024/).

[LTEE09] LTE Encyclopaedia, "*LTE Radio Link Budgeting and RF Planning"*, https://cells.google.com/site/lteencyclopedia/lte-radio-link-budgeting-and-rf-

planning#TOC-2.3.-Downlink-Budget , Dec. 2009.

[Maro15] A. Marotta, *Optimisation of Radio Access Network Cloud Architectures Deployment in LTE Advanced*, M.Sc. Thesis, Instituto Superior Técnico, Lisbon, Portugal, July. 2015. (https://goo.gl/s6M4V2).

[MEDI17] Medium, "*Making 12K 360º VR Streaming a Reality: Why and How We Did It",* https://goo.gl/us5etQ*,* Mar. 2018.

[MEDI18] Medium, "Don't let the FCC take away 3.5 GHz shared spectrum!", https://goo.gl/RZ5ugm, June. 2018.

[MiWE14] MiWEBA, *WP5: Propagation, Antennas and Multi-Antenna Techniques – Deliverable 5.1: Channel Modeling and Characterisation,* Version 1.0, June 2014. (https://goo.gl/CPSC4P).

[MMMA17] mmMagic, *Final mmMagic System Concept,* Deliverable 6.6, July 2017. (https://5g-mmmagic.eu/results/).

[MoLi11] Andreas F. Molisch, *Wireless Communications, Second Edition,* John Wiley & Sons, Ltd., USA, 2011.

[NBNC18] NBN (Australian Telecoms Operator), "*How much data does streaming video, mobiles and TV use?",* https://goo.gl/gPqKT6, Mar. 2018.

[NETF16] NETFLIX, "*Internet Connection Speed Recommendations"*, https://help.netflix.com/en/node/306 , Mar. 2018.

[NETM18] NETMANIAS, "*5G & IoT? We need to talk about latency.",* https://goo.gl/NV5Dnt *,* Mar. 2018.

[NGMN15] NGMN, *NGMN 5G White Paper,* A Deliverable by the NGMN Alliance, Ver. 1.0, Feb. 2015 (https://www.ngmn.org/5g-white-paper/5g-white-paper.html).

[Pere17] J. Pereira, *Multiple Access Strategies for Spatial Modulation,* M.Sc. Thesis, Instituto Superior Técnico, Universidade de Lisboa, May 2017. (https://goo.gl/r7c9Tu).

[Pire15] J. Pires, *LTE Fixed to Mobile Subscribers QoE Evaluation,* M.Sc. Thesis, Instituto Superior Técnico, Universidade de Lisboa, Nov. 2015. (https://goo.gl/og9Lnw).

[ROSC16a] Rohde and Schwarz, *5G Waveform Candidates*, Application Note, June 2016. (https://goo.gl/r57YMk).

[Silv16] H. Silva, *Design of C-RAN Fronthaul for Existing LTE Networks,* M.Sc. Thesis, Instituto Superior Técnico, Universidade de Lisboa, Nov. 2016. (https://goo.gl/VM65oX).

[SMKS17] P. Shulz, M. Matthé, H. Klessing, M. Simsek, G. Fettweis, J. Ansari, S. Ashraf, B. Almeroth, J. Voigt, I. Riedel, A. Puschman, A. Thiel, M. Nuller, T. Elste and M. Windisch, *"Latency Critical IoT Applications in 5G: Perspective on the Design of Radio Interface and Network Architecture",* in IEEE Communications Magazine, Feb. 2017. (https://ieeexplore.ieee.org/document/7842415/).

[Stat16] Statistics Portugal, *Census 2011* (in Portuguese), https://goo.gl/t6Uc7o , Sep.2016.

[Tian16] B. Tianyang, *Analysis of Milimeter Wave and Massive MIMO Cellular Networks,* Ph.D. Thesis, University of Texas, Aug. 2016. (https://goo.gl/aHqAkp).

[UhSH17] D. Uhlir, P. Sedlacek and J. Hosek, *"Practial Overview of Commercial Connected Cars Systems in Europe"*, in 9th International Congress on Ultra-Modern Telecommunications and Control Systems and Workshops (ICUMT), Nov. 2017. (https://goo.gl/KBBeik).

[Vihe16] R. Vihelm, *Outdoor to Indoor Coverage in 5G Networks*, M.Sc. Thesis, Uppsala University, June 2016. (https://goo.gl/5qVHJZ).

[WINN07] WINNER II, *Winner II Channel Models – Part I: Channel Models"*, V.1.2, Feb. 2008. (https://goo.gl/e4QsLd).

[WJSW17] J. Wang, A. Jin, D. Shi, L. Wang, H. Shen, D. Wu, L. Hu, L. Gu, L. Lu, Y. Chen, J. Wang, Y. Saito, A. Benjebbour and Y. Kishiyama, *"Spectral Efficiency Improvement With 5G Technologies: Results from Field Tests"*, in IEEE Journal on Selected Areas in Communications, Vol. 35, No. 8, Aug. 2017. (https://ieeexplore.ieee.org/document/7944631/).

[YaAr17] A. Yazar, H. Arslan, *"Fairness-Aware Scheduling in Multi-Numerology Based 5G New Radio"*, June 2018. (https://goo.gl/QEtii2).

[YaAr18a] A. Yazar, H. Arslan, *"A Flexibility Metric and Optimisation Methods for Mixed Numerologies in 5G and Beyond"*, Feb 2018. (https://goo.gl/drhvho).

[YaAr18b] A. Yazar, B.Pekosz, H. Arslan, *"Flexible Multi-Numerology Systems for 5G New Radio"*, May 2018. (https://goo.gl/3nHuPq).

[YLPY18] L. You, Q. Liao, N. Pappas, D. Yuan, *Resource Optimisation with Flexible Numerology and Frame Structure for Heterogeneous Services,* Jan. 2018 (https://arxiv.org/abs/1801.02066).